

**Institut für Experimentelle Genetik
GSF-Forschungszentrum für Umwelt und Gesundheit,
Neuherberg**



**Identification of Novel Components of
Delta-Notch Signal Transduction**

Sabine Pfister

Vollständiger Abdruck der von der Fakultät Wissenschaftszentrum Wei-
henstephan für Ernährung, Landnutzung und Umwelt der Technischen Universität
München zur Erlangung des akademischen Grades eines

Doktors der Naturwissenschaften

genehmigten Dissertation.

Vorsitzender: Univ.-Prof. Dr. Erwin Grill

Prüfer der Dissertation: 1. Univ.-Prof. Dr. Martin Hrabé de Angelis
2. Priv.-Doz. Dr. Ramón A. Torres Ruiz
3. apl.-Prof. Dr. Jerzy Adamski

Die Dissertation wurde am 15.02.2005 bei der Technischen Universität
München eingereicht und durch die Fakultät Wissenschaftszentrum Wei-
henstephan für Ernährung, Landnutzung und Umwelt am 25.04.2005
angenommen.

Contents

Abstract	4
Zusammenfassung	5
Abbreviations	6
1 Introduction	8
1.1 Core components of Notch signaling	8
1.2 Determination of cell fate	11
1.3 Notch signaling in vertebrates	12
1.4 Notch signaling and human disease	14
1.5 Crosstalk with other signaling pathways	16
1.6 Endocytosis of Delta	17
1.7 Aim of the study	18
2 Methods and Materials	19
2.1 Methods	19
2.1.1 Working with DNA	19
2.1.2 Working with proteins	22
2.1.3 Working with bacteria	25
2.1.4 Working with yeast	26
2.1.5 Yeast two-hybrid system	26
2.1.6 Working with RNA	28
2.1.7 Histological techniques and microscopy	30
2.1.8 Working with mammalian cells	30
2.1.9 Bioinformatics	31
2.2 Materials	34
3 Results	40
3.1 Sequence analysis	40
3.1.1 Conserved NLS and PDZ-binding motif in the cyto- plasmic part of Dll1	40
3.1.2 NLS and PDZ-binding motifs in intracellular domains of mouse Delta and Jagged proteins	40
3.2 Protein-protein interaction studies	42

Contents

3.2.1	Acvrinp1 and Magi-3 are novel Dll1 binding proteins .	42
3.2.2	Acvrinp1 and Magi-3 interact with Dll1 <i>in vitro</i>	46
3.2.3	Acvrinp1 and Magi-3 bind to Jag1 <i>in vitro</i>	46
3.2.4	Modeling of the Acvrinp1 PDZ4 domain complexed with the PDZ-ligand of Dll1	50
3.2.5	Acvrinp1 and Magi-3 interact with Dll1 <i>in vivo</i>	50
3.3	Gene expression studies	52
3.3.1	<i>Acvrinp1</i> and <i>Dll1</i> are partly coexpressed during em- bryogenesis	52
3.3.2	<i>Acvrinp1</i> expression is upregulated in <i>Dll1</i> null mutant embryos	53
3.3.3	<i>Magi-3</i> and <i>Dll1</i> have few common expression do- mains during embryogenesis	53
4	Discussion	57
4.1	Delta-Notch, a bidirectional pathway?	57
4.2	Acvrinp1 and Magi-3 are novel components of Delta-Notch signal transduction	58
4.3	Common function of Acvrinp1 and Dll1 in neurogenesis and follicle formation?	59
4.4	Common function of Magi-3 and Dll1 in neurogenesis and eye development?	60
4.5	Influence of Dll1 on cell adhesion and motility	61
4.6	Delta-Notch and Planar Cell Polarity	61
4.7	Novel Dll1 binding proteins	63
4.8	Outlook	65
	References	66
	Appendix	81
	List of Figures	85
	List of Tables	86
	Danksagung	87
	Lebenslauf	88

Abstract

The evolutionary conserved Notch signal transduction pathway regulates cell fate and cellular differentiation in various tissues and has essential functions in embryonic patterning and tumorigenesis. Cell-cell signaling by the Notch pathway is mediated by the interaction of the transmembrane receptor Notch with its ligands Delta and Jagged presented on adjacent cells. Whereas signal transduction to Notch expressing cells has been described, it is yet unclear whether Delta-dependent signaling may also exist within the Delta expressing cell. To address this question an embryonic cDNA library was screened for proteins binding to the intracellular C-terminal part of mouse Delta1 (Dll1). Two proteins from the MAGUK family, Acvrinp1 and Magi-3, could be identified as novel Dll1 binding proteins. Interactions were verified by pull-down experiments *in vitro* and in a mammalian two-hybrid system *in vivo*. Interacting domains could be delimited to the fourth PDZ domain of Acvrinp1, the fifth PDZ domain of Magi-3 and the PDZ-binding domain of Dll1. A model of the PDZ4 domain of Acvrinp1 complexed with the PDZ-ligand of Dll1 could be generated by homology modeling techniques. Additionally, interactions of Acvrinp1 and Magi-3 with Jagged1 (Jag1), dependent on the PDZ-binding domain of Jag1, were shown *in vitro*. *In situ* expression analyses in mouse embryos revealed that *Dll1* and *Acvrinp1* show partly overlapping but distinct expression patterns, for example, in the central nervous system and the vibrissae buds. Further, expression of *Acvrinp1* was found to be altered in *Dll1* loss-of-function mouse embryos. *Dll1* and *Magi-3* were coexpressed in the neural tube and the eye. These results suggest that, in addition to activating Notch receptors, Dll1 may also mediate intrinsic signals into Dll1 expressing cells. This mechanism may involve interaction with the PDZ proteins Acvrinp1 and Magi-3 and might play a crucial role in cell adhesion and polarity. The novel signal transduction role of Delta has important implications for the understanding of Delta-Notch signaling and the interpretation of Delta mutant phenotypes.

Zusammenfassung

Der evolutionär konservierte Notch-Signaltransduktionsweg reguliert Zellschicksalsentscheidungen und die Differenzierung von Zellen in einer Vielzahl von Geweben und nimmt wichtige Funktionen bei der Musterbildung im Embryo und der Entstehung von Tumoren ein. Die Signalübertragung von Zelle zu Zelle durch den Notch-Signalweg wird durch die Interaktion des transmembranen Rezeptors Notch mit seinen auf angrenzenden Zellen exprimierten Liganden Delta und Jagged ermöglicht. Während die Signalübertragung in die Notch exprimierenden Zellen gezeigt werden konnte, ist es bisher unklar, ob auch eine von Delta abhängige Signalübertragung in die Delta exprimierende Zelle stattfindet. Um sich dieser Frage anzunähern, wurde eine embryonale cDNA Bibliothek nach Proteinen durchsucht, die an den intrazellulären C-terminalen Teil von murinem Delta1 (Dll1) binden. Zwei Proteine, die aus der MAGUK Familie stammen, Acvrinp1 und Magi-3, wurden als neue Dll1 bindende Proteine identifiziert. Die Interaktionen wurden mittels pull-down Experimenten *in vitro* und in einem Säugetier Two-Hybrid System *in vivo* überprüft. Die interagierenden Domänen konnten auf die vierte PDZ Domäne von Acvrinp1, die fünfte PDZ Domäne von Magi-3 und die PDZ-bindende Domäne von Dll1 eingegrenzt werden. Ein Model der 4. PDZ Domäne von Acvrinp1 komplexiert mit dem PDZ-Liganden von Dll1 konnte mittels Homology-Modellierungstechniken erzeugt werden. Zusätzlich konnten Interaktionen von Acvrinp1 und Magi-3 mit Jagged1 (Jag1), abhängig von der PDZ bindenden Domäne von Jag1, *in vitro* gezeigt werden. *In situ* Expressionsanalysen in Mausembryonen offenbarten, dass *Dll1* und *Acvrinp1* teilweise überlappende, aber dennoch unterschiedliche Expressionsmuster zeigen. Darüber hinaus wurde herausgefunden, dass die Expression von *Acvrinp1* in den *Dll1* Verlustmutanten verändert ist. *Dll1* und *Magi-3* waren im Neuralrohr und im Auge coexprimiert. Diese Ergebnisse deuten an, dass Dll1 neben der Aktivierung des Notch Rezeptors auch ein intrinsisches Signal in die Dll1 exprimierenden Zellen übermittelt. Dieser Mechanismus schließt möglicherweise die Interaktion mit den PDZ-Proteinen Acvrinp1 und Magi-3 ein und könnte eine Rolle bei der Zelladhäsion und -polarität spielen. Diese neue Funktion von Delta könnte zu einem besseren Verständnis der Delta-Notch-Signaltransduktion beitragen und bei der Interpretation des Phänotyps von Delta-Verlustmutanten helfen.

Abbreviations

Acvrin1	Activin receptor interacting protein 1
ADAM	A disintegrin and metalloprotease
AGS	Alagille syndrome
APC	Adenomatous polyposis coli
β 3GlcNAcT	O-fucose- β 1, 3-N-acetylglucosaminyltransferase
bHLH	Basic helix-loop-helix
CADASIL	Cerebral autonom dominant arteriopathy with subcortical infarcts and leukoencephalopathy
CBF1	Candida glabrata centromere binding factor 1
<i>C. elegans</i>	<i>Caenorhabditis elegans</i>
CSL	Cbf1/Su(H)/Lag-1
Dll1	Delta-like 1
Dlg	Discs large
Dlg-1	Discs large homolog 1
DSL	Delta/Serrate/Lag-2
<i>E. coli</i>	<i>Escherichia coli</i>
EGF	Epidermal growth factor
EGFR	Epidermal growth factor receptor
Eph	Ephrin receptor
E(spl)	Enhancer of split
Frz-4	Frizzled-4
GUK	Guanylate kinase
GSK	Glycogen synthetase kinase
GST	Glutathione S-transferase
Jag	Jagged
JAK	Janus kinase
LAP	Leucine-rich repeat and PDZ domain
LEF	Lymphocyte enhancer factor
LNG	Lin-12/Notch/Glp-1
JNK	Jun N-terminal kinase
LPM	Lateral plate mesoderm
Ltap	Loop tail associated protein
Magi-3	Membrane associated guanylate kinase inverted 3
MAGUK	Membrane associated guanylate kinase
MAP	Mitogen-activated protein

Abbreviations

MDCK	Madin Darby canine kidney
NiC	Notch intracellular domain
NLS	Nuclear localization signal
PAGE	Polyacrylamide gel electrophoresis
PCP	Planar cell polarity
PDB	Protein data bank
PDZ	PSD-95/Dlg/ZO-1
PDZ-BD	PDZ binding domain
PEST	Proline-, glutamate-, serine-, threonine-rich
PSM	Presomitic mesoderm
RAM	RBPJ κ associated molecule
RBPJ κ	Recombination signal sequence binding protein for J κ genes
RKE	Rat kidney epithelial
<i>S. cerevisiae</i>	<i>Saccharomyces cerevisiae</i>
SD	Spondylocostal dysostosis
SDS	Sodium dodecyl sulfate
SH3	Src-homology 3
S-SCAM	Synaptic scaffolding molecule
SOP	Sensory organ precursor
STAT	Signal transducer and activator of transcription
Su(dx)	Suppressor of deltex
Su(H)	Suppressor of hairless
TACE	TNF α converting enzyme
TAD	Transcriptional activator domain
T-ALL	T-cell acute lymphoblastic leukemias/lymphomas
TBX	T-box
TCF	T-cell factor

1 Introduction

How can a single cell build up a multicellular organism? This question fascinates developmental biologists for decades. One crucial factor for the development of multicellular life is the ability to form biological patterns. Pattern formation is mediated by molecular mechanisms of cell-cell signaling that permit cells to influence each other's fate. One key mechanism in controlling cell-cell communication is the Delta-Notch signal transduction pathway.

1.1 Core components of Notch signaling

The Notch signal transduction pathway controls cell fate and embryonic patterning in vertebrates and invertebrates through local cell interactions. Cell-cell signaling in this pathway is mediated by the interaction of the ligands Delta or Serrate (Jagged in vertebrates) to the Notch receptor expressed on neighboring cells.

Delta and Serrate proteins belong to the DSL (Delta/Serrate/Lag-2) family. DSL proteins are one-pass transmembrane receptors with a variable number of epidermal growth factor (EGF)-like repeats and a DSL domain in the N-terminal extracellular part and a short intracellular domain. In addition, Serrate contains a unique cysteine-rich motif between the EGF repeats and the transmembrane domain. Whereas the function of the EGF motifs remains unclear, it turned out that receptor association is mediated by the DSL domain (FITZGERALD & GREENWALD, 1995; HENDERSON et al., 1997).

Ligands

Notch receptors are transmembrane proteins from the LNG family. The first members isolated were Lin-12 from *C. elegans*, *Drosophila* Notch and Glp-1 from *C. elegans* (GREENWALD, 1985; WHARTON et al., 1985; AUSTIN & KIMBLE, 1987). The extracellular domain of Notch contains several EGF-like and three LNG repeats. The EGF-like motifs mediate interaction with the DSL domain of the ligands (REBAY et al., 1991). A RAM (RBPJκ associated molecule) domain, ankyrin repeats, a transcriptional activator domain (TAD) and a PEST (proline-, glutamate-, serine-, threonine-rich) sequence are found in the intracellular region. Notch is proteolytically cleaved in the secretory pathway by a furin-like convertase (S1 cleavage) and is presented on the cell surface as a heterodimer (BLAUMUELLER et al., 1997; LOGEAT et al., 1998; BARON, 2003).

Receptors

After binding of the ligand the Notch protein is cleaved in its extracellular domain by an ADAM (A disintegrin and metalloprotease) metalloprotease

1 Introduction

such as TACE (TNF α converting enzyme) or Kuzbanian (S2 cleavage) (PAN & RUBIN, 1997; LIEBER et al., 2002; BROU et al., 2000; BARON, 2003). The remaining membrane tethered part of Notch is subsequently cleaved in its transmembrane domain by a presenilin-dependent γ -secretase activity (S3 cleavage) (MUMM et al., 2000; DE STROOPER et al., 1999; BARON, 2003). This regulated processing leads to translocation of the Notch intracellular (N_{Ic}) part into the nucleus (KOPAN et al., 1996) (Fig. 1.1).

In the nucleus, Notch is binding to the CSL (Cbf1/Su(H)/Lag-1) protein *Effector*
Suppressor of hairless (Su(H)) via its RAM domain and ankyrin repeats. This interaction turns Su(H) from a transcriptional repressor into an activator (JARRIAULT et al., 1995).

This results in the upregulation of genes from the *Enhancer of split (E(spl))* *Targets*
locus encoding basic helix-loop-helix (bHLH) factors. These bHLH proteins, in turn, affect the regulation of downstream target genes from the *achate-scute (ac-sc)* complex. (JARRIAULT et al., 1995) (Fig. 1.1).

To switch off the Notch signal, the E3 ubiquitin ligase Suppressor of deltex (Su(dx)) associates with the PEST domain of N_{Ic}. Thereby, N_{Ic} is ubiquitinated and marked for proteasomal degradation (CORNELL et al., 1999).

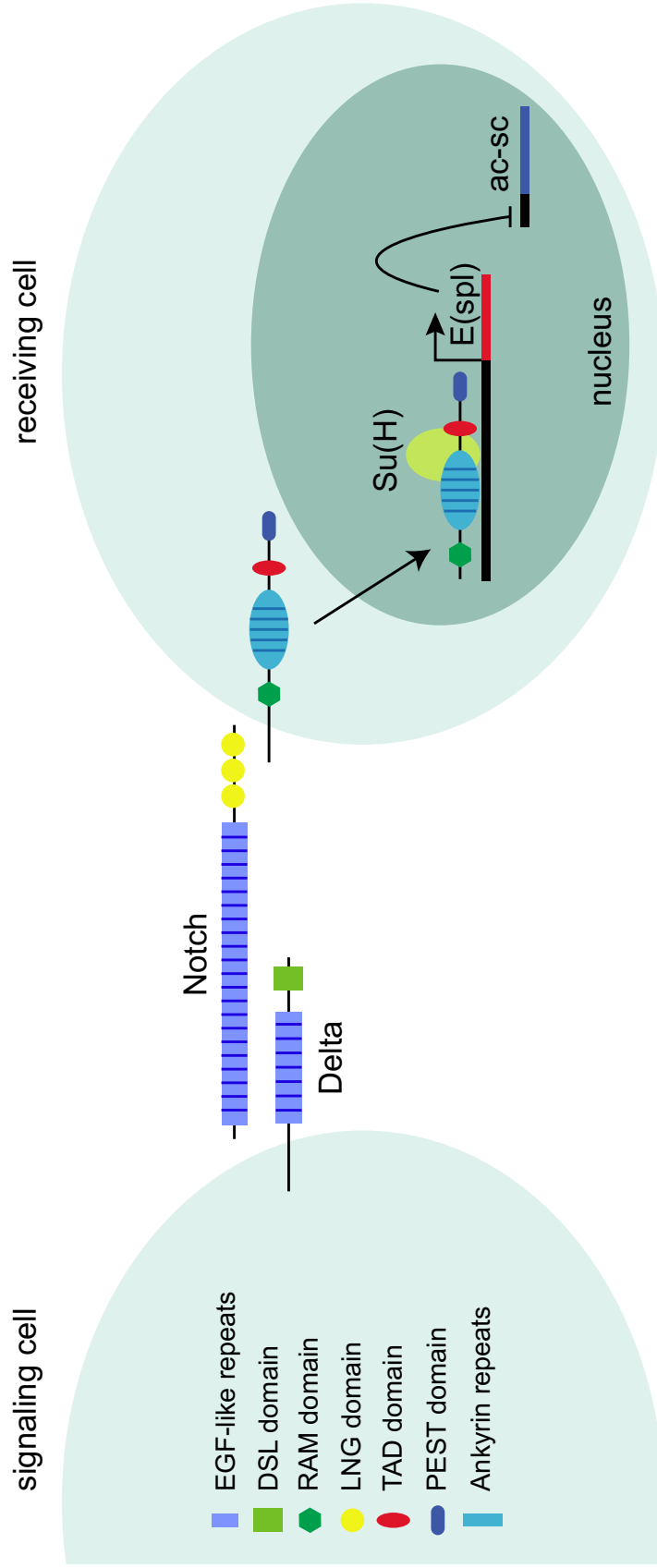


Figure 1.1: Notch signal transduction during lateral inhibition in *Drosophila*. Notch signal transduction is initiated by binding of Delta to Notch. After activation Notch is proteolytically cleaved in its extracellular region and its transmembrane domain. These cleavages release a soluble intracellular form of Notch that is able to translocate into the nucleus. Binding of Nic turns Su(H) into a transcriptional activator of genes from the E(spl) locus. E(spl) genes encode bHLH transcription factors that suppress the expression of proneural genes from the ac-sc complex.

1.2 Determination of cell fate

Delta-Notch signaling mediates cell fate decisions by three processes, called lateral inhibition, lateral specification and lateral induction.

Lateral inhibition describes a process where cells within an equivalence group inhibit neighboring cells from gaining the same developmental fate. This phenomenon is best understood during *Drosophila* neurogenesis. Before initiation of neurogenesis all cells within the neurogenic ectoderm of the fly have the potential to become either a neuronal precursor (neuroblast) or a progenitor of the epidermis (epidermoblast). Cells that express slightly more Delta activate the Notch receptors of neighboring cells. In these Notch bearing cells proneural genes from the *ac-sc* complex are inhibited by bHLH transcription factors from the *E(spl)* locus (Fig. 1.1). The expression of Delta is downregulated in activated Notch-expressing cells. The ability of these cells to inhibit their neighbors is decreased and an initially small difference between two cells is amplified in this regulatory feedback-loop (HEITZLER et al., 1996). Finally, the Delta expressing cells become nascent neurons, whereas Notch bearing cells are caused to adopt the epidermal fate (ARTAVANIS-TSAKONAS et al., 1999). The initially equivalent group of cells is driven to form a salt-and-pepper mosaic (Fig. 1.2a).

Lateral inhibition

Negative feedback-loop

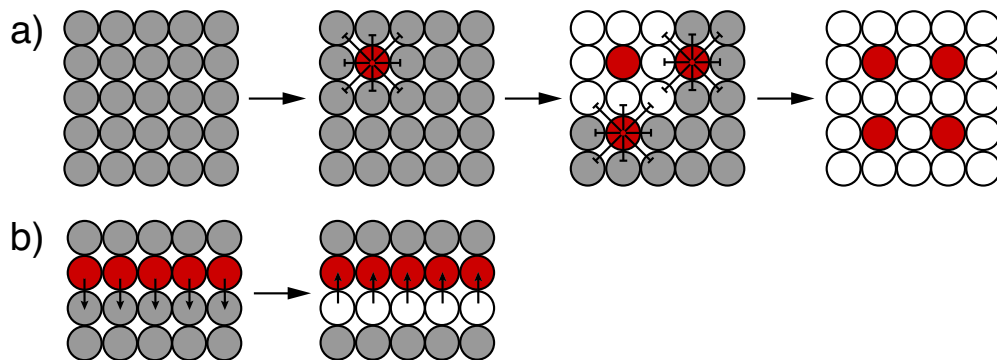


Figure 1.2: Cell fate determination. (a) Lateral inhibition. At the beginning all cells have the same potential (grey). By chance one of the cells (red) expresses slightly more Delta than surrounding cells and activates Notch signaling in its neighbors. The neighboring cells become receiving cells (white) as their expression of Delta is inhibited. The rest of the pattern is now committed. The initially equivalent cells have now different potentials and finally differentiate into cells of different fate. (b) Lateral induction. Inductive signaling typically occurs between nonequivalent cells (red and grey). Serrate expressing cells (red) induce Notch signaling in neighboring cells. These cells signal back as their expression of Delta is upregulated (white). This positive feedback loop finally leads to the formation of a boundary.

In contrast to lateral inhibition, lateral specification occurs between equivalent and nonequivalent cells. One example of lateral specification involves the differentiation of the sensory organ precursors (SOPs) in *Drosophila*. SOP cells divide to produce two cells, whereas only one of the daughter cells receives

Lateral specification

1 Introduction

Numb, an antagonist of Notch. Both daughter cells divide again to form one pair of hair and socket cells and one pair of neuron and sheath. Numb is again asymmetrically distributed during the division and segregates into only one of the two daughter cells. The cells that receive Numb antagonize Notch activity, whereas the other cells adopt the fate associated with Notch activation (SPANNA et al., 1995; FRISE et al., 1996).

Studies on the wing margin of *Drosophila* has shown that Notch signaling is also required for the formation of borders. Fringe, a modulator of Notch signaling, encodes an O-fucose- β 1, 3-N-acetylglucosaminyltransferase (β 3GlcNAcT) that adds O-fucose glycans to the Notch EGF repeats. Thereby, Fringe causes Notch to respond to Delta rather than Serrate. Serrate and Fringe are expressed exclusively in the dorsal part of the developing wing. Serrate expressing cells of the dorsal compartment can only signal to the ventral part of the wing. In response to Serrate activation Delta expression is upregulated in ventral cells. These cells signal back to the dorsal part and induce Serrate expression in the dorsal cells. This positive feedback mechanism results in a localized activation of Notch signaling in adjacent stripes of cells at the wing margin (PANIN et al., 1997; KLEIN & ARIAS, 1998; BRAY, 1998) (Fig. 1.2b). Inductive interactions involve also signaling between nonequivalent cells that express either the LNG receptor or the DSL ligand. One famous example is the induction of mitotic divisions in the germ line of *C. elegans*. The ligand Lag-2, produced by a somatic gonadal cell, the distal tip cell, activates the receptor Glp-1 in the germ line to promote mitosis (CRITTENDEN et al., 1994; HENDERSON et al., 1994).

Lateral induction

Positive feedback-loop

1.3 Notch signaling in vertebrates

Vertebrate homologues have been identified for each of the core components of Notch signal transduction. These include *Notch1-4*; *Delta-like1 (Dll1)*, *Dll3*, *Dll4*, *X-Delta-1* and *C-Delta-1*; Serrate homologues *Jagged1 (Jag1)*, *Jag2* and *C-Serrate-1*; the Su(H) homologue CBF1 (also called RBPJ κ) and Hairy and Enhancer of Split homologues *Hes1*, *Hes5*, *Hes7*, *Hey1* and *Hey2* (DE LA POMPA et al., 1997).

Homologues

In addition, several modulators of Notch signaling were found in vertebrates. The Fringe homologues Radical, Lunatic and Manic fringe are among them (ITOH et al., 2003; CHEN & CASEY CORLISS, 2004; WU et al., 1996; JOHNSTON et al., 1997).

Notch signaling mediates cell fate decisions during many aspects of vertebrate embryonic development. During early neurogenesis, for example, Delta-Notch signaling regulates the differentiation of proliferating cells in the neural tube by lateral inhibition. Thereby, activated Notch represses the neuronal fate (DE LA POMPA et al., 1997; DE BELLARD et al., 2002; GRANDBARBE et al., 2003), Notch pathway mutants exhibit a neurogenic phenotype that is characterised by

Neurogenesis

1 Introduction

an excessive neuronal differentiation (HRABÉ DE ANGELIS et al., 1997; CONLON et al., 1995; OKA et al., 1995). Interestingly, *Dll1* loss-of-function mouse mutants (HRABÉ DE ANGELIS et al., 1997) have more cells in the floorplate and show an increased motor-neuron differentiation, whereas the differentiation of ventral interneurons is decreased. Also, the differentiation of neural progenitors is premature in *Dll1* mutants. These findings indicated that *Dll1* acts as a critical regulator of neuronal differentiation in mice (G. Przemeck, unpublished results). Expression of mouse *Dll1* in nascent neurons but not in cells surrounding them indicates that Delta-Notch signaling also regulates the formation of sensory hair cells in the embryonic inner ear by lateral inhibition (MORRISON et al., 1999).

Moreover, Notch signaling is involved in somitogenesis. Somites are repeating metameric blocks of cells that arise early during development from two sheets of unsegmented mesoderm, called presomitic mesoderm (PSM), lying laterally to both sites of the neural tube. Somites bud from the rostral end of the PSM in an anterior to posterior progression, undergo an mesenchymal to epithelial transition and differentiate. Somite condensation progresses while at the same time new presomitic mesoderm cells are formed from the primitive streak and later from the tail bud. Somite formation is a periodic process, repeated every 90 minutes in chick and every 90-120 minutes in mouse embryos dependent on the axial position (TAM, 1981; AULEHLA & HERRMANN, 2004). Tissues of somatic origin are the axial skeleton and ribs, the skeletal muscles and the dermis of the back. A variety of genes have been identified that show a cyclic expression pattern within the PSM, recurring everytime a new somite is formed. This observation lead to the postulation of a molecular oscillator referred to as the "segmentation clock", which is established and regulated by multiple signaling pathways including those of Notch, Wnt and FGF. The molecular interplay between the various components of these pathways is not fully understood to date. In *Dll1*, *Dll3*, *Notch1* and *RBPJK* loss-of-function mouse mutants the anterior-posterior polarity of somites and the formation of somite boundaries are disturbed, but somite formation is unaffected (HRABÉ DE ANGELIS et al., 1997; KUSUMI et al., 1998; DUNWOODIE et al., 2002; CONLON et al., 1995; OKA et al., 1995). Therefore, although it is well established that the Delta-Notch pathway plays an important role in the clock mechanism, also other factors must be involved.

Somitogenesis

Recently, Notch signaling has also been implicated in the determination of left-right asymmetry. Establishment of the left-right body axis involves four steps: Breaking of the initial symmetry in or near the node, transfer of asymmetric signals to the lateral plate mesoderm (LPM), induction of asymmetric gene expression, such as *Nodal* and *Leftb* in the left LPM and left-right asymmetric morphogenesis of visceral organs. Mice homozygous for a knock-in mutation that places lacZ under the control of the *Dll1* promoter (HRABÉ DE ANGELIS et al., 1997) show left-right defects, namely randomisation of the direction of heart looping and embryonic turning. How *Dll1* influences left-right de-

Left-right development

1 Introduction

velopment remains controversial. Two independent groups reported that *Dll1* mediated Notch signaling is essential for the initiation of *Nodal* expression around the node and that *Nodal* activates asymmetric gene expression in the LPM (KREBS et al., 2003; RAYA et al., 2003). In contrast to this model, Przemeczek et al. suggested that the cause for the observed left-right defects is a failure in the development of proper midline structures. These originate from the node, which is disrupted and deformed in *Dll1* mutant embryos (PRZEMECK et al., 2003).

Furthermore, Notch activity is a crucial factor for the development of several organs. Regulation of the decision between endocrine and exocrine fates in the developing pancreas by lateral inhibition is only one example (APELQVIST et al., 1999).

*Pancreas
development*

In addition, Notch signaling has been shown to affect hematopoiesis. A recombinant soluble form of human DLL1 containing the DSL domain and N-terminal sequences was found to inhibit the differentiation and promote the expansion of hematopoietic progenitor cells in a murine hematopoietic progenitor cell line (HAN et al., 2000). These observations were consistent with the action of human JAG1 and JAG2 in hematopoiesis. Also the purified extracellular domains of human JAG1 and JAG2 increased the number of primitive precursor cell populations in murine and human hematopoietic precursor cells (VARNUM-FINNEY et al., 1998; CARLESSO et al., 1999).

Hematopoiesis

1.4 Notch signaling and human disease

So far four human disorders have been associated with mutations in Notch pathway genes. These include a developmental disorder (Alagille syndrome), a neurological disease (CADASIL), skeletal defects (Spondylocostal dysostosis) and cancer (T-ALL).

Alagille syndrome (AGS) is a developmental disorder that is characterised by neonatal jaundice, a reduced number of bile ducts, congenital heart defects, skeletal defects and eye abnormalities. Other less frequent features of this syndrome include growth retardation, mental retardation and kidney abnormalities. AGS is an autosomal dominant disease with an occurrence of 1 in 70.000 live births. Expressivity of AGS is very variable but penetrance is high (KRANTZ et al., 1997). Two independent groups reported that AGS is caused by mutations in the human *Jagged1* (*JAG1*) gene (LI et al., 1997; ODA et al., 1997). Most mutations identified so far are frame shift, non-sense or splice site mutations and result in truncated JAG1 proteins. Haploinsufficiency was suggested as primary cause for AGS (SPINNER et al., 2001). Recently, a mouse model for AGS could be established. Mice doubly heterozygous for the *JAG1* null allele and a *Notch2* hypomorphic allele exhibit developmental abnormalities characteristic of AGS and might help to understand the molecular mechanisms underlying the disease (MCCRIGHT et al., 2002).

*Alagille
syndrome*

1 Introduction

CADASIL (cerebral autonom dominant arteriopathy with subcortical infarcts and leukoencephalopathy) is an autosomal dominant vascular disorder that manifests in recurrent subcortical ischemic strokes leading to a progressive dementia and death by 65 years of age. Other commonly observed symptoms are migraine with aura and mood disorders (CHABRIAT et al., 1995). The vascular lesions underlying CADASIL affect primarily small cerebral arteries, although the vascular defects are systemic. The frequency of CADASIL is very low. CADASIL usually occurs at a mean age of 45 years and is caused by mutations in the *NOTCH3* gene (JOUTEL et al., 1996). All mutations identified so far result in the gain or loss of a cysteine residue in one of the EGF repeats and might alter the structure of the protein (JOUTEL et al., 1997). Joutel et al. found the ectodomain of NOTCH3 accumulated in cerebral microvasculature of CADASIL patients (JOUTEL et al., 2000). Therefore they suggest that CADASIL mutations impair the clearance of the NOTCH3 ectodomain from the cell surface.

CADASIL

Patients suffering from spondylocostal dysostosis (SD) have a reduced stature resulting from axial skeletal defects like multiple hemivertebrae, rib fusions and deletions. SD is inherited in an autosomal dominant and autosomal recessive manner. Autosomal recessive SD is a rare condition and is caused by mutations in the human *DLL3* gene. Three mutations could be identified so far. Two of them cause truncated DLL3 proteins. The third mutation is a missense mutation in a highly conserved amino acid residue and might affect the structure of DLL3 (BULMAN et al., 2000). Two mouse models for SD have been established. Mice homozygous for the *pudgy* mutation, a spontaneous mutation in the *Dll3* gene, and mice homozygous for a targeted *Dll3* mutation exhibit skeletal defects similar to SD patients (KUSUMI et al., 1998; DUNWOODIE et al., 2002). Phenotypic analyses revealed that delayed and irregular somite formation is the reason for the observed skeletal defects.

Spondylocostal dysostosis

Human NOTCH1 has been implicated in T-cell acute lymphoblastic leukemias/lymphomas (T-ALL). Three T-ALL patients examined exhibited chromosomal translocation that lead to the expression of truncated NOTCH1 proteins containing most or all of the cytoplasmic domain (ELLISEN et al., 1991). Studies in *Drosophila* and *C. elegans* suggest that truncated forms of LNG family members are constitutively active (STRUHL et al., 1993). This constitutive activation of the Notch pathway might affect cellular differentiation without blocking the potential of cells to divide and may promote tumorigenesis.

T-ALL

The diversity of the described disorders shows the broad spectrum of Notch activity in man.

1.5 Crosstalk with other signaling pathways

During embryonic development an impressive amount of different cell types have to be created by few signaling pathways that mediate interaction between the cells. To create such a diversity common signaling pathways have to be connected to each other. Also the Notch signal transduction pathway is integrated into such a network.

Recently, a crosstalk between the Notch and the JAK-STAT pathway has been reported (KAMAKURA et al., 2004). JAK-STAT signaling is activated as extracellular signaling molecules, like cytokines and growth factors, bind to specific receptors on the cell surface. A subsequent cascade of phosphorylation events involving JAK (janus kinase) finally leads to the phosphorylation of the transcription factor STAT (signal transducer and activator of transcription). Phosphorylated STATs dimerize and migrate into the nucleus where they activate specific target genes. Like Notch, STATs have been implicated in tumorigenesis and the regulation of cell fates (LEVY & DARNELL, 2002). A direct interaction between JAK2, STAT3 and the Notch primary targets Hes1 and Hes5 was shown (KAMAKURA et al., 2004). It has been suggested that the observed association facilitates the complex formation between JAK2 and STAT3, thus promoting STAT3 phosphorylation and activation. Furthermore STAT3 seems to be crucial for the maintenance of radial glial cells and differentiation of astrocytes by Notch signaling in the CNS (KAMAKURA et al., 2004).

JAK-STAT

Notch and Epidermal Growth Factor Receptor (EGFR) pathways cooperate, among others, in the regulation of cell fate specifications in the *Drosophila* eye. Thereby, activation of EGFR induces the differentiation of photoreceptor cells and promotes their expression of Delta. Overexpression of Delta is mediated by Sno and Ebi, two proteins that antagonize a repressor function of Su(H). Delta, in turn, induces neighboring cells to become nonneural cone cells (TSUDA et al., 2002). Antagonistic effects of Notch and EGFR signaling have also been described. During the formation of the adult chordotonal organ of *Drosophila* SOPs are continuously accumulated from a proneural cluster. Notch signaling is required to limit the number of SOPs, but does not prevent multiple SOP formation because EGFR signaling overcomes Notch-mediated lateral inhibition by opposing the repression of proneural genes from the ac-sc complex (ZUR LAGE & JARMAN, 1999).

EGFR

Several connections to the Wnt signaling cascade have also been suggested. Wnt signaling is initiated by binding of a Wnt family member to its receptor Frizzled. The Frizzled protein then activates Disheveled, allowing it to become an inhibitor of a glycogen synthetase kinase-3 (GSK-3). GSK-3, when active, prevents the dissociation of β -catenin from the APC (adenomatous polyposis coli) complex, which targets β -catenin for proteasomal degradation. β -catenin is then translocated to the nucleus and activates Wnt responsive genes in complex with LEF/TCF (lymphocyte enhancer factor/T-cell factor). At the wing margin of *Drosophila* Wnt signaling induces the formation of sensory bristles,

Wnt

1 Introduction

whereas activated Notch provides an inhibitory signal. Thereby, Wnt signaling overcomes Notch suppression through a direct interaction of Disheveled and Nlc that inhibits Notch activity (AXELROD et al., 1996). In addition, studies in *Drosophila* revealed an alternative Notch signal transduction pathway independent of Su(H) and mediated by Deltex (RAMAIN et al., 2001). This novel signaling mode seems to be regulated by elements of the Wingless signaling pathway, like Disheveled and the *Drosophila* GSK-3 homolog Shaggy. The results of several new studies indicate that an interplay between the Wnt and Delta-Notch pathway is also required for proper vertebrate somitogenesis (AULEHLA et al., 2003; AULEHLA & HERRMANN, 2004; GALCERAN et al., 2004; HOFMANN et al., 2004). Disruption of Wnt signaling affects the cyclic expression of Notch pathway genes, whereas cyclic expression of Axin2, a Wnt pathway gene, is maintained when Notch signaling is impaired (AULEHLA et al., 2003). Therefore, Wnt signaling was placed upstream of the Delta-Notch pathway in somitogenesis. Two independent groups now proposed that Wnt exerts its effect on Delta-Notch signaling via its downstream transcription factors LEF/TCF (GALCERAN et al., 2004; HOFMANN et al., 2004). It could be demonstrated that LEF/TCF cooperate with the T-box transcription factor TBX6 to directly activate the transcription of Dll1 in the PSM and tail bud. The variety of connections to other signaling pathways shows again the central role of the Delta-Notch pathway during embryonic development.

1.6 Endocytosis of Delta

Several groups reported that the shed ectodomain of Notch is endocytized in complex with Delta by the ligand expressing cell. In *Drosophila* this endocytosis is dependent on Dynamin and the RING-type E3 ubiquitin ligase Neuralized (PARKS et al., 2000; LAI et al., 2001; PAVLOPOULOS et al., 2001). In vertebrates the zebrafish Ring-type E3 ubiquitin ligase Mind bomb is involved in the same process (ITOH et al., 2003; CHEN & CASEY CORLISS, 2004). It has been suggested that ubiquitin ligases interact with the intracellular domains of Delta ligands to promote their ubiquitinylation and internalization. This might lead to physical changes required for the proteolytic cleavage that releases the Notch extracellular domain (S2 cleavage), which undergoes transendocytosis. As a result, the remaining Notch fragment becomes susceptible to cleavage by γ -secretase activity (S3 cleavage) (PARKS et al., 2000; LAI et al., 2001; PAVLOPOULOS et al., 2001; ITOH et al., 2003; CHEN & CASEY CORLISS, 2004). Recently, a *Mind bomb* loss-of-function mouse mutant line could be established. The fact that *Mind bomb* null mutants display neurogenesis and somitogenesis defects is consistent with the observation that ubiquitinylation and endocytosis of Delta ligands is required for effective Notch signaling (K. Artzt, personal communication).

1.7 Aim of the study

In the last decades signal transduction to Notch expressing cells has been studied in detail but it is still unclear if Delta-dependent signaling occurs also within Delta expressing cells. To address this question, proteins interacting with the intracellular domain of mouse Dll1 should be identified with help of a yeast two-hybrid approach. Interactions obtained in yeast should be confirmed by GST pull-down experiments *in vitro* and in a mammalian two-hybrid system *in vivo*. The major interacting domains should be delimited and a structural model of the interactions should be created by homology modeling techniques. Also, interesting candidate proteins should be tested for interaction with Jag1 *in vitro*. In addition, tissue coexpression should be checked by *in situ* expression analyses in wildtype and *Dll1* loss-of-function mouse embryos. The elucidation of processes within the Delta bearing cells are important for the understanding of Delta-Notch signaling and so far unresolved questions concerning Delta-mutant phenotypes.

What happens inside the Delta expressing cells?

2 Methods and Materials

2.1 Methods

2.1.1 Working with DNA

Plasmid isolation from bacteria

Plasmid containing bacteria were incubated in LB-Amp or LB-Kan medium overnight at 37 °C and 200 rpm. Depending on the desired amount of DNA the culture volume was set to 5 or 50 ml. For isolation of plasmid DNA NucleoSpin Plasmid (#740588; Macherey-Nagel) or NucleoBond PC 100 kits (#740573; Macherey-Nagel) were used according to the manufacturer's protocol.

Plasmid isolation from yeast

To isolate plasmid DNA from yeast 1 ml of an overnight culture was centrifuged for 3 min at 14000 rpm at room temperature. The supernatant was discarded and the pellet was resuspended in 500 μ l S-buffer. The solution was incubated at 37 °C for 30 min. After addition of 100 μ l Lysis buffer the suspension was vortexed and left at 65 °C for 30 min. 166 μ l 3 M potassium acetate was added and the solution was chilled on ice, followed by centrifugation at 14000 rpm for 10 min at 4 °C. The supernatant was transferred to a new Eppendorf tube and DNA was precipitated with 800 μ l 100 % ethanol for 10 min on ice. The sample was centrifuged afterwards at 14000 rpm at 4 °C for 15 min. The DNA pellet was washed with 500 μ l 70 % ethanol, air dried and resuspended in 50 μ l sterile water.

Determination of DNA concentration

DNA concentration was estimated by measuring the optical density at 260 nm with an UV-spectrophotometer (DU530; Beckmann). Multiplication of the measured value by 50 (double stranded DNA concentration at $OD_{260}=1$) and the dilution factor gives DNA concentration in μ g/ml.

Purification of DNA

For isolation of DNA fragments from restriction digestions, bands of the desired size were cut out from an agarose gel and were extracted with the QIAquick gel extraction kit (#28704; QIAGEN). PCR products can be purified with

2 Methods and Materials

the QIAquick PCR purification kit (#28104; QIAGEN). Both kits were used according to the manufacturer's protocol.

Agarose gel electrophoresis

Due to their negative charge DNA molecules can migrate in an electric field. Agarose gel electrophoresis takes advantage of this property and allows the separation of DNA fragments according to their molecular weights. For agarose gel electrophoresis DNA samples were mixed with 6 x loading dye (#R0611; MBI Fermentas) at a ratio of 5:1 and were applied to 0,8 % - 2 % agarose gels containing 1 $\mu\text{g}/\text{ml}$ ethidium bromide. The gels were run at 120 V in 1 x TBE buffer in a gel chamber (Sub-Cell GT; Biorad). DNA was visualised afterwards by UV excitation (254 nm) of intercalated ethidium bromide.

Restriction digestion of DNA

1 μg plasmid DNA was typically digested with 1 U of the respective restriction enzyme. Buffer conditions were adopted from the manufacturer's protocol. The reactions were incubated for 90 min at 37 °C. Success of the restriction was checked by agarose gel electrophoresis.

Ligation

Ligation of a linearised vector with the desired insert is catalysed by the enzyme T4-DNA-Ligase. Usually 100 ng vector DNA was mixed with the 3 x molar amount of insert DNA and 2.5 U T4-DNA-Ligase in a total volume of 10 μl . Alternatively 1-4 μl of PCR product was used for ligation into pCRII, pcDNA3.1 (#K4600-01 and #K4800-01; Invitrogen) or pGEM (#A1380; Promega) from the TA-Cloning kits. The reactions were incubated overnight at 16 °C.

Polymerase Chain Reaction (PCR)

For specific amplification of DNA fragments from cDNA or plasmid DNA PCR reactions were performed. The following standard mixture was used:

50 ng DNA template
1 x PCR buffer
0.2 mM of each dNTP
1.5 mM MgCl_2
0.25 μM of each primer
2.5 U DNA-Polymerase
ad 20 μl H_2O

2 Methods and Materials

At first, double-stranded DNA was separated into single strands at 95 °C for 30 sec (**denaturation**). The temperature for subsequent primer **annealing** is dependent on the melting temperature of the oligonucleotides used and was determined empirically. Usually 30 sec were sufficient for annealing. **Elongation** was performed with an appropriate DNA-Polymerase at 72 °C for 1 min/kb fragment length. These three steps were repeated 25-35 times dependent on the desired amount of DNA. Pfu DNA-Polymerase was used for cloning, Taq DNA-Polymerase for the detection of plasmid containing *E. coli* clones. PCR was performed in Stratagene's RoboCycler 96.

Cloning

For generation of the expression constructs pGBKT7*Dll1*cyto, pGEX*Dll1*cyto, pGEX*Jag1*cyto, pcDNA3*Acvrin1* GUKWW, pcDNA3*Acvrin1* PDZ1-5, pcDNA3*Acvrin1* ΔPDZ4-5, pcDNA3*Acvrin1* PDZ4-5, pcDNA3*Acvrin1* ΔPDZ5, pcDNA3*Acvrin1* PDZ5, pcDNA3*Magi-3* PDZ1-5, pACT*Dll1*cyto, pBIND*Acvrin1* and pBIND*Magi-3* PDZ1-5 the respective cDNA sequences were amplified by PCR from template plasmids. Due to its high accuracy Pfu DNA-Polymerase was used for all PCR reactions. For addition of 3' A-overhangs PCR reactions were incubated with 1 U Taq DNA-Polymerase for 10 min at 72 °C and subsequently subcloned into pCR2.1 (#K4500-40; Invitrogen), pGEM (#A1380; Promega) or pcDNA3.1 (#K4800-01; Invitrogen) by TA-Cloning according to the manufacturer's instructions. The cDNA inserts were released by restriction digestion and cloned into the desired vectors according to standard protocols (SAMBROOK et al., 1989). For the creation of RNA probes the cDNA sequences of *Acvrin1* PDZ1-5 and *Magi3* PDZ1-5 were amplified by PCR and directly introduced into pCRII by TA-Cloning (#K4600-40; Invitrogen). Primers and restriction sites are listed in the appendix. All constructs were sequenced by Dr. W. Metzger (Sequiserie).

In vitro mutagenesis

Site-directed mutagenesis is used to make point mutations, switch amino acids, and delete or insert single or multiple amino acids. In this study site-directed mutagenesis was performed to delete the PDZ-binding domains of *Dll1* and *Jag1*. Two primers each were designed that contained the desired mutation and annealed to the same sequence on opposite strands of the pGEX*Dll1*cyto or pGEX*Jag1*cyto construct (see Appendix). Extension of these primers during PCR with Pfu DNA-Polymerase generated the mutated plasmids pGEX*Dll1*cytoΔPDZ-BD and pGEX*Jag1*cytoΔPDZ-BD. Afterwards, the PCR reactions were treated with DpnI to digest the parental DNA templates and were transformed into *E. coli* DH5α. Finally the constructs were checked by sequencing.

2.1.2 Working with proteins

Expression and purification of GST fusion proteins

For expression and purification of the recombinant proteins 50 ml LB-Amp medium was inoculated with an overnight culture of pGEX*DIII*cyto, pGEX*DIII*cyto Δ PDZ-BD, pGEX*Jag1*cyto or pGEX*Jag1*cyto Δ PDZ-BD in *E. coli* BL21 at a ratio of 1:100. Cultures were grown at 37 °C and 200 rpm to an OD₆₀₀ of 0.7. Protein expression was induced by addition of 0.5 mM IPTG and cultivation was continued for 3 h. Afterwards, cells were harvested by centrifugation (10 min, 4000 rpm, 4 °C). Supernatants were discarded and pellets were resuspended in 2.5 ml Lysis buffer containing 2.5 μ l 1000 x Protease inhibitors (#1697498; Roche Diagnostics) and 5 μ l Lysozyme solution. Afterwards, the cells were cracked by repeated freezing in liquid nitrogen and thawing in a 30 °C waterbath. After addition of 5 μ l Benzonase (10 U/ μ l) and 150 μ l 100 mM MgCl₂ suspensions were incubated for 45 min at room temperature and centrifuged (45 min, 4500 rpm, 4 °C) afterwards. GST fusion proteins could be purified by incubation with 100 μ l PBS washed Glutathione Sepharose 4B beads (#17-0756-01; Amersham Biosciences) overnight at 4 °C with shaking. The next day, mixtures were centrifuged (2 min, 3200 rpm, 4 °C), supernatants were discarded and beads were washed three times with 1 ml cooled PBS. To elute the GST fusion proteins, beads were incubated with 500 μ l Elution buffer for 1 h at room temperature with shaking. For removal of glutathione the protein solutions were dialysed in 6 mm dialysis tubings (#44104; Serva Electrophoresis) against PBS at 4 °C (3 x 1h).

SDS-Polyacrylamide gel electrophoresis (PAGE)

Expression and purity of the isolated proteins were checked by SDS-polyacrylamide gel electrophoresis (PAGE) according to Schägger and von Jagow (SCHÄGGER & VON JAGOW, 1987). Following mixtures were sufficient to pour 2 mini-gels (Mini-PROTEAN 3 system; Bio-Rad):

10% Resolving Gel:	
30 % Acrylamide, 0.8 % Bisacrylamide	3.3 ml
Gel buffer	3 ml
50 % Glycerol	2.5 ml
H ₂ O	1 ml
TEMED	20 μ l
10 % APS	50 μ l
Total volume	10 ml

2 Methods and Materials

4% Stacking Gel:	
30 % Acrylamide, 0.8 % Bisacrylamide	670 μ l
Gel buffer	670 μ l
H ₂ O	3.67 ml
TEMED	7 μ l
10 % APS	40 μ l
Total volume	5 ml

Protein samples were mixed with an equal volume of 1 x SDS-sample buffer and boiled for 8 min. Probes and a molecular marker (#345-0125; Bio-Rad) for estimation of protein sizes were applied to the gels. Gels were run at 80 V until protein samples passed the stacking gel. Electrophoresis was continued at 120 V. After gel run was completed gels were stained with Coomassie staining solution for 30 min, destained with 7 % acetic acid and dried for 1 h at 80 °C with vacuum (Model 583 Gel Dryer, Bio-Rad). For separation of proteins with different molecular weights for the pull-down experiments 4-12 % precasted gradient gels (#345-0125; Bio-Rad) were run with MES buffer (#161-0789; Bio-Rad).

Western blotting

To analyse protein samples with specific antibodies proteins were separated by SDS-PAGE and transferred to a PVDF membrane (#EH-2222; Pall). The PVDF membrane was cut to the size of the gel and moistened with methanol. Afterwards, the membrane and the gel were incubated in blotting buffer for 10 min. Two pieces of gel-size filter paper were soaked in blotting buffer and put onto the anode plate of a semi-dry blotting device (#107-3848; Bio-Rad) followed by the membrane, the gel and another two soaked pieces of filter paper. Blotting was performed for 30 min at 20 V. After transfer of the proteins the membrane was blocked with 5 % skimmed milk powder in PBS for 30 min at room temperature. Subsequently, the membrane was incubated with the primary antibody diluted in 0.5 % skimmed milk powder in PBS overnight at 4 °C. The next day, the membrane was washed with PBS and incubated with an appropriate peroxidase labeled secondary antibody diluted in 0.5 % skimmed milk powder in PBS for 2 h at room temperature. After washing detection was performed in detection buffer until protein bands became visible. Staining could be stopped with tap water. The membrane was dried for storage.

Protein concentration measurement

For protein concentration measurement a modified protocol of Markwell (MARKWELL et al., 1981) according to the Lowry method (LOWRY et al., 1951) was used. Protein samples were diluted in deionised water to a maximum final concentration of 100 μ g/ml. A dilution series of BSA standard solution in deionised water was prepared to give final concentrations of 0-100 μ g/ml.

2 Methods and Materials

250 μ l protein samples or standard dilutions were mixed with 750 μ l Solution C and incubated for 10 min at room temperature. Afterwards, 75 μ l Solution D was added. The samples were mixed and left for 45 min in the dark. Within the next 45 min the absorption at 660 nm was measured. Concentration of the protein samples was determined by interpolation from the standard curve.

***In vitro* translation and ^{35}S -Methionine labeling**

The TNT T7 Quick Coupled Transcription/Translation System (#L1170; Promega) was used for a one step transcription/translation of *Acvrin1*, the *Acvrin1*-deletion constructs and *Magi-3* PDZ1-5 in pcDNA3 or pcDNA3.1 vector (Invitrogen). Protein products were labeled at the same time with ^{35}S -Methionine (#AG1594; Amersham Biosciences) according to the manufacturer's protocol.

GST pull-down assay

For the verification of protein-protein interactions *in vitro* GST pull-down assays were performed (Fig. 2.1). 1.5 μ g of the respective GST fusion protein was bound to 5 μ l glutathione-sepharose 4B beads (#17-0756-01; Amersham Biosciences) in PBS for 2 h at 4 °C. After sedimentation (2 min, 4000 rpm, 4 °C) the supernatant was removed and the beads were washed three times in 200 μ l cooled PBS and incubated with 10 μ l of the *in vitro* translated probe in 200 μ l binding buffer for 2 h at 4 °C. Beads were washed three times in 200 μ l washing buffer for 20 min at 4 °C before they were overlayed with 10 μ l SDS-sample buffer and boiled for 8 min. After 5 min centrifugation at 14000 rpm the supernatant was analysed by SDS-PAGE and autoradiography (Phosphoimager Fuji FLA-3000, 16h exposure).

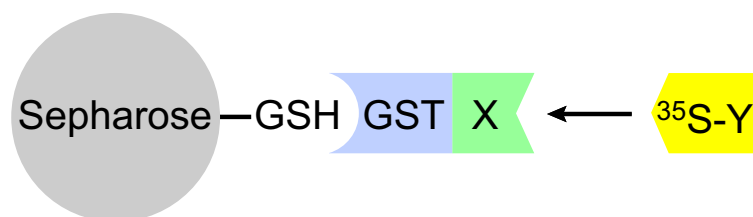


Figure 2.1: GST pull-down assay. Protein X is expressed in fusion with GST. The GST fusion protein is immobilized on a glutathione-sepharose matrix and incubated with *in vitro* translated and ^{35}S -Methionine labeled protein Y. Several washing steps are performed to remove unbound protein Y. If protein X and protein Y interact with each other, radioactivity is kept in the sample and can be detected by SDS-PAGE and autoradiography

2.1.3 Working with bacteria

Storage and growing

Bacteria are grown in LB medium at 37 °C with shaking (200 rpm) or incubated on LB agar plates at 37 °C overnight. For long term storage 1 ml of an overnight culture is mixed with 500 μ l 80 % glycerol in a cryotube vial and put into a -80 °C freezer until usage.

Preparation of chemically competent *E. coli*

250 ml LB medium with 20 mM MgSO₄ were inoculated with 2.5 ml of an overnight culture of *E. coli* DH5 α , JM107 or BL21 (1:100) and incubated at 37 °C to OD₆₀₀=0.4-0.6. The bacterial suspension was cooled down to 4 °C and centrifuged (15 min, 4500 rpm, 4 °C) afterwards. The pellet was resuspended in 100 ml cold TFB1, left on ice for 5 min and centrifuged again. Supernatant was discarded and bacteria were resuspended in 10 ml cold TFB2. After 15-60 min incubation on ice, the suspension was divided into 100 μ l portions, quick-frozen in liquid nitrogen and stored at -80 °C.

Preparation of electrocompetent *E. coli*

10 ml of an overnight culture of *E. coli* XL1-blue was diluted with 1 l LB medium (1:100) and incubated at 37 °C until it reached an OD₆₀₀ of 0.5-0.8. The culture was cooled down on ice and centrifuged at 4500 rpm and 4 °C for 15 min. The pellet was washed with 1 l, 500 ml and 20 ml ice cold 10 % glycerol before it was resuspended in 10 ml ice cold 10 % glycerol. 50 μ l aliquots were prepared, frozen in liquid nitrogen and stored at -80 °C until usage.

Heat-shock transformation

Usually, 2 μ l of plasmid DNA or a ligation reaction was mixed with 100 μ l of thawed chemically competent *E. coli* (BL21, DH5 α , JM107 or TOP10). The reaction was kept on ice for about 30 min. After heat-shock at 42 °C for 45 sec, bacteria were grown in 250 μ l LB medium at 37 °C for 1 h with shaking (200 rpm). Finally, the reaction mixture was plated onto appropriate selection media.

Electroporation

For transformation into electrocompetent *E. coli* XL1-blue, one aliquot of the bacteria was thawed, mixed with 2 μ l of plasmid DNA or a ligation reaction and incubated on ice for 10 min. Afterwards, the suspension was transferred to a sterile electroporation cuvette (#165-2086; Biorad) and pulsed at 200 Ω , 2.5 kV and 25 mF (Gene Pulser II; Biorad). After subsequent addition of 1 ml LB

2 Methods and Materials

medium bacteria were transferred to an Eppendorf tube, incubated for 1 h at 37 °C with shaking and finally plated on LB agar.

2.1.4 Working with yeast

Storage and growing

Yeast can be cultivated in liquid medium with shaking (250 rpm) or on solid agar plates. The optimal cultivation temperature is 30 °C. To store yeasts for a longer period of time 1 ml of an overnight culture is mixed with 500 μ l 80 % glycerol in a cryotube. The vial can be stored at -80 °C for several years.

Transformation into yeast

300 ml YPDA or SD medium (for pretransformed yeasts) were inoculated with 30 ml of an overnight culture and incubated at 30 °C with shaking (250 rpm) until the culture has reached the stationary phase (OD_{600} between 0.4 and 0.6). After incubation the culture was centrifuged at 1000 rpm for 5 min at 4 °C. Supernatant was discarded and the pellet was resuspended in 1.5 ml 1 x TE/1 x LiAc (1:1) to make the yeast cells competent. For transformation 100 μ l competent yeast cells were mixed with 0.1 μ g plasmid DNA, 0.1 mg salmon testes carrier DNA (#D-9156; Sigma) and 600 μ l PEG/LiAc. The mixture was vortexed and incubated for 30 min at 30 °C and 200 rpm. After incubation 70 μ l DMSO was added and the solution was mixed by gentle inversion. Heat-shock was done at 42 °C for 15 min. After cooling down the cells on ice, they were collected by centrifugation (14000 rpm; 5 sec). The pellet was resuspended in 0.5 ml 1 x TE. 100 μ l of the suspension was plated on each SD agar plate. Plates were incubated up-side-down at 30 °C until colonies appeared. Transformation efficiency was calculated as follows:

$$\frac{cfu \times total\ suspension\ vol. (\mu l)}{vol.\ plated (\mu l) \times dilution\ factor \times DNA\ used (\mu g)} = cfu/\mu g\ DNA$$

2.1.5 Yeast two-hybrid system

The yeast two-hybrid system is a valuable tool for the identification of novel protein-protein interactions. In a Gal4-based system the bait gene is expressed as a fusion to the Gal4 DNA-binding domain, while another gene from a cDNA library is expressed as fusion to the Gal4 activation domain. When bait and library fusion proteins interact, the two domains of Gal4 are brought into proximity, thus activating transcription of several reporter genes (Fig. 2.2). In this study the MATCHMAKER Two-Hybrid System 3 (#630303; Clontech) was used to screen a mouse day 11 embryo cDNA library (#638868; Clontech) for proteins binding to the intracellular domain of Dll1.

2 Methods and Materials

Testing the bait for autonomous reporter gene activation

The bait construct pGBKT7*Dll1*cyto was transformed into the yeast strain AH109 that is *His*, *Ade*, *Trp* and *Leu* deficient. The *Trp* gene on pGBKT7 allowed the positive selection of plasmid containing yeasts. One of the positive clones was streaked out onto SD/-*Trp*, SD/-*His*/-*Trp* and SD/-*Ade*/-*Trp* to test the bait for autonomous activation of the reporter genes *His* and *Ade*. Plates were incubated for four days at 30 °C.

Screening a pretransformed library by yeast mating

A 50 ml culture of pGBKT7*Dll1*cyto in *S. cerevisiae* AH109 was incubated overnight (30 °C and 250 rpm) until the culture exceeded an OD₆₀₀ of 0.8. The culture was centrifuged (10 min, 1000 rpm, 4 °C) and the pellet was resuspended in 5 ml of the remaining supernatant. Meanwhile, 1 ml of the pretransformed cDNA library in the *His*, *Ade*, *Trp* and *Leu* deficient yeast strain Y187 was thawed in a waterbath at room temperature. The vector pACT2 with the *Leu* selection marker has been used for library construction. 10 µl of the library was taken to determine its titer afterwards. Both transformed yeast strains were then cocultivated in a 2 l Erlenmeyer flask with 44 ml YPDA-Kan medium for the formation of diploid cells. Incubation was continued for 24 h at 30 °C and 50 rpm. The next day, the mating mixture was centrifuged at 1000 rpm at 4 °C for 10 min. The pellet was washed twice with 50 ml YPDA-Kan that has been used to rinse the Erlenmeyer flask. Finally the pellet was resuspended in 10 ml YPDA-Kan and the total volume was noted down to be able to estimate the number of clones screened afterwards. The entire suspension was plated in the following way: 100 µl of a 1:10, 1:100, 1:1000 and 1:10000 dilution were spread on SD/-*Trp*, SD/-*Leu* and SD/-*Leu*/-*Trp* plates (Ø 10 cm) to determine the mating efficiency. These plates were incubated for four days at 30 °C. The remaining suspension was spread on large QDO plates (Ø 15 cm) with X-α-Gal at 250 µl per plate. Plates were left at 30 °C for 14 days.

Calculating mating efficiency and number of clones screened

Colonies grown on the SD/-*Trp*, SD/-*Leu* and SD/-*Leu*/-*Trp* plates that had 30-300 cfu were counted. The viable cfu/ml on each type of SD medium was calculated:

$$\frac{cfu \times 1000 \mu l}{vol. plated (\mu l) \times dilution factor} = \# viable cfu/ml$$

cfu/ml on SD/-*Leu* = viability of Y187 partner

cfu/ml on SD/-*Trp* = viability of AH109 partner

cfu/ml on SD/-*Leu*/-*Trp* = viability of diploids

2 Methods and Materials

The obtained values were used for the determination of the mating efficiency:

$$\frac{\#cfu/ml\ of\ diploids}{\#cfu/ml\ of\ limiting\ partner\ (= Y187)} \times 100 = \% Diploid$$

The number of clones screened was estimated in the following way:

$$\#cfu/ml\ diploids \times resuspension\ vol. = \#of\ clones\ screened$$

Plasmid library titering

For the calculation of the library titer the 10 μ l library aliquot was diluted with 1 ml YPDA-Kan medium (dilution A) at first. 10 μ l of dilution A was then added to 1 ml YPDA-Kan (dilution B). 10 μ l from dilution A mixed with 50 μ l YPDA-Kan as well as 50 μ l and 100 μ l aliquots from dilution B were spread onto SD/-Leu plates. After four days incubation at 30 °C colonies on plates with 30-300 colonies were counted. The titer (cfu/ml) was calculated as follows:

$$\frac{\#colonies}{plating\ volume\ (ml) \times dilution\ factor} = cfu/ml$$

Selection and characterisation of interacting proteins

Plasmids were isolated from blue yeast colonies grown on QDO plates with X- α -Gal and transformed into *E. coli* XL1-blue. The bacterial suspensions were plated on LB-Amp medium to rescue the library plasmids only. The library vector pACT2 but not the bait vector pGBKT7 contains the *Amp* resistance gene. Plasmids were isolated from *E. coli* and sequenced. Finally the obtained sequences were compared to those in the NCBI database by BLAST search (www.ncbi.nlm.nih.gov/BLAST/).

2.1.6 Working with RNA

Embryo dissection and fixation

For embryo collection C3HeB/FeJ mice or mice carrying a *DIII*^{lacZ} knock-in-allele (HRABÉ DE ANGELIS et al., 1997) were used. *DIII*^{lacZ} mice were maintained on a mixed 126Sv;C56BL/6J background. For whole mount *in situ* hybridization experiments embryos were fixed in 4 % PFA in DEPC-PBS overnight at 4 °C. The next day, the embryos were dehydrated through 25, 50 and 75 % methanol in DEPC-PBS for 10 min minimum each at 4 °C. Afterwards, the embryos were bleached in 6 % H₂O₂ in methanol for 1 h at 4 °C and again dehydrated in 100 % methanol for 10 min minimum at 4 °C. Embryos were subsequently stored at -20 °C.

2 Methods and Materials

Generation of RNA probes

For generation of DIG labeled *Dll1* (BETTENHAUSEN et al., 1995), *Acvrinpl* and *Magi3* sense and antisense RNA probes from linearised cDNA clones the DIG RNA labeling mix (#1277073; Roche) was used according to the manufacturer's instructions.

Whole mount *in situ* hybridization

For whole mount *in situ* hybridizations the previously described protocol by Spörle and Schughart (SPÖRLE & SCHUGHART, 1998) was modified:

First of all, the embryos were rehydrated through 75, 50 and 25 % methanol in DEPC-PBS for 10 min minimum each on ice. After several washing steps in PBT on ice (2 x 10 min and 1 x 5 min) embryos older than 9 days were treated with proteinase K (10 µg/ml in proteinase K buffer) at room temperature. Incubation time was dependent on the developmental stages: E10 - 1 min, E11 - 5 min, E12 - 8 min. To stop proteinase K digestion embryos were washed with 2 mg/ml glycine in PBT (2 x 5 min) and in PBT (2 x 5 min) on ice. Afterwards, the embryos were incubated in RIPA buffer for 10 min, washed in PBT (2 x 5 min) and fixed for exactly 20 min with 4 % PFA/0.2 % glutaraldehyde in PBT on ice. The embryos were washed again in PBT on ice followed by a 10-minutes incubation in hybe buffer/PBT (1:1) at room temperature. Embryos were washed in hybe buffer for 10 min and prehybridised for 3 h in hybe buffer with 100 µg/ml tRNA at 68 °C. Meanwhile, the DIG labeled RNA probe was denatured at 90 °C for 3 min and stored on ice until usage. Finally, hybridization was performed with a 1:100 dilution of DIG labeled RNA probe in 100 µg/ml tRNA in hybe buffer overnight at 68 °C.

The next day, the embryos were washed with hybe buffer at 65 °C (2 x 30 min). After cooling down the embryos were washed for 5 min each with hybe buffer/RNase solution (1:1) and RNase solution at room temperature. Afterwards, a 60-minutes incubation in 100 µg/ml RNase A in RNase solution at 37 °C was performed to remove the unbound RNA probe. The embryos were then washed in RNase solution/SSC-Fa-T at room temperature (5 min) and in SSC-Fa-T at 65 °C (2 x 5 min, 3 x 10 min and 5 x 30 min). The embryos were again cooled down to room temperature and were washed in SSC-Fa-T/1 x TBST (1:1) (5 min), 1 x TBST (2 x 10 min) and MABT (2 x 10 min) at room temperature. While the embryos were incubated in 10 % blocking reagent (#1096176; Roche) in MABT for 1 h, the anti-DIG-AP antibodies were preadsorbed in a dilution of 1:5000 in 1 % blocking reagent in MABT. The embryos were finally incubated in this antibody solution at 4 °C overnight.

The next day, the unbound antibodies were removed by several washing steps in MABT (3 x 5 min) and TBST (3 x 5 min, 8 x 1 h) at room temperature. Embryos were left in TBST overnight at 4 °C. TBST was changed the next morning. Alkaline phosphatase staining was started in the afternoon. Therefore, the embryos were washed with alkaline phosphatase buffer at room temperature (2

2 Methods and Materials

x 5 min) before they were stained with alkaline phosphatase staining solution at 4 °C in the dark. To stop the staining procedure the embryos were washed in alkaline phosphatase buffer (3 x 10 min) and fixed in 4 % PFA/PBS overnight at 4 °C. In this solution embryos can be stored for years without losing their staining.

2.1.7 Histological techniques and microscopy

Cryosections

For cryopreservation stained embryos from whole mount *in situ* hybridization experiments were incubated in 30 % sucrose/PBS in a falcon tube until they sank to the bottom. Afterwards, the embryos were left in 7.5 % gelatine/30 % sucrose in PBS for 2 h at 42 °C. For hardening embryos were transferred to petri dishes. The embedded embryos were cut out from gelatine, were overlaid with Cryoblock (#41-3020-00; medite Medizintechnik) and sectioned at 35 μ m at -35 °C (Kryostat kompakt CM1850; Leica). Cryosections were finally mounted using Kaiser's Glycerin-gelatine (#1.09242.0100; Merck).

Microscopy

Pictures from stained embryos were taken with the stereo microscope MZ 95 from Leica equipped with a digital camera. For documentation of the Cryosections the Axioplan 2 microscope from Zeiss in combination with a digital camera was used. Contrast and color levels were adjusted with Adobe Photoshop 7, when necessary.

2.1.8 Working with mammalian cells

Storage and growing of HeLa cells

HeLa cells were grown in RPMI 1640 medium (#61870-010; Gibco) containing 10 % FBS (#26140-079; Gibco) and 1 x Penicillin-Streptomycin solution (#15140-122; Gibco) at 37 °C and 5 % CO₂. The confluent culture was splitted 1:4 to 1:6 every 3-5 days using Trypsin-EDTA (#25300-054; Gibco). For long-term storage HeLa cells in the exponential growth phase were collected by centrifugation (3000 rpm, 5 min), resuspended in 1 ml freezing medium (RPMI 1640 medium with 20 % FBS and 10 % DMSO) and transferred to a cryopreservation vial. Cells were slowly cooled down to -80 °C and were finally put into a liquid nitrogen container. To grow stored cells the culture was quickly thawed from -160 °C to 37 °C, cells were collected by centrifugation (3000 rpm, 5 min) and were transferred to a new culture flask containing the appropriate medium.

2 Methods and Materials

Transfection

HeLa cells were grown to 50 % confluency and were transfected with FuGENE 6 Transfection Reagent (#1815091; Roche) according to the manufacturer's protocol.

Mammalian two-hybrid assay

For the verification of the Dll1-Acvrin1 and Dll1-Magi-3 interactions in mammalian cells a mammalian two-hybrid assay was performed three times using the CheckMate Mammalian Two-Hybrid System (#E2440; Promega) according to the manufacturer's protocol (Fig. 2.3). pBIND*Acvrin1* (0.78 μ g) or pBIND*Magi-3* PDZ1-5 (0.52 μ g) coding for a Acvrin1 or Magi-3 fusion protein with the DNA binding domain of Gal4, and pACT*Dll1*cyto (0.48 μ g) coding for a Dll1cyto fusion protein with the transcription activation domain of VP16, were cotransfected with the reporter plasmid pG5-luc (0.4 μ g) into human HeLa cells at equal molar amounts. After 48 hours the cells were lysed. Quantification of luciferase reporter gene expression was done using the Dual-Luciferase Reporter Assay System (#E1910; Promega) according to the manufacturer's instructions. Luciferase activities were measured as triplicate values and normalized to the Renilla luciferase activity of the pBIND vector.

2.1.9 Bioinformatics

Alignments

Amino-acid sequences were aligned using ClustalW (www.ebi.ac.uk/clustalw). Alignments were visualised using BioEdit (www.mbio.ncsu.edu/BioEdit/bioedit.html).

Homology modeling

The ribbon model of the fourth PDZ domain of Acvrin1 complexed with the Dll1 PDZ-ligand was generated by the use of SWISS-MODEL (<http://swissmodel.expasy.org>). SWISS-MODEL is a server for automated comparative modeling of 3D protein structures. First, the amino-acid sequence of Acvrin1 PDZ4 was compared to experimental protein structures stored in the Protein Data Bank (PDB) (<http://www.rcsb.org/pdb/index.html>). Suitable templates with sequence identities above 25 % were automatically selected. Afterwards, the target sequence and templates were superimposed. The created model was visualised using PyMOL (<http://pymol.sourceforge.net/>).

2 Methods and Materials

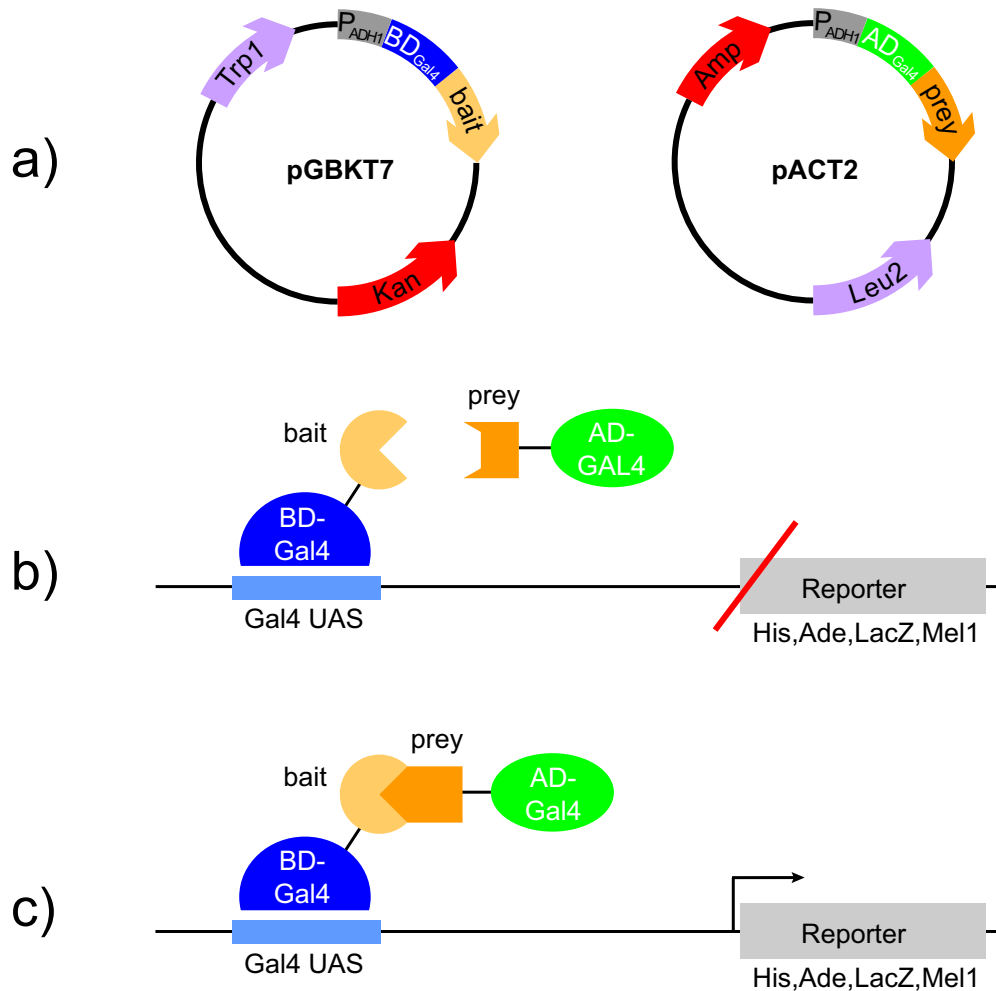


Figure 2.2: The Gal4 yeast two-hybrid system. (a) The bait gene is cloned into pGBKT7 containing a kanamycin resistance gene (Kan) and the *Trp1* nutritional marker. The cDNA library is cloned into pACT2 containing an ampicillin resistance gene (Amp) and the *Leu2* nutritional marker (b) The bait gene is expressed as a fusion to the Gal4 DNA-binding domain (BD-Gal4) binding to upstream activating sequences (UASs) on the yeast chromosome, while the genes from the cDNA library are expressed as a fusion to the Gal4 activation domain (AD-Gal4). If bait and prey are not able to interact with each other, reporter genes are not transcribed. (c) When bait and library fusion proteins interact, BD-Gal4 and AD-Gal4 are brought into proximity, thus activating transcription of the reporter genes His, Ade, LacZ and Mel1

2 Methods and Materials

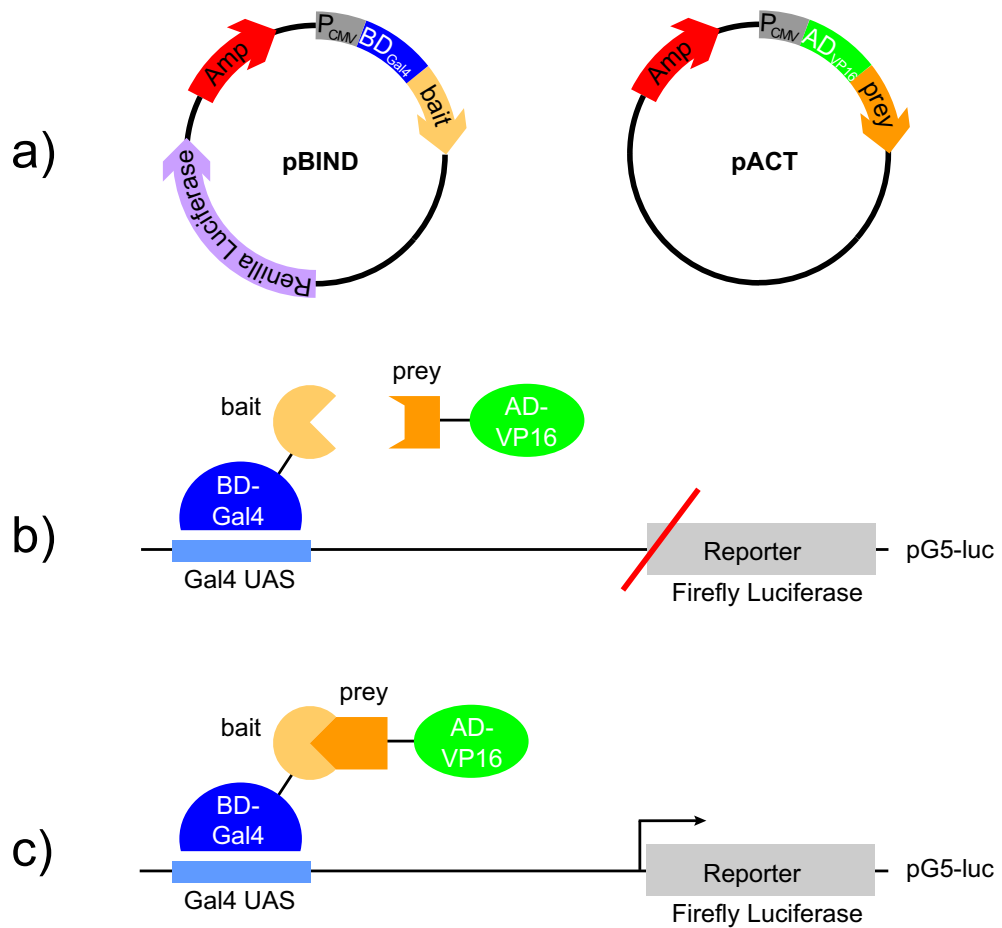


Figure 2.3: The mammalian two-hybrid system. (a) The bait gene is cloned into pBIND containing an ampicillin resistance gene (Amp) and Renilla Luciferase coding sequence that allows the normalization of transfection efficiency. The prey gene is cloned into pACT containing another ampicillin resistance gene. (b) The bait gene is expressed as a fusion to the Gal4 DNA-binding domain (BD-Gal4) binding to upstream activating sequences (UASs) on the pG5-luc plasmid, while the prey gene is expressed as a fusion to the VP16 activation domain (AD-VP16). If bait and prey are not able to interact with each other, reporter genes are not transcribed. (c) When bait and library fusion proteins interact, the BD-Gal4 and AD-VP16 are brought into proximity, thus activating transcription of the Firefly Luciferase reporter

2.2 Materials

Buffers and media

General buffers

- 1 x PBS:
8.4 mM Na₂HPO₄, 1.8 mM NaH₂PO₄, 150 mM NaCl (pH 7.4)

Plasmid isolation from yeast

- S-buffer:
10 mM potassium phosphate pH 7.2, 50 mM β-mercaptoethanol, 10 mM EDTA pH 8.0, adjust to pH 7.5, add 50 μg/μl Zymolase before use
- Lysis buffer:
25 mM Tris-HCl pH 7.5, 25 mM EDTA pH 8.0, 2.5 % SDS, adjust to pH 7.5
- 3 M potassium acetate pH 5.5

Agarose gel electrophoresis

- 10 x TBE:
108 g Tris base, 55 g boric acid, 9.3 g EDTA (pH 8)

Purification of GST fusion proteins

- Lysis buffer:
50 mM Tris-HCl pH 7.8, 500 mM NaCl, 1 mM EDTA
- Lysozyme solution:
50 mg/ml Lysozyme in PBS
- Elution buffer:
10 mM reduced glutathione (#G-4251; Sigma) in 50 mM Tris-HCl pH 8

SDS-PAGE

- Gel buffer:
3 M Tris-HCl pH 8.45, 0.3 % SDS
- Cathode buffer:
100 mM Tris, 100 mM tricine, 0.1 % SDS
- Anode buffer:
200 mM Tris-HCl pH 8.9

2 Methods and Materials

- SDS-sample buffer:
50 % glycerol, 160 mM Tris-HCl pH 6.8, 5 % β -mercaptoethanol, 2 % SDS, 0.02 % bromphenol blue
- Coomassie staining solution:
500 mg Coomassie Brilliant Blue G-280, 200 ml methanol, 5 ml acetic acid, ad 300 ml H₂O

Western blotting

- Blotting buffer:
48 mM Tris, 39 mM glycine, 1.3 mM SDS, 20 % methanol
- 5 x staining buffer:
6.5 mM NaH₂PO₄, 35.7 mM Na₂HPO₄, 0.75 M NaCl, 0.5 M imidazol, 0.25 % Tween-20 (pH 7.5)
- CoCl₂-solution:
10 mg/ml CoCl₂
- Detection buffer:
25 ml 1 x staining buffer, 100 μ l CoCl₂-solution, 10 μ l H₂O₂, 3 mg DAB

Protein concentration measurement

- Solution A:
2 % Na₂CO₃, 0.7 % NaOH, 0.16 % sodium tartrate, 1 % SDS
- Solution B:
4 % CuSO₄ x 5 H₂O
- Solution C:
100 A + 1 B
- Solution D:
Folin-Ciocalteu's phenol reagent/H₂O (1:1)
- BSA standard solution:
0.1 mg/ml BSA (#A-8531; Sigma) in H₂O

GST pull-down assay

- Binding buffer:
100 mM NaCl, 50 mM KH₂PO₄ pH 7.4, 1 mM MgCl₂, 10 % glycerol, 0.1 % Tween-20, 1.5 % BSA (#01400; Biomol)
- Washing buffer:
100 mM NaCl, 50 mM KH₂PO₄ pH 7.4, 1 mM MgCl₂, 10 % glycerol, 0.1 % Tween-20

2 Methods and Materials

Preparation of chemically competent *E. coli*

- TFB1:
30 mM KAc, 100 mM RbCl, 10 mM CaCl₂, 50 mM MnCl₂, 10 % glycerol, adjust pH to 5.8 with KAc, sterile filtrate
- TFB2:
10 mM MOPS, 75 mM CaCl₂, 10 mM RbCl, 15 % glycerol, adjust pH to 6.5 with KOH, sterile filtrate

Transformation into yeast

- 10 x TE buffer:
100 mM Tris-HCl, 10 mM EDTA (pH 7.5)
- 10 x LiAc:
1 M lithium acetate pH 7.5
- PEG/LiAc:
dissolve 3 g PEG in 3.5 ml H₂O at 60 °C, add 750 µl 10 x TE and 750 µl 10 x LiAc

Whole mount *in situ* hybridization

- DEPC-H₂O:
0.01 % DEPC in H₂O, incubate overnight, autoclave
- DEPC-PBS:
0.01 % DEPC in PBS, incubate overnight, autoclave
- PBT:
0.1 % Tween-20 in DEPC-PBS
- Proteinase K buffer:
20 mM Tris-HCl pH 7.5, 1 mM EDTA, autoclave twice
- RIPA buffer:
0.05 % SDS, 150 mM NaCl, 1 % NP40, 0.5 % sodium deoxycholate, 1 mM EDTA, 50 mM Tris-HCl (pH 8.0) in DEPC-H₂O
- Heparin solution:
100 mg/ml heparin (#H3149; Sigma) in DEPC-H₂O
- Hybe buffer:
50 % deionized formamide, 5 x SSC, 0,05 % heparin solution, 0.1 % Tween-20 in DEPC-H₂O, adjust to pH 6 with 1 M citric acid
- tRNA:
10 µg/µl in DEPC-H₂O, phenolise 2 x, store at -20 °C

2 Methods and Materials

- RNase solution:
500 mM NaCl, 10 mM Tris-HCl pH 7.5, 0.1 % Tween-20
- RNase A:
10 $\mu\text{g}/\mu\text{l}$ RNase A in 10 mM sodium acetate pH 7.4, heat to 100 °C for 15 min, cool down to RT, store at -20 °C
- 20 x SSC:
3M NaCl, 300 mM sodium citrate pH 7
- SSC-Fa-T:
2 x SSC, 50 % formamide, 0.1 % Tween-20
- 10 x TBST:
1.36 M NaCl, 26.8 mM KCl, 250 mM Tris-HCl pH 7.5, 1 % Tween-20
- MAB:
100 mM maleic acid, 150 mM NaCl, adjust to pH 7.5 with solid sodium hydroxide
- MABT:
0.1 % Tween-20 in MAB
- Alkaline Phosphatase buffer:
100 mM NaCl, 50 mM MgCl_2 , 100 mM Tris-HCl pH 9.5, 2 mM levamisole, 0.1 % Tween-20
- Staining solution:
Alkaline phosphatase substrate (#1442074; Roche), 2 mM levamisole, 0.1 % Tween-20, centrifuge, use supernatant for staining

Media for bacterial culture

- LB-medium:
10 g NaCl, 10 g bacto-tryptone, 5 g yeast extract, (15 g bacto-agar for plates), add 1 l H_2O
For antibiotic selection add 50 mg/ml ampicillin or kanamycin
For blue-white screening add 2 ml X- β -Gal solution (20 mg/ml in DMF) and 40 μl 1 M IPTG

Media for yeast culture

- YPDA medium:
20 g bacto-peptone, 10 g yeast extract, (25 g bacto-agar for plates), add 960 ml H_2O , autoclave, add 40 ml 50 % glucose (autoclaved), 3 ml 1 % adenine (sterile filtrated)
For matings add 12 mg/l kanamycin

2 Methods and Materials

- SD medium:
6.7 g yeast nitrogen base without amino acids, 0.6 g DO-supplement without adenine, histidine, leucine, tryptophane, (25 g bacto-agar for plates), ad 960 ml H₂O, autoclave, add 40 ml 50 % glucose (autoclaved) add for specific selection:
2 ml 1 % adenine (sterile filtrated)
2 ml 1 % histidine (sterile filtrated)
6 ml 1 % leucine (sterile filtrated)
4 ml 1 % tryptophane (sterile filtrated)
add for α -galactosidase assay: 1 ml X- α -Gal solution (20 mg/ml in DMF)

Vectors

pCRII-TOPO Dual Promoter	(#K4600-40; Invitrogen)
pCR2.1-TOPO	(#K4500-40; Invitrogen)
pGEM T-easy	(#A1380; Promega)
pcDNA3	(Invitrogen)
pcDNA3.1	(Invitrogen)
pGEX Δ BamHI	modified pGEX-2T (LEENDERS et al., 1996)
pGBKT7	(#630303; Clontech)
pGADT7	(#630303; Clontech)
pACT2	(#630303; Clontech)
pBIND	(#E2440; Promega)
pACT	(#E2440; Promega)
pG5-luc	(#E2440; Promega)

Enzymes

Restriction enzymes	(MBI Fermentas)
PfuTurbo DNA-Polymerase	(#600250; Stratagene)
T4-DNA-Ligase	(#M0202S; New England Biolabs)
Taq DNA-Polymerase	(#EP0404; MBI Fermentas)
Lysozyme	(#105281; Merck)
Zymolase	(#L2524; Sigma)
Benzonase	(#E8263; Sigma)
RNase A	(#R4875; Sigma)
Proteinase K	(#1000144; Roche)
T7 RNA-Polymerase	(#EP0111; MBI Fermentas)
RNase Inhibitor	(#EO0311; MBI Fermentas)
DNaseI	(#776785; Roche)

2 Methods and Materials

Bacterial and yeast host strains, cell lines

<i>E. coli</i> BL21-CodonPlus(DE3)-RP	(Stratagene)
<i>E. coli</i> TOP10	(Invitrogen)
<i>E. coli</i> JM107	(Stratagene)
<i>E. coli</i> DH5 α	(Invitrogen)
<i>E. coli</i> XL-1 blue	(Stratagene)
<i>S. cerevisiae</i> AH109	(Clontech)
<i>S. cerevisiae</i> Y187	(Clontech)
HeLa-Human cervix carcinoma	(DSMZ)

Chemicals

General chemicals were obtained in p.a. quality from the companies Merck, Roth, Sigma or Biomol. Ingredients for bacterial and yeast media were purchased from Difco or Clontech

Radiochemicals

³⁵S-Methionine (#AG1594; Amersham Biosciences)

Primers

Oligonucleotides were kindly provided by Utz Linzner or purchased from MWG.

Antibodies

mouse anti-GST	(#13-6700; Zymed)
goat anti-mouse IgG+IgM (H+L) HRP	(#115-035-044; Dianova)
anti-DIG-AP antibodies	(#1093274; Roche)

3 Results

3.1 Sequence analysis

3.1.1 Conserved NLS and PDZ-binding motif in the cytoplasmic part of Dll1

Findings related to the function of the intracellular part of Delta and its homologues are controversial. For example, the expression of intracellular truncated forms of *Drosophila* Delta and Serrate or of *Xenopus* X-Delta-1 have dominant-negative effects (CHITNIS et al., 1995; SUN & ARTAVANIS-TSAKONAS, 1996). In contrast, the deletion of the cytoplasmic part of Lag-2 in *C. elegans* generates a hyperactive protein (HENDERSON et al., 1994).

To find out more about the function of the intracellular part of Delta-like1 (Dll1), the mouse protein sequence was screened for targeting signals and binding motifs. A signal for nuclear localization (NLS) could be identified at amino acids 688-691 (RKRP) of the intracellular C-terminal part (Fig. 3.1). It belongs to the class of monopartite, SV-40 like nuclear localization sites that are characterized by a single cluster of hydrophobic amino acids.

Furthermore, the 4 C-terminal amino acids of Dll1 (ATEV) form a PDZ-binding motif (PSD-95/Dlg/ZO-1). So far four classes of PDZ-binding sites could be identified (FANNING & ANDERSON, 1999; JELEN et al., 2003; NOURRY et al., 2003). The motif found can be assigned to class I that is determined by the consensus sequence X-T/S-X-V/L/I (one letter amino acid code). Both motifs are conserved among Delta homologues from different vertebrate species, suggesting that these domains may be functionally important (Fig. 3.1).

3.1.2 NLS and PDZ-binding motifs in intracellular domains of mouse Delta and Jagged proteins

An alignment of the intracellular domains of the three mouse Delta (Dll1, Dll3, Dll4) and two Jagged (Jag1, Jag2) proteins revealed that NLS and PDZ-binding motifs are present in some but not all murine Notch ligands. Sites for nuclear localization could be identified in the Dll1 sequence and directly after the transmembrane domain of both Jagged homologues. PDZ-binding domains were found in Dll1, Dll4 and Jag1 (Fig. 3.2). In contrast to the identical class I motifs found in the Delta sequences, the Jag1 PDZ-binding ligand (EYIV) belongs

3 Results

DII1 mouse	570	RLKLLQKHQPPPEPCGG	ETETMNNLANCQ	REKDVSVSIIIG
DII1 rat	562	RLKLLQKHQPPPDPCGG	ETETMNNLANCQ	REKDVSVSIIIG
DII1 human	570	RLRLQKHRRPPADPCRG	ETETMNNLANCQ	REKDISVSIIG
C-Delta-1 chicken	578	RLKVVQKRHHQPEACRS	ETETMNNLANCQ	REKDISVSIIG
X-Delta-1 xenopus	571	RVRVQKRRHQPEACRGE	SKTMMNNLANCQ	REKDISVSIIG
DeltaD zebrafish	571	RLKLLQQRSSQIID-SH	SEIETMNNLTTNRS	REKDLISVSIIG
DII1 mouse	609	ATQIKNTNKKADDFHGD	HGAKKSSFKVRYPT	VDYNLVRDLK
DII1 rat	601	ATQIKNTNKKADDFHGD	HGADKSSFKARYPT	VDYNLVRDLK
DII1 human	609	ATQIKNTNKKADDFHGD	HSADKNGFKARYPA	VDYNLVQDLK
C-Delta-1 chicken	617	ATQIKNTNKKVDFHSD	-NSDKNGYKVRYP	PSVDYNLVHELK
X-Delta-1 xenopus	610	TTQIKNTNKKIDFLSE	SNNEKNGYKPRYP	PSVDYNLVHELK
DeltaD zebrafish	610	ATQVKNITNKKVDFQSD	-GDKNGFKSRYS	SLVDYNLVHELK
DII1 mouse	649	GDEATVRDTHSKRDTKC	QSQSSAGEEKIAP	-TLRGG EIPD
DII1 rat	641	GDEATVRDAHSKRDTKC	QSQSSVGEEEKSTS	-TLRGG EVPD
DII1 human	649	GDDTAVRDAHSKRDTKC	QPPQSSGEEKGTPT	TLRGG EASE
C-Delta-1 chicken	656	NEDS-VKEEHGKCEAKC	ETDYSEAEKSAVQL	KSS-DTSE
X-Delta-1 xenopus	650	NEDS-PKEERSKCEAKC	SSNDSDSDEVDNS	VHSKR--DSSE
DeltaD zebrafish	648	QEDLGKEDSERSEATKC	EPLDSDSEEEKHRN	HLSK--DSSE
DII1 mouse	688	RKRPEESVYSTSKDTKY	QSVYVLSAEKDEC	VIATEV
DII1 rat	680	RKRPEESVYSTSKDTKY	QSVYVLSAEKDEC	VIATEV
DII1 human	689	RKRPDSSGCGSTSKDTKY	QSVYVLSAEKDEC	VIATEV
C-Delta-1 chicken	694	RKRPEESVYSTSKDTKY	QSVYVLSAEKDEC	VIATEV
X-Delta-1 xenopus	687	RKRPEESVYSTSKDTKY	QSVYVLSAEKDEC	VIATEV
DeltaD zebrafish	686	RKRTEESLCLC--KDTKY	QSVFVLSAEKDEC	VIATEV

Figure 3.1: Amino-acid sequence comparison of intracellular domains of DII1 homologues from various vertebrate species. Identical amino acids are boxed. Similar residues are shaded in grey. Gaps that were introduced for the alignment are shown as hyphens. Amino-acid positions are indicated on the left. The predicted nuclear localization signal is shaded in blue, the PDZ-binding motif is shaded in green.

DII1	570	RLKLLQKHQPPPEPCGG	ETETMNNLANCQ	REKDVSVSIIIGA		
DII4	555	QLRLRR--PDDE----	SREAMNNLSDFQKD	-----NLIPA		
DII3	514	-----	-----	-----		
DII1	610	TQIKNTNKKADDFHGDH	GAEKSSF-KVRYPT	VDYNLVRDLK		
DII4	584	AQLKNTNQQKELEVDCG	LDKSNCGKLNHTLD	YNLAPGLL		
DII3	514	-RRRGPGQDTGTRLLS	GTREPSVHTL	LPDALNNRLQLQD--		
DII1	649	GDEATVRDTHSKRDTKC	QSQSSAGEEKIAPT	TLRGG EIPD		
DII4	624	G-----RGSM	PGKYP--HSDKSLG	-EKVPLRLHS-EKPE		
DII3	550	G-----	AG-----	DGP		
DII1	688	RKRPEESVYSTSKDTKY	QSVYVLSAEKDEC	VIATEV		
DII4	654	CR--ISAICSPRDSMY	QSVCLISEERNEC	VIATEV		
DII3	557	SS--ADWNHPEDGDS	RSIYVIPAP--SIY	AREEA		
Jag1	1094	RKRKRKPS	SHTHSAPE	DNNTTNNVREQLNQIK	NPIEKHGANT	
Jag2	1109	RKRKRKER	ERSR-LPRDE	STNNQWAPLNPI	IRNPIERP	GGSG
Jag1	1134	VPIKDYENKNSKMSK	IR-----	THNSEVEE	EED	
Jag2	1148	LGTGGHKDILYQCK	NFTPPPRRAGEAL	PGPAGHGAGG	EDE	
Jag1	1160	DMDKHQQKVRFAKQ	PVYTLVDREEKAP	SGTPTKHPN	MTN-	
Jag2	1185	EDEELSRGDGDSPE	AEKFI	SHKFTKDP	SCSLGRPAC	MAPG
Jag1	1199	-KQDNRDLES	AQSLNRMEY	IV		
Jag2	1228	PKVDNR	AVRS	TKDVR	RRAGRE-	

Figure 3.2: Amino-acid sequence comparison of intracellular domains of mouse Delta and Jagged proteins. Identical amino acids are boxed. Similar residues are shaded in grey. Gaps that were introduced for the alignment are shown as hyphens. Amino-acid positions are indicated on the left. Predicted nuclear localization signals are shaded in blue, PDZ-binding motifs are shaded in green.

3 Results

to class II. X-Ψ-X-Ψ (Ψ means hydrophobic amino acid) is the consensus sequence for this group (FANNING & ANDERSON, 1999; JELEN et al., 2003; NOURRY et al., 2003).

3.2 Protein-protein interaction studies

3.2.1 Acvrinp1 and Magi-3 are novel Dll1 binding proteins

In order to isolate proteins binding to the cytoplasmic domain of Dll1 (Dll1_{cyto}), a GAL4-based yeast two-hybrid system was used. Approximately 2.3×10^8 independent clones of a cDNA library of 11 days old mouse embryos were screened with the intracellular part of Dll1 (amino acids 569-722) as bait. After positive selection prey plasmids of the obtained clones were isolated and sequenced. Altogether 15 proteins could be identified (Table 3.1). Two of them are members of the membrane associated guanylate kinase (MAGUK) family. MAGUK proteins consist of a catalytically inactive guanylate kinase (GUK) domain, Tryptophane-rich (WW) or Src-homology 3 (SH3) domains and several PDZ domains. Each of these modules mediates interactions with different proteins. Therefore, MAGUK proteins are able to coordinate the assembly of multiprotein-signaling complexes at specific subcellular sites (FANNING & ANDERSON, 1999; JELEN et al., 2003; NOURRY et al., 2003).

Activin receptor interacting protein 1 (Acvrinp1), also known as Magi-2 (Membrane associated guanylate kinase inverted 2), is one of the PDZ proteins isolated. The obtained clones contained nucleotides 2195-3076 of the Acvrinp1 coding sequence corresponding to PDZ4 and the N-terminal part of PDZ5 of the protein, followed by 18 additional nucleotides that did not belong to the Acvrinp1 sequence (Fig. 3.5a). The other PDZ protein is called Membrane associated guanylate kinase inverted 3 (Magi-3). The isolated Magi-3 clones contained nucleotides 923-1126 coding for the fifth PDZ domain. Both, the Acvrinp1 and Magi-3 clones showed strong induction of reporter genes in yeast, which indicates that the proteins are true interactors of Dll1.

Synaptic scaffolding molecule (S-SCAM) from rat was the first Acvrinp1 homologue that had been previously identified (HIRAO et al., 1998). It has been reported that S-SCAM assembles various components at synaptic junctions (HIRAO et al., 1998; OHTSUKA et al., 1999; IDE et al., 1999; YAO et al., 1999; HIRAO et al., 2000; XU et al., 2001; NISHIMURA et al., 2002; HIRABAYASHI et al., 2004; MEYER et al., 2004). Analyses of *Dll1* mutant embryos in our institute demonstrated that Dll1 plays a crucial role during neurogenesis (G. Przemeck, unpublished results). Therefore, Acvrinp1 was selected for further investigations. Magi-3 was also chosen due to its high structural and amino-acid sequence similarity (46 % identity) to Acvrinp1 (Fig. 3.3).

3 Results

Acvrinp1 Magi-3	1 1	MSKSLKKKSHWT SKVHESV IGRN-PEGQLGFELKGAENGGFPYLGVEK - - - -PGKVAYESGSKLVSEELLLEVNETP MSKTLKKKKHHL SKVQECACVSWAGPPGDLGAE I RGGAEERGEFPYLGRLRDEAGGGGTCV VSGKAPSPGDVLLLEVNGTP
Acvrinp1 Magi-3	74 81	VAGLTI RDVLAV I KHCKDPLRLKCVKQGGIVDKDLRHYLNRFQKGSVDHELQOI RDNLYLRTVPC TTRPHKEGEVPGV VSGLTNRDTLAV I RHFREPI RLKTVKPGKVINKDLRHYLSLQFQKGSIDHKLQQV I RDNLYLRTI PCTTRAPRDGEVPGV
Acvrinp1 Magi-3	154 161	DYIFITVEEFMELEKSGALLESGTYDGNFYGT PKPPAEAPAPLLN - VTDQI LPGA TP SAEGKRKRKNSVTNMEKASIEPPE DYNFISVEQKALEESGALLESGTYDGNFYGT PKPPAEPSFPQDPVDQVLFDFNEFDTESQRKRTTSVSKMERMDSSLPE
Acvrinp1 Magi-3	233 241	EEEE - RPVVNGVVI TPESSEHEDKSAGASGETPSQYPAPVYSQPEELKQMDDTKPTKPEENEDS DPLPDNWE MAY EEEEDEKAVNGSGSMETREM - - HSETSDCWMKT VPS - - - - - YNQTN - - - - SSMDFRNYMMRDEN - - LEPLPKNWE MAY
Acvrinp1 Magi-3	312 307	TEKGEVYFIDHNTKTTSWLDPRLAKKAKPPEECKENELPYGWEKIDDP IYGTYYVDH I NRRTQFENPVLEAKRKLQQHNM TDTGMIYFIDHNTKTTTWLDPRLCKKAKAPEDCEDGELPYGWEKIEDPQYGTYYVDHLNQTQFENPVVEEAKRKKQLG - - * * * * *
Acvrinp1 Magi-3	392 384	PHELGA KPLQAPGFREKPLFTRDASQLKGTFLSTLLKKS NMFGFT I IGGDEPDEF LQVKSVIDGPA A QDGKMETGDV - - - - - QAEI HSAKT DVERAHFTRDPSQLKGLV RASLKKSTMGFGFT I IGGDRPDEF LQVKNVLKDGPA A QDGKIAPGDV ‡
Acvrinp1 Magi-3	472 460	IYVINEVCVLGHTHADVVVKLFQSVP I GQSVNLVLCRGYPLPFDPEDPANS MVPP LAIMERPPV MVNGRHNYETYLEY I S I V D I N G N C V L G H T H A D V V Q M F Q L V P V N Q Y V N L T L C R G Y P L P D D S E D P V D I V A A T P V I N G Q S - - L T K G - - - - E T C M N - - T * * * * *
Acvrinp1 Magi-3	552 532	RTSQSVPI DTRPPHSLHSM PADGQLDGTYPVVHDDNVSMASGATQAE LMTLTI V KGAQGF GFT I A D S P T G Q R V K Q I L QDFKLGAMVLDQNGKSGQ I L A S D - R L N G - - P S E S S E Q R A S L A S S G S S Q P E L V T I P L I K G P K G F G F A I A D S P T G Q K V K M I L ‡
Acvrinp1 Magi-3	632 609	DIQGCPLCEGDL IVEINQQNVQNL SHTEVVD I LKDCPVGSETSL I HRGGFFSPWKT PKPMMDR WENQGSPQ TSLSAPA DSQWCQGLQKGD I KEIYHQNVQNL THLQVVEVLKQ F P V G A D V P L L I R G G P C S P T K A K T K T D T K E N S G S L E T I N - - E P * * * * *
Acvrinp1 Magi-3	712 687	VPQNLFPFPA LHRSSFPDS TEAFDPRKPDPEL YEKSRAI YESRQQVPPRTSFRMDS SSGKPDYKEL DVHLRRMESGFGFR I P Q M P F P P S I R S G S P - - - - - K L D P S E V Y L K S K T L Y E D K P - - - - - P N T K D L D V F L R R K Q E S G F G F R ‡
Acvrinp1 Magi-3	792 743	I L G G D E P G O P I L I G A V I A M G S A D R D G R L H P G D E L V Y V D G I P V A G K T H R Y V I D L M H H A A R N G Q V N L T V R R K V L C G G E P C P E V L G G D G P D Q S I Y I G A I P L G A A E K D G R L R A A D E L M C I D G I P V K G S H K Q V L D L M T T A A R N G H V L L T V R R K I F Y G - E K Q P E * * * * *
Acvrinp1 Magi-3	872 822	NGRSPGSVSTHHSSPRSDYATYSNSNHAAPSSNASPPEGFASHLSQTSDVV IHRKENEGFGFVISSLNRPESGATITVP D - - ESHQAFSQNGSPR - - - - - LNRAELPTRSAPQEA Y - - - - - D V T L Q R K E N E G F G F V I L T S K S K P P P G - - - V I P ‡
Acvrinp1 Magi-3	952 881	HKIGRIDGSPADRC AKLVKVDRI LA VNGQS I NMPHADIVKL I KDAGLSVTLRI PQEELNSPTSA PSEKQSPMAQQH HKIGRVIDGSPADRCGLKVG DHI SAVNGQS I V D L S H D N I V Q L I K D A G V T V T L T V A E E E H H G P P S G T N S A R Q S P - A L Q H
Acvrinp1 Magi-3	1032 960	SPLAQQSPLAQPSPATPNSPV AQPAPPQLQLQGHENS YRSEVKARQDV KPD I RQPF T D Y R Q P P L D Y R Q P P G D Y S Q P P R P M G Q A Q - - - - - A N H I P G D R I A L E G - - - - - E I G R D V C S S Y R H S W S D H K H - - - - -
Acvrinp1 Magi-3	1112 998	PLDYRQHS PDTRQYPLSDYRQPQDFDYFTVDMEKGA KGF GFS I RGGREYKMDLYVLR LAEDGPA I R N G R M R V G D Q I I E I N - - - - - L A Q P D T A V I S V G S R H N Q S L G C Y P V E L E R G P R G F G F S L R G G K E Y N M G L F I L R L A E D G P A I K D G R I H V G D Q I V E I N ‡
Acvrinp1 Magi-3	1192 1074	GESTRDMTHARA I E L I K S G R R R V R L L L K R G T G Q V P E Y G M V P S S L S M C M K S D K H G S P Y F Y L L G H P K D T G E P T Q G I T H T R A I E L I Q A G G N K V L L L R P G T G L I P D H G L A P S G L C S Y V K P E Q H - - - - -

Figure 3-3: Amino-acid sequence alignment of Acvrinp1 and Magi-3. Domains are shown as annotated by Ensemble (www.ensembl.org). PDZ domains are shaded in green, the guanylate kinase domains are shaded in orange and WW domains are shaded in yellow. Asterisks indicate the conserved GLGF motif and histidine typical for class I PDZ domains.

3 Results

Table 3.1: Proteins interacting with Dll1 as identified by two-hybrid screening

gene	symbol ¹	accession number	amino acid residues ²	functions and references
Activin receptor interacting protein 1	Acrinp1	NM_015823	733-1025	Scaffolding molecule at synaptic junctions Interaction with Atrophin-1, a protein containing polyglutamine repeats in patients with the neurodegenerative disorder DRPLA Regulation of activin-mediated signaling by assembly of activin signaling molecules at specific subcellular sites (SHOJI et al., 2000; TSUCHIDA et al., 2001) (HIRAO et al., 1998; OHTSUKA et al., 1999; IDE et al., 1999; YAO et al., 1999; HIRAO et al., 2000; XU et al., 2001; NISHIMURA et al., 2002; HIRABAYASHI et al., 2004; MEYER et al., 2004) (WOOD et al., 1998)
Calstentenin-1	Clstn1	NM_023051	82-259	Modulation of postsynaptic Ca ²⁺ -signaling (VOGT et al., 2001; HINTSCH et al., 2002)
Similar to DNA-binding protein		XM_140546	7-333	unknown
Elastin microfibril interface located protein 1	Emilin1	NM_133918	954-1017	Extracellular matrix glycoprotein involved in elastogenesis and cell adhesion Involved in placenta formation and initial organogenesis (BRESSAN et al., 1993; DOLIANA et al., 1999; COLOMBATTI et al., 2000; ZANETTI et al., 2004) (BRAGHETTA et al., 2002)
Similar to Glutaminyli-tRNA-Synthetase	GlnRS	BC023023	446-548	mRNA translation (CAVARELLI & MORAS, 1993; FREIST et al., 1997)
High mobility group nucleosomal binding domain 2	Hmgn2	NM_016957	1-70	Transcriptional enhancement by modulation of chromatin structure (BUSTIN et al., 1995; PARANJAPE et al., 1995; TRIESCHMANN et al., 1995a; TRIESCHMANN et al., 1995b)
Membrane associated guanylate kinase inverted 3	Magi-3	AF213258	923-1126	Positioning of tumor suppressor PTEN near components of AKT/PTB pathway at epithelial tight junctions Target of oncogenic HPV E6 proteins for proteasomal degradation Positioning of substrates for RPRPβ at the plasma membrane Alteration of subcellular localization of HTLV-1 oncoprotein Tax1 Regulation of JNK signaling as scaffold protein for Frizzled and Ltap Scaffolding molecule at synaptic junctions (THOMAS et al., 2002) (ADAMSKY et al., 2003) (OHASHI et al., 2004) (YAO et al., 2004) (MEYER et al., 2004)

3 Results

gene	symbol ¹	accession number	amino acid residues ²	functions and references
Ribosomal protein S23	Rps23	NM_024175	24-95	Translation (PESTOVA et al., 2001)
Riken cDNA 1110019N10		NM_026753	6-163	unknown
Riken cDNA 2010310H23		AK008561	540-577	unknown
PEST-containing nuclear protein	Penp	XM_132579	1-136	Nuclear protein involved in cell-cycle regulation (MORI et al., 2002; MORI et al., 2004)
Proliferating cell nuclear antigen	Pcna	BC005778	148-260	DNA replication, Okazaki fragment processing, DNA repair, DNA synthesis, DNA methylation, chromatin remodeling and cell cycle regulation (MAGA & HUBSCHER, 2003)
Sidekick 2	Sdk-2	XM_1111104	569-847	Adhesion protein required for pattern formation in the eye of <i>Drosophila</i> (NGUYEN et al., 1997)
Splicing factor serine-rich 2	Sfrs2	NM_011358	118-221	Synaptic adhesion molecule that directs laminar targeting of neurites (YAMAGATA et al., 2002; ABBAS, 2003)
Ubiquitin C	Ubc	NM_019639	13-109 and 796-886	mRNA splicing (FU, 1995; MANLEY & TACKE, 1996) Targeting proteins for degradation (WEISSMAN, 2001)

¹ gene symbols according to The Jackson Laboratory Mouse Genome Informatics database (www.informatics.jax.org), where applicable
² as identified in two-hybrid system

3.2.2 Acvrinp1 and Magi-3 interact with Dll1 *in vitro*

To gather independent evidence for the interaction between Dll1 and Acvrinp1, a direct *in vitro* assay was performed using an ³⁵S-Methionine labeled Acvrinp1 probe and an affinity purified GSTDll1cyto fusion protein. The progress of recombinant protein expression and purification is shown in Fig. 3.4. As expected, Acvrinp1 bound to GSTDll1cyto but not to GST alone (Fig. 3.5b). This result confirms the interaction between Acvrinp1 and Dll1cyto found in the yeast two-hybrid screen.

To delimit the region of Acvrinp1 that is interacting with Dll1cyto, a series of deletion mutants of Acvrinp1 was tested in the *in vitro* system (Fig. 3.5). It was evident that all mutants containing PDZ4 of Acvrinp1 were able to bind to the intracellular part of Dll1, whereas all proteins lacking this domain displayed no interaction. In agreement with the protein part obtained in the yeast two-hybrid screen (Fig. 3.5a) it is likely that PDZ4 of Acvrinp1 is a key domain for binding to Dll1.

To confirm that the PDZ-binding motif of Dll1 is essential for binding to Acvrinp1, the last four C-terminal amino acids of Dll1cyto were deleted (Fig. 3.4) and this mutant was tested for interaction with Acvrinp1 (Fig. 3.7a). As expected, no positive signal could be detected. These results indicate that the association of Dll1 and Acvrinp1 is most likely mediated by binding of the C-terminus of Dll1 to the fourth PDZ domain of Acvrinp1.

The interaction between Magi-3 and Dll1 was tested by *in vitro* pull-down assays, too. Therefore, Magi-3 cDNA coding for PDZ domains 1-5 was amplified from mouse d10 cDNA (Fig. 3.6). The obtained cDNA sequence was translated *in vitro* and labeled with ³⁵S-Methionine. As expected, PDZ domains 1-5 of Magi-3 bound to GSTDll1cyto but not to the truncated form of Dll1 with deleted PDZ-binding domain (Fig. 3.7b). Interaction with the negative control GST was also not observed. The previous two-hybrid screen has shown that PDZ5 of Magi-3 is sufficient for the interaction with Dll1. These results indicate that Dll1 binds to the fifth PDZ domain of Magi-3 via its C-terminus.

3.2.3 Acvrinp1 and Magi-3 bind to Jag1 *in vitro*

To find out if also Jag1 is able to interact with Acvrinp1 and Magi-3, GST pull-down assays were performed. Therefore, the cytoplasmic part of Jag1 was expressed as a GST fusion protein (GSTJag1cyto) in *E. coli* and purified by affinity chromatography (Fig. 3.4). Jag1cyto bound specifically to Acvrinp1 and Magi-3 in the *in vitro* system (Fig.3.7). To examine whether the PDZ-binding domain of Jag1 is involved in the interactions, a truncated Jag1 protein with deletion of the four C-terminal amino acids (GSTJag1ΔPDZ-BD) was prepared (Fig.3.4). As expected, no interactions with Acvrinp1 and Magi-3 could be detected (Fig.3.7). These results demonstrate that Jag1 specifically interacts with Acvrinp1 and Magi-3 *in vitro* via its PDZ-binding domain.

3 Results

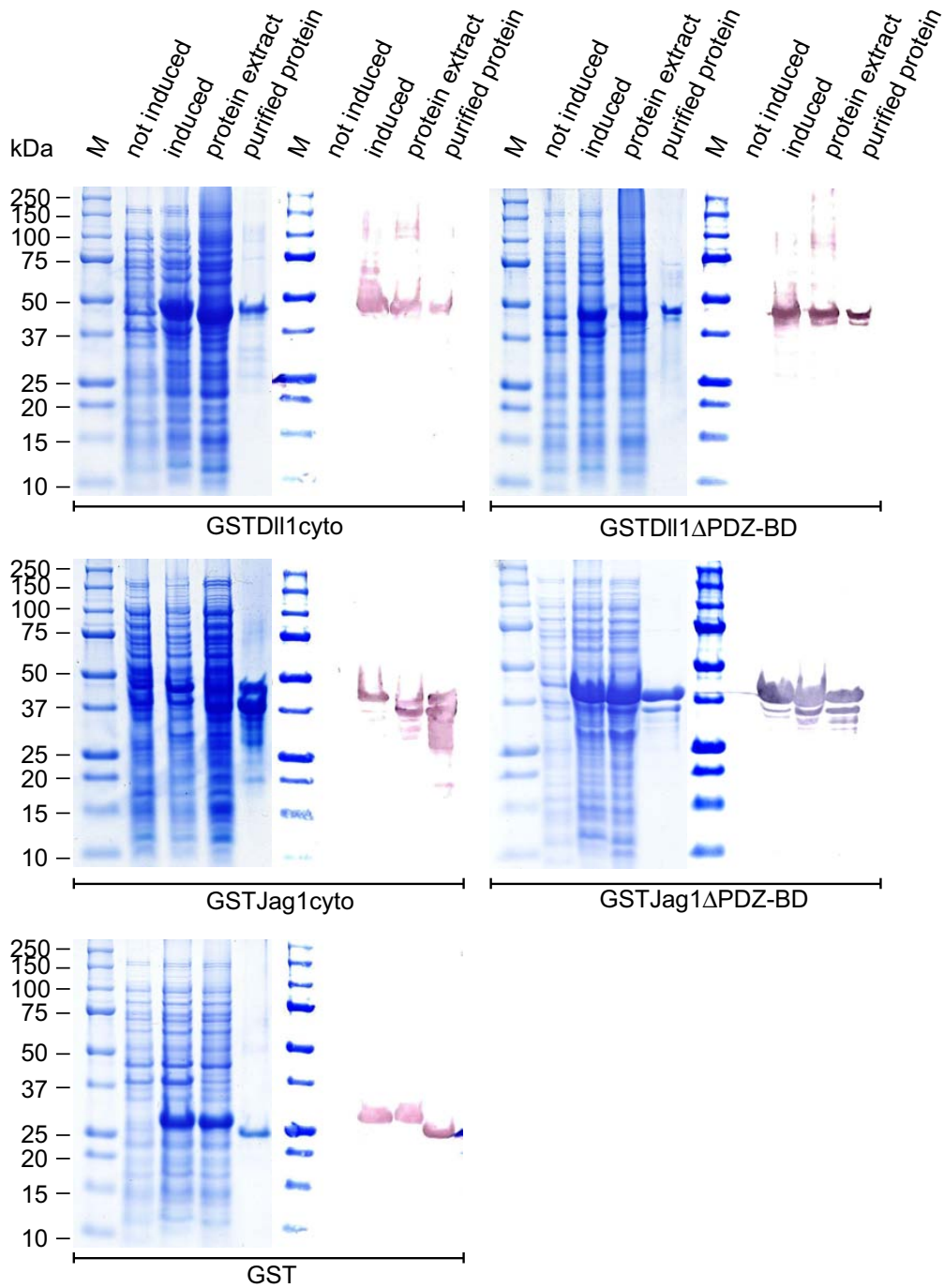


Figure 3.4: Induction and purification of GST fusion proteins. On the left 10 % SDS-PAGE gels stained with Coomassie Brilliant Blue are shown. On the right proteins are detected with an anti-GST antibody by western blotting. GST, GSTDII1cyto, GSTΔPDZ-BD, GSTJag1cyto, GSTJag1ΔPDZ-BD could be overexpressed in the induced *E. coli* BL21 cultures. No basal protein expression could be detected in bacteria that were not induced. All proteins are found in the soluble fraction after protein extraction and could be purified at a concentration of approximately 1 $\mu\text{g}/\mu\text{l}$. The molecular weight of the obtained proteins is in accordance with the calculated values (GST: 29 kDa, GSTDII1cyto: 43.8 kDa, GSTDII1ΔPDZ-BD: 43.4 kDa, GSTJag1cyto: 41.3 kDa, GSTJag1ΔPDZ-BD: 40.8 kDa). Molecular mass markers (M) are shown in kDa on the left.

3 Results

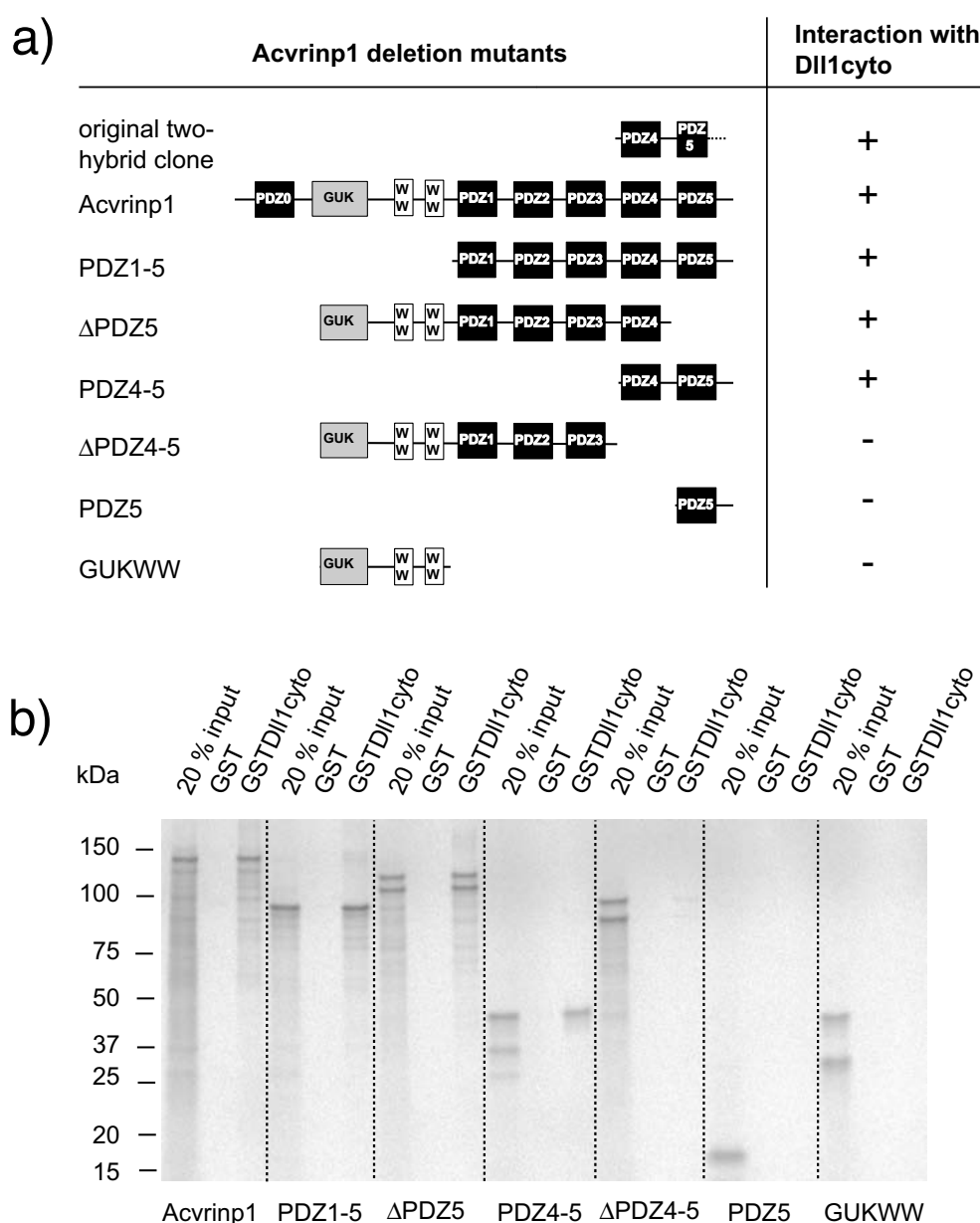


Figure 3.5: Interaction of DII1cyto and Acvrip1 *in vitro*. (a) Schematic illustration of Acvrip1 and the Acvrip1-deletion mutants. GUK domains are illustrated as grey boxes, WW domains as white boxes and PDZ domains as black boxes. The additional amino acids of the original two-hybrid positive clone are shown as dotted line. In the right panel interaction (+) or no interaction (-) with DII1cyto is indicated. (b) Interaction of DII1cyto and Acvrip1 or Acvrip1 deletion mutants as tested by GST pull-down assays. Acvrip1 and the deletion mutants containing PDZ1-5 (PDZ1-5), PDZ4-5 (PDZ4-5) and the mutant with deletion of PDZ5 (Δ PDZ5) were bound by GSTDII1cyto but not by GST alone. The mutants containing the guanylate kinase and WW domains (GUKWW), PDZ5 (PDZ5) and the mutant lacking PDZ 4-5 (Δ PDZ4-5) displayed no interaction with GSTDII1cyto and GST. Acvrip1 probes used for the GST pull-down assays are shown in the left lanes (20% input). Multiple bands represent alternative methionine translation products. Molecular mass markers are shown in kDa on the left.

3 Results

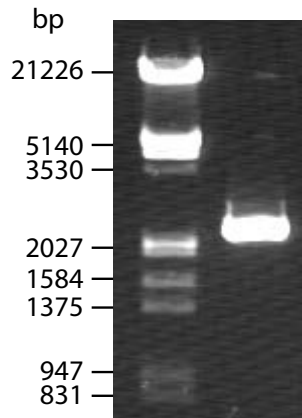


Figure 3.6: Generation of Magi-3 cDNA. A DNA base pair ladder is shown on the left. The 2200 bp PCR product coding for PDZ1-5 of Magi-3 is shown on the right.

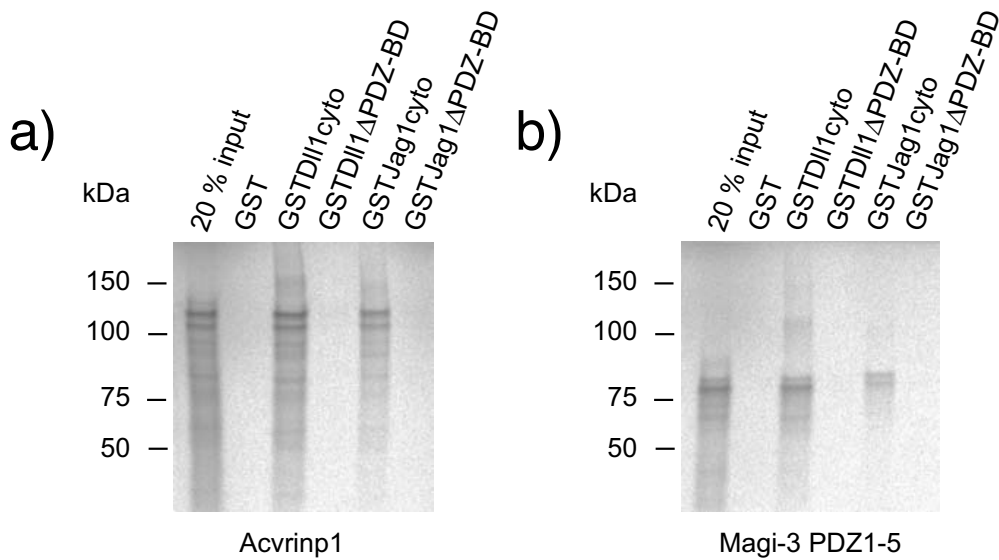


Figure 3.7: Interaction of DII1cyto and Jag1cyto with Acvrip1 and Magi-3 *in vitro*. (a) No interaction could be detected between Acvrip1 and GST (Lane 2), between Acvrip1 and a GSTDII1cyto fusion protein with deleted PDZ-binding domain (GSTDII1ΔPDZ-BD) (Lane 4) and between Acvrip1 and a GSTJag1cyto fusion protein with deleted PDZ-binding domain (GSTJag1ΔPDZ-BD) (Lane 6). Acvrip1 was specifically bound by GSTDII1cyto (Lane 3) and GSTJag1cyto (Lane 5). (b) Magi-3 displayed interaction with GSTDII1cyto (Lane 3) and GSTJag1cyto (Lane 5), but not with GST (Lane 2), GSTDII1ΔPDZ-BD (Lane 4) and GSTJag1ΔPDZ-BD (Lane 6). Acvrip1 and Magi-3 probes used for the GST pull-down assays are shown in the left lanes (20% input). Multiple bands represent alternative methionine translation products. Molecular mass markers are shown in kDa on the left.

3.2.4 Modeling of the Acvrinp1 PDZ4 domain complexed with the PDZ-ligand of Dll1

To get a visual impression on the interaction between the Acvrinp1 PDZ4 domain and the PDZ-ligand of Dll1, a structural model was created via the Swiss-Model server (Fig. 3.8). As characteristic for PDZ domains (FANNING & ANDERSON, 1999; JELEN et al., 2003; NOURRY et al., 2003), the PDZ4 domain of Acvrinp1 forms a partially opened barrel consisting of six β strands (β A to β F). The open sides of the barrel are each capped with an α helix (α A and α B). The N- and C-termini of PDZ domains are usually close to each other indicating that PDZ domains are modular signaling domains (FANNING & ANDERSON, 1999; JELEN et al., 2003; NOURRY et al., 2003). Also the N- and C-terminal residues of the Acvrinp1 PDZ4 domain are in close vicinity. Binding of the PDZ-binding domain of Dll1 occurs as an antiparallel β sheet in an extended groove formed by the β B strand and the α B helix. The C-terminus of ligands usually binds to the so called "carboxylate-binding loop" within this groove (FANNING & ANDERSON, 1999; JELEN et al., 2003; NOURRY et al., 2003). The carboxylate-binding loop contains the conserved sequence K/R-X-X-X-G- Ψ -G- Ψ (Ψ means hydrophobic amino acid), called GLGF motif. The carboxylate of the ligand forms hydrogen bonds with the main chain amides of the last three residues of the GLGF motif and is further coordinated to the R or K residue by a water molecule. The side chain of the ligand at the -2 position is in direct contact with the side chain of the first residue of the α B helix. In class I PDZ domains the α B1 residue is a His. The N-3 nitrogen of the His forms hydrogen bonds to the hydroxyl group of the Ser/Thr residue at the -2 position of type I PDZ ligands (FANNING & ANDERSON, 1999; JELEN et al., 2003; NOURRY et al., 2003). The GLGF motif (R925, G930, F931, G932, F933) as well as the characteristic His residue (H988) could be identified in the amino acid sequence and structure of Acvrinp1 PDZ4 (Fig.3.3 and 3.8). Therefore, the Acvrinp1 PDZ4 domain could be identified as typical class I PDZ domain.

3.2.5 Acvrinp1 and Magi-3 interact with Dll1 *in vivo*

To verify the results obtained in yeast and *in vitro*, the protein interactions between Dll1 and Acvrinp1 and between Dll1 and Magi-3 were tested using a mammalian two-hybrid system. The cytoplasmic part of Dll1 was expressed as a fusion protein with the transcription activation domain of VP16, whereas Acvrinp1 and Magi-3 were present as fusion proteins with the DNA-binding domain of Gal4. Dll1 and Acvrinp1 as well as Dll1 and Magi-3 were transiently expressed in the HeLa cell line and tested for interaction with the help of a luciferase reporter gene. Coexpression of VP16 and Gal4 was used as negative control and should show no activation of the luciferase reporter gene. As expected, a specific interaction of Acvrinp1 and the intracellular domain of Dll1 was observed. Respectively, the relative luciferase activity was increased

3 Results

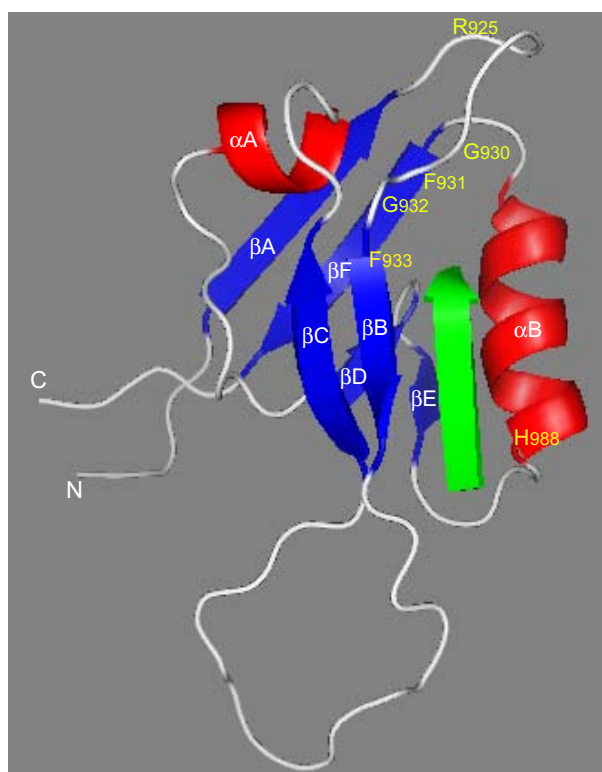


Figure 3.8: Structural model of the Acvrinp1 PDZ4 domain complexed the C-terminal peptide (IATEV) of Dll1: α helices and β strands of Acvrinp1 PDZ4 are shown in red and blue. The PDZ-binding domain of Dll1 is shown in green as a β sheet antiparallel to the β B strand. Numbering of α helices and β strands and the position of N- and C-termini of Acvrinp1 PDZ4 are indicated. Amino-acid residues required for ligand binding are highlighted in yellow.

nearly 13 fold compared to the negative control, whereas cells transfected with Acvrinp1 or Dll1cyto alone exhibited no significant activation of luciferase expression (Fig. 3.9). Only weak (5 fold) increase of luciferase activity was observed after cotransfection of Magi-3 and Dll1cyto, while Magi-3 alone already showed a 2 fold increase in comparison to the negative control. Transfections with the positive control proteins MyoD and Id showed 48 fold activation, which confirms the functionality of the system. These data suggest that at least Acvrinp1 specifically interacts with Dll1 in mammalian cells.

3 Results

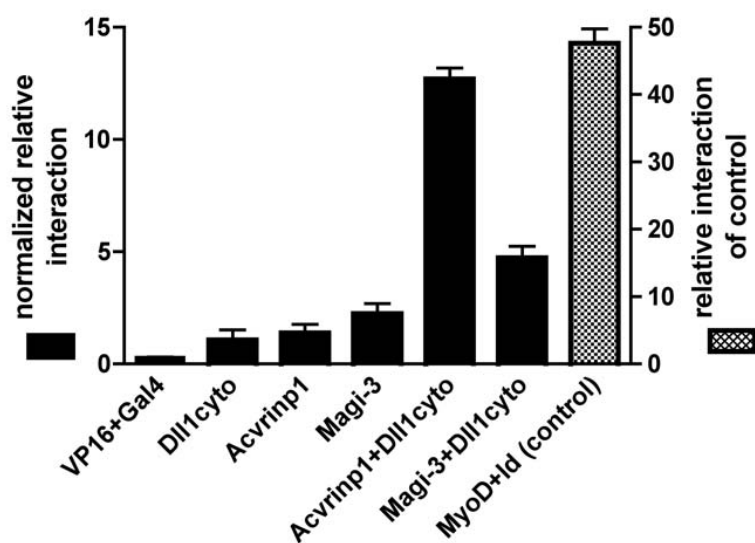


Figure 3.9: Interaction of Dll1cyto with Acvrinp1 and Magi-3 in HeLa cells analyzed using a mammalian two-hybrid system. pBIND*Acvrinp1* or pBIND*Magi-3* PDZ1-5 coding for an Acvrinp1 or Magi-3 fusion protein with the DNA-binding domain of Gal4, and pACT*Dll1cyto* coding for a Dll1cyto fusion protein with the transcription activation domain of VP16, were cotransfected with the reporter plasmid pG5-luc into human HeLa cells. After 48 hours the cells were lysed and luciferase activity was quantified. Interaction levels are shown on the left and right as relative luciferase activities of cell lysates. Values given are the mean of triplicate measurements and are normalized to the Renilla luciferase activity of the pBIND vectors. The value obtained with the negative control was set to 1. Relative luciferase activities after transfection with Acvrinp1, Magi-3 and Dll1cyto or cotransfections are analyzed as indicated. As negative and positive controls cotransfections of VP16 and Gal4 or MyoD and Id are shown.

3.3 Gene expression studies

3.3.1 *Acvrinp1* and *Dll1* are partly coexpressed during embryogenesis

To examine whether *Dll1* and *Acvrinp1* also have overlapping domains of expression in the organism in which they could potentially interact during embryogenesis, whole mount *in situ* hybridizations were performed on mouse embryos from day 8.5 to day 12.5 of gestation (E8.5 to E12.5). During this period, *Dll1* mRNA is expressed in a dynamic pattern, for example, in the paraxial mesoderm, somites, and subsets of cells in the nervous system (Fig. 3.10d-f) (HRABÉ DE ANGELIS et al., 1997; BETTENHAUSEN et al., 1995; BECKERS et al., 1999; MORRISON et al., 1999). At E8.5 *Acvrinp1* expression was not detectable by *in situ* hybridization and only weak signals were found in presumptive neural tissue at E9.5 (Fig. 3.10o and data not shown). At later stages, *Acvrinp1* was expressed in a distinct pattern in developing neural tissues, pharyngeal arches, the genitalia, and in parts of the developing facial region (Fig.

3 Results

3.10a-c, m). The expression of *Acvrinp1* in the developing central nervous system was in some areas similar to the expression of *Dll1* (Fig. 3.10d-f). Cross sections through the neural tube at E11.5 and E12.5 revealed that both *Acvrinp1* and *Dll1* are expressed in the mantle layer of the dorsal neural tube (Fig. 3.10g, h, j, k). The overlapping expression domain includes the region where neural crest cells emerge from the neural tube. Other regions of overlapping expression domains with *Dll1* include the vibrissae primordia, where both genes are expressed in the dermal condensations underlying the epidermis (Fig. 3.10i, l).

3.3.2 *Acvrinp1* expression is upregulated in *Dll1* null mutant embryos

To gain further insight into the relationship of both genes *Acvrinp1* expression was analysed in *Dll1* null-mutant embryos. *Acvrinp1* expression was found to be upregulated in mutant embryos (Fig. 3.10m, n). At E10.5 high transcript levels were detected in regions, which normally express *Acvrinp1* at E11.5 in wild-type embryos (compare Fig. 3.10n with 3.10a). Premature *Acvrinp1* expression was also found at E9.5 in a region where ventral motorneurons emerge (Fig. 3.10o, p).

3.3.3 *Magi-3* and *Dll1* have few common expression domains during embryogenesis

To compare the expression patterns of *Magi-3* and *Dll1* whole mount *in situ* hybridizations were performed on mouse embryos from day 8.5 to day 14.5 of embryonic development. No *Magi-3* transcripts could be detected earlier than E9.5 (data not shown). At E9.5 *Magi-3* was expressed in the eyes, nasal pits and hindgut endoderm lying lateral to the neural tube (Fig. 3.11a, b). *Magi-3* expression in trigeminal and cranial nerves innervating the first and second branchial arch occurs at E9.5 but becomes stronger at E10.5 (Fig. 3.11b, c). At E10.5 and E11.5 additional expression domains include the pharyngeal arches, the developing heart and the fore- and hindlimb buds (Fig. 3.11c, d). At E12.5 and E13.5 *Magi-3* expression becomes visible in the neural tube and the developing snout (Fig. 3.11e, f). In the neural tube, *Magi-3* and *Dll1* are coexpressed in the dorsal region (Fig. 3.11g, j). In addition, *Magi-3* transcripts are detectable in tissue surrounding the vibrissae buds, whereas at the same time *Dll1* is expressed within the follicles (Fig. 3.11h, k). Coexpression of *Magi-3* and *Dll1* could be detected in the eye lens at E14.5 (Fig. 3.11i, l). In contrast to *Acvrinp1*, no differences in the intensity of *Magi-3* expression were observed in *Dll1* null-mutant embryos (compare Fig. 3.11a and b).

3 Results

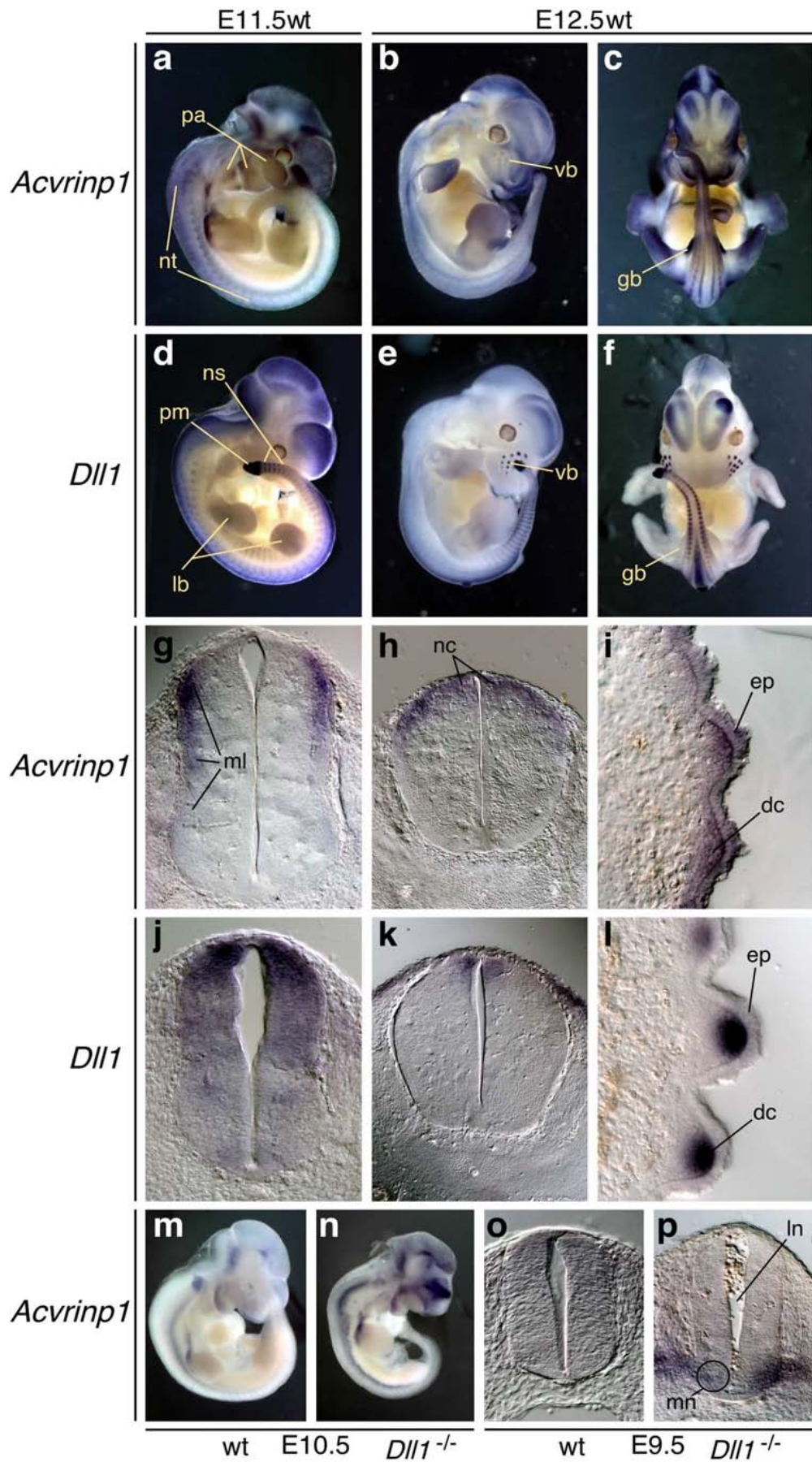


Fig. 3.10

3 Results



Figure 3.10: Comparison of *Acvrinp1* and *Dll1* gene expression. a-f, m, n show whole mount *in situ* hybridizations. g, h, j, k, o, p show cryo-sections at the level of the forelimb bud and i, l cryo-sections of vibrissae buds of whole mount *in situ* hybridized embryos. (a) At E11.5 *Acvrinp1* is expressed in a distinct pattern in the developing nervous system, the pharyngeal arches and in the facial region. (b, c) At E12.5 *Acvrinp1* transcripts are detected in the nervous system, the developing limbs, the vibrissae buds and in the genital bud. (d-f) *Dll1* is expressed in a distinct pattern in the nervous system, the presomitic mesoderm, newly formed somites and in the vibrissae buds. (g) At E11.5 *Acvrinp1* is expressed in the mantle layer of the entire neural tube with stronger expression in the dorsal half. (h) At E12.5 *Acvrinp1* transcripts are present in the dorsal half of the neural tube including the uppermost neural crest region. (i) In the vibrissae buds *Acvrinp1* is expressed both in the epidermal layer and in the dermal condensations. (j) At E11.5 *Dll1* is present throughout the entire neural tube with a stronger expression in the dorsal part including the mantle layer. (k) At E12.5 high transcript levels of *Dll1* exist in the dorsal most part of the neural tube. (l) In the vibrissae buds *Dll1* transcripts are present at high levels in the dermal condensations. (m, n) In *Dll1* null-mutant embryos at E10.5 *Acvrinp1* expression is upregulated, for example, in the neural tube. (o, p) In the neural tube of *Dll1* null-mutants at E9.5 premature *Acvrinp1* expression is present in the region of developing motorneurons. Since *Dll1* null-mutants are haemorrhagic, blood cells are visible in the lumen of the neural tube. Abbreviations: dc, dermal condensations; ep, epidermal layer; gb, genital bud; lb, limb; ln, lumen of the neural tube; ml, mantle layer of the neural tube; mn; region of developing motorneurons; nc, region of neural crest cell emergence; ns, newly formed somites; nt, neural tube; pa, pharyngeal arches; pm; presomitic mesoderm; vb, vibrissae bud.



Figure 3.11: Analysis of *Magi-3* gene expression. a-f, h, i, k, l show whole mount *in situ* hybridizations. g and j show sections through the neural tube at the forelimb bud. (a, b) At E9.5 *Magi-3* is expressed in the hindgut endoderm, the nasal pits and the eyes of wild type and *Dll1* null-mutant embryos. (c, d) At E10.5 and E11.5 *Magi-3* transcripts are detected in the eyes, the nasal pits, the limb buds, the developing heart and the trigeminal and cranial nerves innervating the first and second branchial arches. (e, f) At E12.5 and E13.5 *Magi-3* expression is present in the developing facial region, the limbs and the central nervous system. (g, j) In the neural tube the highest transcript levels of *Magi-3* and *Dll1* exist in the dorsal region. (h, k) In the snout *Magi-3* is expressed in tissue surrounding the vibrissae buds, whereas *Dll1* transcripts are detectable in the follicles. (i, l) At E14.5 *Magi-3* and *Dll1* are coexpressed in the eye lens. Abbreviations: ey, eye; he, heart; hg, hindgut; le, lens; lb, limb; np, nasal pits; nt, neural tube; pa, pharyngeal arches; V, trigeminal nerve; VII, cranial nerve; vb, vibrissae bud

3 Results

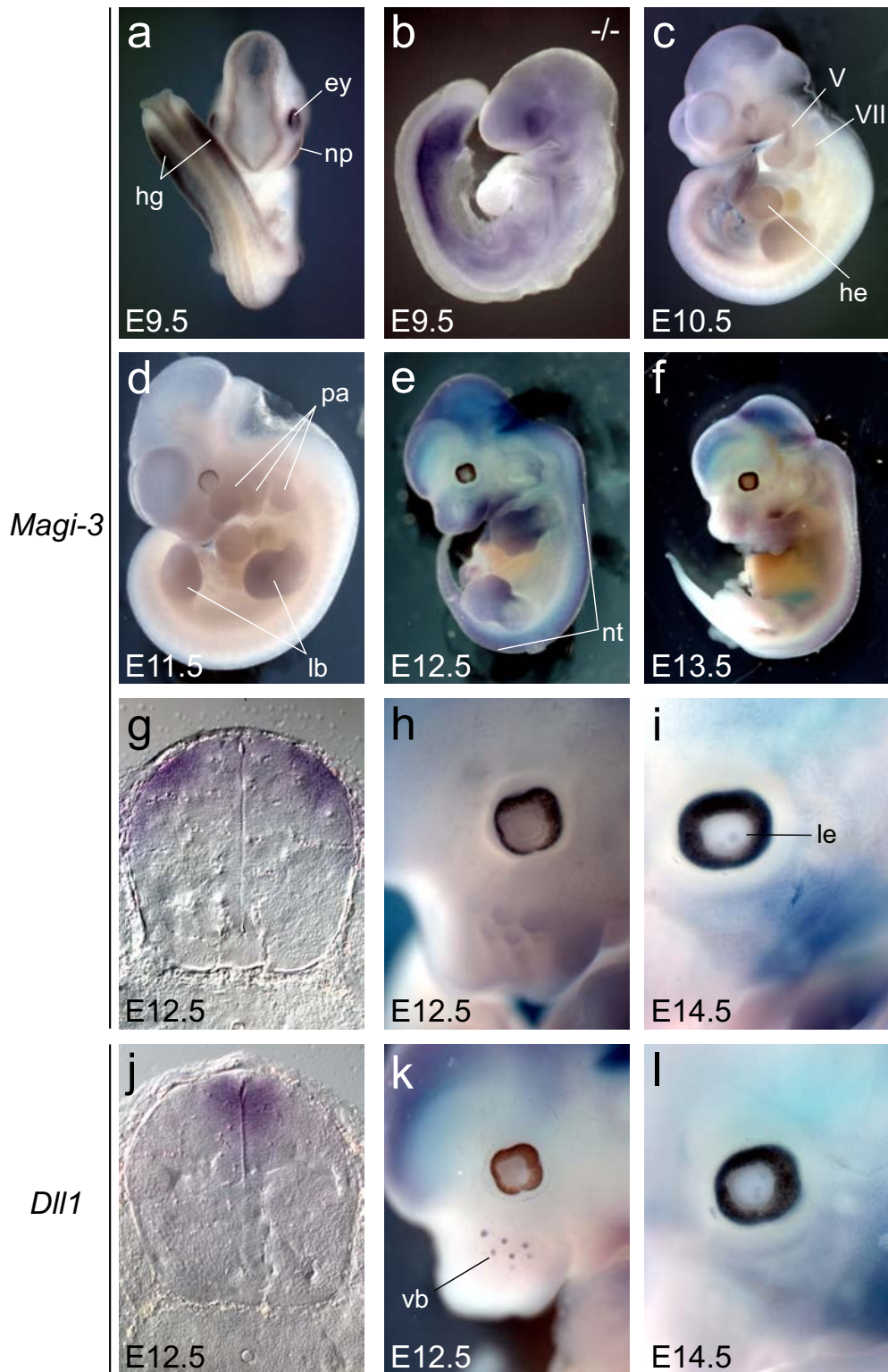


Fig. 3.11

4 Discussion

4.1 Delta-Notch, a bidirectional pathway?

The sequence analyses of DSL ligands described in this thesis indicated that the intracellular domains of Dll1, Jag1 and Jag2 might be able to enter the nucleus. Indeed, it could be shown by other groups that exactly these DSL proteins undergo the same proteolytic cleavages that affect the Notch receptors after ligand binding. Proteolysis occurs first in the extracellular region by an ADAM metalloprotease such as TACE or Kuzbanian, followed by intermembranous cleavage mediated by a presenilin-dependent γ -secretase activity. The sequential cleavages result in the production of soluble intracellular domains which then localize at least in part to the nucleus (BLAND et al., 2003; IKEUCHI & SISODIA, 2003; LAVOIE & SELKOE, 2003; SIX et al., 2003). These findings raise the possibility that intracellular domains of DSL proteins may play a role in nuclear signaling events in the ligand expressing cell and thus implicate a novel intrinsic signaling pathway dependent on the DSL ligand.

Nuclear localization

In this work, PDZ-binding motifs could be identified at the C-termini of Dll1, Dll4 and Jag1. Taking into consideration the described function of PDZ proteins in the assembly of intracellular multi-protein signaling complexes (FANNING & ANDERSON, 1999), it seems reasonable to implicate that interactions of the intracellular domains of DSL ligands with PDZ domain containing proteins may be another trigger for an intrinsic signal. Recent investigations support this idea. It has been reported that neoplastic transformation of RKE cells expressing human Jag1 involves a PDZ protein dependent signaling into the Jag1 expressing cell (ASCANO et al., 2003). Moreover, it has been suggested that the inhibitory influence of Dll1 on cell motility is mediated by a PDZ dependent mechanism (LOWELL & WATT, 2001; SIX et al., 2004). Both, nuclear localization of the cytoplasmic domain and the ability to interact with PDZ proteins, indicate that DSL proteins may have two distinct functions: (1) as ligands to initiate Notch signaling in neighboring cells and (2) as receptors to initiate an intrinsic PDZ-dependent signaling mechanism. Such a mode of signaling has recently been discovered in the ephrin/Eph pathway, indicating that at least in some developmental context signaling is bidirectional (KULLANDER & KLEIN, 2002).

Interaction with PDZ proteins

Bidirectional signaling?

In addition, the existence of different combinations of NLS and PDZ-binding motifs may be a reason for the observed functional differences between the DSL ligands and may account for the functional diversity of Notch signaling.

Functional differences of Notch ligands

4 Discussion

Table 4.1: Existence of NLS, PDZ-binding domains (PDZ-BD) and Fringe-dependent inhibition of vertebrate DSL ligands

	NLS	PDZ-BD	Fringe
Dll1	+	+	-
Dll3	-	-	-
Dll4	-	+	-
Jag1	+	+	+
Jag2	+	-	+

Different temporal and spatial expression and the inhibitory influence of Fringe proteins on Jagged rather than Delta proteins may contribute to this diversity (Tab. 4.1). In the present study Acvrinp1 and Magi-3 have been identified as novel Dll1 and Jag1 binding proteins. Recently, it has been shown that Dlg-1 (discs large 1) is able to interact with Dll1 *in vitro* and *in vivo*, whereas no interaction of Dlg-1 with Jag1 could be detected (SIX et al., 2004). Moreover, *in vitro* interaction of Dll1, but not Jag1, with Scribble was observed in our institute (C. Höfer, unpublished results). On the other hand, the ras-binding protein AF6 was found to be specifically associated with Jag1 in a direct yeast two-hybrid assay (HOCK et al., 1998; ASCANO et al., 2003). The observation that Dll1 and Jag1 partly interact with distinct PDZ proteins might provide another explanation for the functional differences of Notch ligands.

4.2 Acvrinp1 and Magi-3 are novel components of Delta-Notch signal transduction

In the present study, Acvrinp1 and Magi-3 were identified as novel Dll1 binding proteins in a yeast two-hybrid approach. The fact that the interactions could be confirmed *in vitro* by GST pull-down assays strongly supports their specificity. The interaction between Acvrinp1 and Dll1 could even be shown *in vivo* in a mammalian two-hybrid system whereas the association of Magi-3 and Dll1 was found to be too weak for strong activation of the luciferase reporter. In addition, the interaction of Dll1 with Acvrinp1 and Magi-3 has later been confirmed by an independent group (WRIGHT et al., 2004). Wright et al. isolated all three known MAGI proteins, Magi-1, Acvrinp1 (also known as Magi-2) and Magi-3 from an adult mouse whole brain lysate using a C-terminal peptide of human Dll1.

Interactions are specific

Processes mediated by Acvrinp1 and Magi-3 are typical for MAGUK proteins: Synaptic scaffolding molecule (S-SCAM) from rat was the first Acvrinp1 homologue previously identified (HIRAO et al., 1998). It has been reported that

Functions

4 Discussion

S-SCAM acts as scaffolding molecule at synaptic junctions (HIRAO et al., 1998; OHTSUKA et al., 1999; IDE et al., 1999; YAO et al., 1999; HIRAO et al., 2000; XU et al., 2001; NISHIMURA et al., 2002; HIRABAYASHI et al., 2004; MEYER et al., 2004). Moreover, Acvrinp1 was implicated in the regulation of activin-mediated signaling by assembly of activin signaling molecules at specific sub-cellular sites (SHOJI et al., 2000; TSUCHIDA et al., 2001). The positioning of tumor suppressor PTEN near components of the AKT/PTB pathway is supported by Acvrinp1 and Magi-3 as well (WU et al., 2000a; TOLKACHEVA et al., 2001; VAZQUEZ et al., 2001; WU et al., 2000b). The results of recent investigations indicate that Magi-3 positions substrates for RPTP β at the plasma membrane (ADAMSKY et al., 2003) and plays a role in the regulation of JNK signaling as scaffold protein for Frizzled and Ltap (YAO et al., 2004). Recently, Magi-3 has also been detected at synaptic junctions (MEYER et al., 2004). The identification of two such scaffolding molecules as intracellular Dll1 binding proteins leads to the assumption that Dll1 might mediate an intrinsic signal transduction pathway dependent on Acvrinp1 and Magi-3.

The performed GST pull-down assays revealed that the PDZ-binding domain of Dll1 mediates the interaction with Acvrinp1 and Magi-3. The fourth PDZ domain of Acvrinp1 could be identified as major interacting domain. The presented structural model revealed that the association of Acvrinp1 PDZ4 and Dll1 is an interaction between a class I PDZ domain and a class I PDZ-ligand. The fifth PDZ domain of Magi-3 was found to be sufficient for the interaction with Dll1 in yeast. Interactions of Dll1 with other PDZ domains of Magi-3 have not been tested and can therefore be not excluded. Wright et al., for example, suggested that an interaction of Dll1 with PDZ4 of Magi-3 will also be likely possible since the fourth PDZ domains of all members of the MAGI protein family are conserved (WRIGHT et al., 2004). The interactions of Jag1 with Acvrinp1 and Magi-3 *in vitro* were found to be dependent on the PDZ-binding domain of Jag1. Nevertheless, this is surprising as interactions of type II PDZ binding motifs with type I PDZ domains have not been described to date. Therefore, the classification of PDZ-binding motifs and PDZ domains might have to be reconsidered.

Interacting domains

4.3 Common function of Acvrinp1 and Dll1 in neurogenesis and follicle formation?

The described expression analysis revealed that *Acvrinp1* is partly co-expressed with *Dll1* in the vibrissae primordia during mouse embryonic development. It has been reported that Dll1 plays a predominant role in the segregation of mesenchymal cells forming the dermal condensations of vibrissae follicles (FAVIER et al., 2000). The overlapping expression domains of *Acvrinp1* and *Dll1* in the developing nervous system include the region of neural crest cell emergence in the dorsal neural tube. It has been already described that

Common and independent functions

4 Discussion

Dll1 has essential functions in the migration and differentiation of neural crest cells (DE BELLARD et al., 2002). Also, *Acvrin1* has been implicated in neuronal processes. Several groups reported that *Acvrin1* functions as scaffolding molecule to assemble various components at synaptic junctions (HIRAO et al., 1998; OHTSUKA et al., 1999; IDE et al., 1999; YAO et al., 1999; HIRAO et al., 2000; XU et al., 2001; NISHIMURA et al., 2002; HIRABAYASHI et al., 2004; MEYER et al., 2004). Therefore, *Acvrin1* may be essential for the ability of the nervous system to remodel its connections in order to adjust the organism in response to changing conditions, referred to as "synaptic plasticity". The observed regional and temporal coexpression indicate that *Acvrin1* and *Dll1* cooperate during neurogenesis and follicle formation.

It is remarkable that the expression patterns of *Acvrin1* and *Dll1* are not completely overlapping. *Dll1* is, for example, highly expressed in the presomitic mesoderm and in somites, whereas *Acvrin1* mRNA was absent in these tissues. On the other hand, strong expression of *Acvrin1* could be detected in the genital buds where *Dll1* is not expressed. In addition, interactions of *Acvrin1* with several proteins, other than *Dll1*, have been observed. These include, for example, Atrophin-1, the tumor suppressor PTEN and Activin receptor type IIA (WOOD et al., 1998; SHOJI et al., 2000; TSUCHIDA et al., 2001; WU et al., 2000a; TOLKACHEVA et al., 2001; VAZQUEZ et al., 2001). A connection between the Delta-Notch pathway and these molecules has not been reported so far. These findings implicate that *Acvrin1* and *Dll1* have common functions as well as functions that are independent from each other.

Comparing expression patterns of *Acvrin1* in wild type and *Dll1* loss-of-function mouse embryos, an upregulation of *Acvrin1* transcription was found. One reason of this might be a direct influence of *Dll1* on *Acvrin1* transcription. On the other hand, *Acvrin1* might be expressed in tissues that differentiate prematurely in *Dll1* knock-out mice. A premature neuronal differentiation has been already observed in these mutants (G. Przemec, unpublished results).

Dll1
regulates
Acvrin1
expression

4.4 Common function of *Magi-3* and *Dll1* in neurogenesis and eye development?

Comparison of *Magi-3* and *Dll1* expression patterns revealed that both genes are expressed in the dorsal part of the neural tube at E12.5 and in the eye lenses at E14.5. These data indicate that *Magi-3* and *Dll1* have a common function in neuronal development and formation of the eye. Expression of *Magi-3* in the lenses of neonatal mice has already been shown (NGUYEN et al., 2003).

In contrast to *Acvrin1*, the intensity of *Magi-3* expression was not increased in *Dll1* loss-of-function mutants, which suggests that the expression of *Magi-3* is independent from *Dll1*.

Magi-3
expression is
independent
from *Dll1*

4.5 Influence of Dll1 on cell adhesion and motility

Dll1 is highly expressed in human keratinocytes. These stem cells signal, via the conventional Notch signaling pathway, to neighboring cells to make them differentiate into transit amplifying cells (LOWELL & WATT, 2001). In addition, *Dll1* promotes the cohesiveness of these stem cells either by an inhibition of cell motility and/or by promoting cell adhesion. Interestingly, the effect of *Dll1* on cell cohesiveness is dependent on its intracellular domain including the PDZ-binding motif but is independent from Notch activity (LOWELL & WATT, 2001). Motility was also found to be reduced in mouse embryo fibroblast cells (3T3) stably transfected with *Dll1*. Deletion of the PDZ-binding motif completely abolished this inhibitory effect but had no influence on Notch activation (SIX et al., 2004). Recently, it has been reported that zebrafish embryos injected with a splice-blocking morpholino that deprives DeltaD of its C-terminal valine show mislocalization of primary sensory neurons in the dorsal part of the neural tube, the Rohon-Beard neurons (WRIGHT et al., 2004). This observation suggests that the interaction of DeltaD with PDZ proteins regulates the migration of Rohon-Beard neurons and possibly other neurons in the neural tube. Again, Notch signaling was unaffected by disruption of the PDZ-binding domain. These different lines of evidence strongly indicate that the interaction of *Dll1* with PDZ proteins influences cell adhesion and cell motility independent from Notch activation. There are several possibilities for the underlying molecular mechanism: (1) The *Dll1*-PDZ complex associates with cortical actin and might regulate the reorganisation of the actin cytoskeleton to form lamellipodia and filopodia during cell migration (LOWELL & WATT, 2001). (2) *Dll1* might promote cellular adhesion by recruitment of PDZ proteins to sites of cell-cell contacts. Thereby protein complexes could be formed that are involved in the establishment of cell-cell junctions (SIX et al., 2004). (3) The *Dll1*/PDZ complex might exert its effect on cell adhesion and motility by regulating gene expression cell-autonomously (IKEUCHI & SISODIA, 2003; LAVOIE & SELKOE, 2003; SIX et al., 2003). The fact that the PDZ-binding domain of *Dll1* is not needed for Notch activation is not too surprising because several DSL proteins lacking the PDZ-binding motif have been shown to be effective Notch ligands (DUNWOODIE et al., 1997; LUO et al., 1997).

Mechanism?

4.6 Delta-Notch and Planar Cell Polarity

The establishment of cellular polarity is a crucial step in the development of epithelial tissues. In addition to apical/basal polarity, the epithelial cells of many tissues are also polarized along an axis that is orthogonal to the apical/basal axis. This form of epithelial polarity is known as planar cell polarity (PCP) or tissue polarity (FANTO & MCNEILL, 2004). A key for the development of

4 Discussion

planar polarity is the evolutionary conserved PCP pathway. In *Drosophila* PCP signaling is required for the regular arrangement of ommatidia in the eye, the formation and directionality of hairs in the wing and the arrangement of sensory bristles in the thorax (ADLER, 2002). The molecular mechanism of PCP signaling has not been completely elucidated. However, several PCP pathway components have been identified, among them the Wnt receptor Frizzled and Dishevelled, a cytoplasmic protein required for Frizzled signal transduction (FANTO & MCNEILL, 2004). The involvement of Frizzled and Dishevelled indicates an overlap with the canonical Wnt signaling pathway. However, PCP does not involve the downstream components of the canonical Wnt pathway, such as β -catenin and LEF/TCF but seems to be rather mediated by small GTP-ases and a cascade of mitogen-activated protein (MAP) kinases from the JNK (Jun N-terminal kinase) family. Therefore, the PCP pathway is also called non-canonical Wnt pathway (FANTO & MCNEILL, 2004).

A cross-talk between the Delta-Notch and PCP pathway has already been described during patterning of the compound eye in *Drosophila* (TOMLINSON & STRUHL, 1999). The *Drosophila* eye is composed of several hundred ommatidia that exist in two chiral forms, depending on the position at the ventral or the dorsal half of the eye. Each ommatidium contains 8 photoreceptor cells. Chirality is specified by an extracellular gradient of a Frizzled activating ligand from the dorsoventral midline (the equator) to the poles of the eye. Therefore, the cell of the R3/R4 pair of presumptive photoreceptor cells, which is closest to the equator, has the highest Frizzled activity and takes the R3 fate, whereas the other cell adopts the R4 fate. The initially small difference in Frizzled activity leads to high Delta activity in the presumptive R3 and high Notch activity in the presumptive R4 cell, stabilising the cell fate decision. As consequence, the R4 cells move asymmetrically relative to the R3 cells initiating the appropriate chiral pattern of the remaining cells of the ommatidium (TOMLINSON & STRUHL, 1999). How Delta and Notch activity is directed by PCP signaling components remains to be further elucidated.

The vertebrate equivalent of the PCP pathway has been implicated in neural tube closure and convergent extension cell movements during gastrulation and has been found to be responsible for the polarised orientation of stereociliary bundles in the inner ear (WALLINGFORD et al., 2000; WALLINGFORD & HARRLAND, 2002; CURTIN et al., 2003; MONTCOUQUIOL et al., 2003).

So far, a connection between the PCP and Delta-Notch pathway has not been described in vertebrates. Recently, it has been reported that Magi-3 functions as a scaffold for Frizzled-4 (Frz-4) and Ltap (loop tail associated protein) to activate the PCP pathway via JNK (YAO et al., 2004). Ltap has been genetically linked to the LAP (leucine-rich repeat and PDZ domain) family member *Scribble* (MURDOCH et al., 2001; MURDOCH et al., 2003). It has been speculated that the molecular basis of this genetic interaction might be a direct protein-protein interaction between the PDZ-binding domain of Ltap and one or several of the 4 PDZ domains of Scribble. Interestingly, *Dll1*, Ltap and

Cross-talk in Drosophila

Cross-talk in vertebrates?

4 Discussion

Scribble are partly coexpressed in mouse embryos, for example, in the neural tube excluding the floor-plate region, in the cochlea of the inner ear and in vibrissae buds. Also, the phenotypes of *Ltap* (*loop-tail*), *Scribble* (*circletail*) and *Dll1* loss-of-function mouse embryos are similar in some respect. An irregular segmentation of somites, an enlarged floor-plate and an abnormal inner ear development could be identified in all the three mutants (GREENE et al., 1998; MURDOCH et al., 2001; KIBAR et al., 2001; MURDOCH et al., 2003; HRABÉ DE ANGELIS et al., 1997; PRZEMECK et al., 2003; MORRISON et al., 1999). The identification of Magi-3 as component of Delta-Notch and PCP signaling and the similarity of expression patterns and mutant phenotypes is a first indication of a cross-talk between the two pathways during embryogenesis of vertebrates. In addition, the expression of *Notch1* was found to be downregulated in the presomitic mesoderm of *Ltap* mutants, suggesting that the proper expression of Notch1 is dependent on *Ltap* (GREENE et al., 1998). Furthermore, immunohistochemical analyses revealed that the expression of *Scribble* is modified in *Dll1* null mutant embryos, which indicates that *Dll1* influences the expression of *Scribble* (G. Przemeck, preliminary results).

Recently, it could be shown in our institute by *in vitro* pull-down assays and coimmunoprecipitation experiments that *Dll1* is able to interact with *Scribble* (C. Höfer, unpublished results). *Scribble* has been genetically linked to another PDZ protein, *Dlg*, during the establishment of cell polarity in developing epithelia in *Drosophila* (BILDER et al., 2000). Moreover, *Dlg* has been physically linked to *Scribble*. Coimmunoprecipitation analyses revealed that *Dlg* and *Scribble* are held together by the adapter protein GUK-holder at the neuromuscular junction of *Drosophila* forming a tripartite complex (MATHEW et al., 2002). The observed colocalization of human *Scribble* and mammalian *Dlg* in MDCK cells strongly suggests the conservation of the physical linkage in mammals (DOW et al., 2003). Interestingly, *Dlg-1* has been identified as novel protein interacting with the C-terminal PDZ-binding motif of *Dll1* but not *Jag1* (SIX et al., 2004). Also, the expression patterns of *Dll1* and *Dlg-1* are partly overlapping during embryonic development, for example, in neural tissue, the presomitic mesoderm and somites (CARUANA & BERNSTEIN, 2001). It's an interesting idea that *Dll1*, *Magi-3*, *Ltap*, *Scribble* and *Dlg-1* might be components of a multiprotein signalling complex regulating cell polarity (Fig. 4.1). Due to the high structural and sequence similarity of *Magi-3* and *Acvrinp1*, *Acvrinp1* might be able to replace *Magi-3* to regulate PCP signaling.

4.7 Novel *Dll1* binding proteins

Besides *Acvrinp1* and *Magi-3*, other novel *Dll1* binding proteins could be identified in the presented yeast two-hybrid assay. Among them were several proteins that have been already described as typical false-positives, namely Glutaminyl-tRNA-Synthetase (*GlnRS*), Riboso-

False-positives

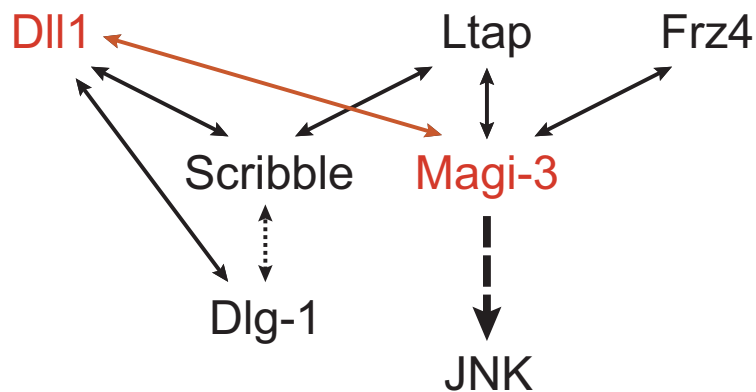


Figure 4.1: Model of JNK activation by Magi-3. Dll1 might be recruited to a multi-protein signaling complex regulating PCP signaling by interactions with the PDZ domain containing proteins Magi-3, Scrib and Dlg-1. Solid arrows indicate direct protein-protein interactions. Indirect interaction between Scrib and Dlg-1 via a so far unknown adapter protein is shown as dotted line. Activation of the JNK signaling cascade is indicated as fat dashed arrow.

mal protein S23 (Rps23), Proliferating cell nuclear antigen (PCNA), Splicing factor arginine/serine-rich 2 (Sfrs2) and Ubiquitin C (Ubc) (<http://www.fccc.edu/research/labs/golemis/InteractionTrapInWork.html>).

False-positives activate reporter gene activity where no protein-protein interaction is involved.

The performed yeast two-hybrid assay revealed also an interaction of Dll1 with the extracellular matrix glycoprotein Elastin microfibril interface located protein 1 (Emilin-1) and the synaptic adhesion molecules Calsyntenin-1 (Clstn1) and Sidekick 2 (Sdk-2). Nevertheless, a physical association is very unlikely as the determined binding domains of these proteins lie outside the cell.

Two of the isolated positive yeast clones contained RIKEN cDNA sequences (1110019N10 and 2010310H23) with unknown function. Further analyses of the corresponding protein sequences with respect to conserved domains and binding motifs might provide valuable informations about the function of the unknown proteins in context with Delta-Notch signaling.

Novel interactors

The association of Dll1 with nuclear proteins, like High mobility group nucleosomal binding domain 2 (Hmgn2), PEST-containing nuclear protein (Pcnp) and a so far unknown DNA-binding protein, supports the theory that Dll1 is involved in nuclear signaling events in the ligand expressing cell.

4.8 Outlook

This thesis at hand gives a first insight into the function of the intracellular domains of DSL proteins. *Acvrinp1* and *Magi-3* were identified as novel components of the Delta-Notch pathway. Now the challenge is to elucidate the function of these proteins in context with Delta-Notch signaling.

The results of the presented expression analyses indicate that the interactions of *Dll1* with *Acvrinp1* and *Magi-3* are of significance for embryonic development, for example, during neurogenesis and follicle morphogenesis. To further characterize the function of these interactions *Acvrinp1*, *Magi-3* and the PDZ-binding domain of *Dll1* could be disrupted by gene targeting (knock-out) or gene silencing by RNAi (knock-down) in mice. Comparison of the loss-of-function mutant phenotypes should give a deeper insight into the requirement of the observed interactions for proper embryonic development. In addition, whole mount *in situ* hybridizations with Notch pathway genes could show if the absence of *Acvrinp1*, *Magi-3* or the *Dll1* PDZ-binding motif has any influence on Notch activation and signal transduction.

*Knock-out,
knock-down*

Informations concerning the subcellular localization of the proposed *Dll1*/PDZ complex could be useful to find out more about the influence of *Dll1* on cell polarity. Therefore, transfected or stable cell lines expressing *Dll1*cyto and *Acvrinp1* or *Dll1*cyto and *Magi-3* could be generated. Also the migratory behaviour and the disruption of cell adhesion markers could be monitored in these cells to elucidate the function of *Dll1* on cell motility and adhesion.

*Subcellular
localization*

Moreover, the identification of proteins interacting with *Acvrinp1* and *Magi-3* could help to clarify their role in embryonic development. Therefore, an embryonic cDNA library could be screened with *Acvrinp1* and *Magi-3* as bait in a yeast two-hybrid approach. Interesting interactions could be confirmed by GST pull-down assays *in vitro* and in a mammalian two-hybrid system *in vivo*. The obtained binding partners might also be associated with the intracellular domains of *Dll1* and *Jag1* via the PDZ proteins and might therefore provide valuable informations about the intrinsic function of DSL ligands.

*Two-hybrid
screen*

Acvrinp1 was found to be upregulated in *Dll1* null-mutant mice. How the absence of *Dll1* influences the expression of *Acvrinp1* is still unknown. Identification and functional characterisation of the *Acvrinp1* promoter(s) could prove to be helpful. For promoter identification a variety of bioinformatic tools are available in the institute. The obtained results should be verified by activity measurements of promoter constructs in appropriate cell lines expressing *Acvrinp1*. Furthermore, one hybrid and/or gel-shift assays could shed light on the question which transcription factors might regulate the expression of *Acvrinp1*.

*Promoter
analysis*

Together with the presented data these further studies on the proposed intrinsic signaling activity of Delta will help to understand the complexity of Delta-Notch signal transduction, Delta function and the phenotypes of Delta mutants.

References

- Abbas, L (2003). Synapse formation: let's stick together. *Curr Biol*, 13(1):R25–7.
- Adamsky, K, Arnold, K, Sabanay, H & Peles, E (2003). Junctional protein MAGI-3 interacts with receptor tyrosine phosphatase beta (RPTP beta) and tyrosine-phosphorylated proteins. *J Cell Sci*, 116(Pt 7):1279–89.
- Adler, P N (2002). Planar signaling and morphogenesis in *Drosophila*. *Dev Cell*, 2(5):525–35.
- Apelqvist, A, Li, H, Sommer, L, Beatus, P, Anderson, D J, Honjo, T, Hrabé de Angelis, M, Lendahl, U & Edlund, H (1999). Notch signalling controls pancreatic cell differentiation. *Nature*, 400(6747):877–81.
- Artavanis-Tsakonas, S, Rand, M D & Lake, R J (1999). Notch signaling: cell fate control and signal integration in development. *Science*, 284(5415):770–6.
- Ascano, J M, Beverly, L J & Capobianco, A J (2003). The C-terminal PDZ-ligand of JAGGED1 is essential for cellular transformation. *J Biol Chem*, 278(10):8771–9.
- Aulehla, A & Herrmann, B G (2004). Segmentation in vertebrates: clock and gradient finally joined. *Genes Dev*, 18(17):2060–7.
- Aulehla, A, Wehrle, C, Brand-Saberi, B, Kemler, R, Gossler, A, Kanzler, B & Herrmann, B G (2003). Wnt3a plays a major role in the segmentation clock controlling somitogenesis. *Dev Cell*, 4(3):395–406.
- Austin, J & Kimble, J (1987). *glp-1* is required in the germ line for regulation of the decision between mitosis and meiosis in *C. elegans*. *Cell*, 51(4):589–99.
- Axelrod, J D, Matsuno, K, Artavanis-Tsakonas, S & Perrimon, N (1996). Interaction between Wingless and Notch signaling pathways mediated by *dishevelled*. *Science*, 271(5257):1826–32.
- Baron, M (2003). An overview of the Notch signalling pathway. *Semin Cell Dev Biol*, 14(2):113–9.

References

- Beckers, J, Clark, A, Wunsch, K, Hrabé de Angelis, M & Gossler, A (1999). Expression of the mouse Delta1 gene during organogenesis and fetal development. *Mech Dev*, 84(1-2):165–8.
- Bettenhausen, B, Hrabé de Angelis, M, Simon, D, Guenet, J L & Gossler, A (1995). Transient and restricted expression during mouse embryogenesis of Dll1, a murine gene closely related to Drosophila Delta. *Development*, 121(8):2407–18.
- Bilder, D, Li, M & Perrimon, N (2000). Cooperative regulation of cell polarity and growth by Drosophila tumor suppressors. *Science*, 289(5476):113–6.
- Bland, C E, Kimberly, P & Rand, M D (2003). Notch-induced proteolysis and nuclear localization of the Delta ligand. *J Biol Chem*, 278(16):13607–10.
- Blaumueller, C M, Qi, H, Zagouras, P & Artavanis-Tsakonas, S (1997). Intracellular cleavage of Notch leads to a heterodimeric receptor on the plasma membrane. *Cell*, 90(2):281–91.
- Braghetta, P, Ferrari, A, de Gemmis, P, Zanetti, M, Volpin, D, Bonaldo, P & Bressan, G M (2002). Expression of the EMILIN-1 gene during mouse development. *Matrix Biol*, 21(7):603–9.
- Bray, S (1998). Notch signalling in Drosophila: three ways to use a pathway. *Semin Cell Dev Biol*, 9(6):591–7.
- Bressan, G M, Daga-Gordini, D, Colombatti, A, Castellani, I, Marigo, V & Volpin, D (1993). Emilin, a component of elastic fibers preferentially located at the elastin-microfibrils interface. *J Cell Biol*, 121(1):201–12.
- Brou, C, Logeat, F, Gupta, N, Bessia, C, LeBail, O, Doedens, J R, Cumano, A, Roux, P, Black, R A & Israel, A (2000). A novel proteolytic cleavage involved in Notch signaling: the role of the disintegrin-metalloprotease TACE. *Mol Cell*, 5(2):207–16.
- Bulman, M P, Kusumi, K, Frayling, T M, McKeown, C, Garrett, C, Lander, E S, Krumlauf, R, Hattersley, A T, Ellard, S & Turnpenny, P D (2000). Mutations in the human delta homologue, DLL3, cause axial skeletal defects in spondylocostal dysostosis. *Nat Genet*, 24(4):438–41.
- Bustin, M, Trieschmann, L & Postnikov, Y V (1995). The HMG-14/-17 chromosomal protein family: architectural elements that enhance transcription from chromatin templates. *Semin Cell Biol*, 6(4):247–55.
- Carlesso, N, Aster, J C, Sklar, J & Scadden, D T (1999). Notch1-induced delay of human hematopoietic progenitor cell differentiation is associated with altered cell cycle kinetics. *Blood*, 93(3):838–48.

References

- Caruana, G & Bernstein, A (2001). Craniofacial dysmorphogenesis including cleft palate in mice with an insertional mutation in the discs large gene. *Mol Cell Biol*, 21(5):1475–83.
- Cavarelli, J & Moras, D (1993). Recognition of tRNAs by aminoacyl-tRNA synthetases. *FASEB J*, 7(1):79–86.
- Chabriat, H, Vahedi, K, Iba-Zizen, M T, Joutel, A, Nibbio, A, Nagy, T G, Krebs, M O, Julien, J, Dubois, B & Ducrocq, X (1995). Clinical spectrum of CADASIL: a study of 7 families. Cerebral autosomal dominant arteriopathy with subcortical infarcts and leukoencephalopathy. *Lancet*, 346(8980):934–9.
- Chen, W & Casey Corliss, D (2004). Three modules of zebrafish Mind bomb work cooperatively to promote Delta ubiquitination and endocytosis. *Dev Biol*, 267(2):361–73.
- Chitnis, A, Henrique, D, Lewis, J, Ish-Horowicz, D & Kintner, C (1995). Primary neurogenesis in *Xenopus* embryos regulated by a homologue of the *Drosophila* neurogenic gene Delta. *Nature*, 375(6534):761–6.
- Colombatti, A, Doliana, R, Bot, S, Canton, A, Mongiat, M, Mungiguerra, G, Paron-Cilli, S & Spessotto, P (2000). The EMILIN protein family. *Matrix Biol*, 19(4):289–301.
- Conlon, R A, Reaume, A G & Rossant, J (1995). Notch1 is required for the coordinate segmentation of somites. *Development*, 121(5):1533–45.
- Cornell, M, Evans, D A, Mann, R, Fostier, M, Flasz, M, Monthatong, M, Artavanis-Tsakonas, S & Baron, M (1999). The *Drosophila melanogaster* Suppressor of deltex gene, a regulator of the Notch receptor signaling pathway, is an E3 class ubiquitin ligase. *Genetics*, 152(2):567–76.
- Crittenden, S L, Troemel, E R, Evans, T C & Kimble, J (1994). GLP-1 is localized to the mitotic region of the *C. elegans* germ line. *Development*, 120(10):2901–11.
- Curtin, J A, Quint, E, Tsipouri, V, Arkell, R M, Cattanach, B, Copp, A J, Henderson, D J, Spurr, N, Stanier, P, Fisher, E M, Nolan, P M, Steel, K P, Brown, S D M, Gray, I C & Murdoch, J N (2003). Mutation of *Celsr1* disrupts planar polarity of inner ear hair cells and causes severe neural tube defects in the mouse. *Curr Biol*, 13(13):1129–33.
- De Bellard, M E, Ching, W, Gossler, A & Bronner-Fraser, M (2002). Disruption of segmental neural crest migration and ephrin expression in delta-1 null mice. *Dev Biol*, 249(1):121–30.

References

- De la Pompa, J L, Wakeham, A, Correia, K M, Samper, E, Brown, S, Aguilera, R J, Nakano, T, Honjo, T, Mak, T W, Rossant, J & Conlon, R A (1997). Conservation of the Notch signalling pathway in mammalian neurogenesis. *Development*, 124(6):1139–48.
- De Strooper, B, Annaert, W, Cupers, P, Saftig, P, Craessaerts, K, Mumm, J S, Schroeter, E H, Schrijvers, V, Wolfe, M S, Ray, W J, Goate, A & Kopan, R (1999). A presenilin-1-dependent gamma-secretase-like protease mediates release of Notch intracellular domain. *Nature*, 398(6727):518–22.
- Doliana, R, Mongiat, M, Bucciotti, F, Giacomello, E, Deutzmann, R, Volpin, D, Bressan, G M & Colombatti, A (1999). EMILIN, a component of the elastic fiber and a new member of the C1q/tumor necrosis factor superfamily of proteins. *J Biol Chem*, 274(24):16773–81.
- Dow, L E, Brumby, A M, Muratore, R, Coombe, M L, Sedelies, K A, Trapani, J A, Russell, S M, Richardson, H E & Humbert, P O (2003). hScrib is a functional homologue of the Drosophila tumour suppressor Scribble. *Oncogene*, 22(58):9225–30.
- Dunwoodie, S L, Clements, M, Sparrow, D B, Sa, X, Conlon, R A & Beddington, R S P (2002). Axial skeletal defects caused by mutation in the spondylocostal dysplasia/pudgy gene Dll3 are associated with disruption of the segmentation clock within the presomitic mesoderm. *Development*, 129(7):1795–806.
- Dunwoodie, S L, Henrique, D, Harrison, S M & Beddington, R S (1997). Mouse Dll3: a novel divergent Delta gene which may complement the function of other Delta homologues during early pattern formation in the mouse embryo. *Development*, 124(16):3065–76.
- Ellisen, L W, Bird, J, West, D C, Soreng, A L, Reynolds, T C, Smith, S D & Sklar, J (1991). TAN-1, the human homolog of the Drosophila notch gene, is broken by chromosomal translocations in T lymphoblastic neoplasms. *Cell*, 66(4):649–61.
- Fanning, A S & Anderson, J M (1999). PDZ domains: fundamental building blocks in the organization of protein complexes at the plasma membrane. *J Clin Invest*, 103(6):767–72.
- Fanto, M & McNeill, H (2004). Planar polarity from flies to vertebrates. *J Cell Sci*, 117(Pt 4):527–33.
- Favier, B, Fliniaux, I, Thelu, J, Viallet, J P, Demarchez, M, Jahoda, C A & Dhouailly, D (2000). Localisation of members of the notch system and the differentiation of vibrissa hair follicles: receptors, ligands, and fringe modulators. *Dev Dyn*, 218(3):426–37.

References

- Fitzgerald, K & Greenwald, I (1995). Interchangeability of *Caenorhabditis elegans* DSL proteins and intrinsic signalling activity of their extracellular domains in vivo. *Development*, 121(12):4275–82.
- Freist, W, Gauss, D H, Ibba, M & Soll, D (1997). Glutaminyl-tRNA synthetase. *Biol Chem*, 378(10):1103–17.
- Frise, E, Knoblich, J A, Younger-Shepherd, S, Jan, L Y & Jan, Y N (1996). The *Drosophila* Numb protein inhibits signaling of the Notch receptor during cell-cell interaction in sensory organ lineage. *Proc Natl Acad Sci U S A*, 93(21):11925–32.
- Fu, X D (1995). The superfamily of arginine/serine-rich splicing factors. *RNA*, 1(7):663–80.
- Galceran, J, Sustmann, C, Hsu, S-C, Folberth, S & Grosschedl, R (2004). LEF1-mediated regulation of Delta-like1 links Wnt and Notch signaling in somitogenesis. *Genes Dev*, 18(22):2718–23.
- Grandbarbe, L, Bouissac, J, Rand, M, Hrabé de Angelis, M, Artavanis-Tsakonas, S & Mohier, E (2003). Delta-Notch signaling controls the generation of neurons/glia from neural stem cells in a stepwise process. *Development*, 130(7):1391–402.
- Greene, N D, Gerrelli, D, Van Straaten, H W & Copp, A J (1998). Abnormalities of floor plate, notochord and somite differentiation in the loop-tail (Lp) mouse: a model of severe neural tube defects. *Mech Dev*, 73(1):59–72.
- Greenwald, I (1985). *lin-12*, a nematode homeotic gene, is homologous to a set of mammalian proteins that includes epidermal growth factor. *Cell*, 43(3 Pt 2):583–90.
- Han, W, Ye, Q & Moore, M A (2000). A soluble form of human Delta-like-1 inhibits differentiation of hematopoietic progenitor cells. *Blood*, 95(5):1616–25.
- Heitzler, P, Bourouis, M, Ruel, L, Carteret, C & Simpson, P (1996). Genes of the Enhancer of split and achaete-scute complexes are required for a regulatory loop between Notch and Delta during lateral signalling in *Drosophila*. *Development*, 122(1):161–71.
- Henderson, S T, Gao, D, Christensen, S & Kimble, J (1997). Functional domains of LAG-2, a putative signaling ligand for LIN-12 and GLP-1 receptors in *Caenorhabditis elegans*. *Mol Biol Cell*, 8(9):1751–62.

References

- Henderson, S T, Gao, D, Lambie, E J & Kimble, J (1994). lag-2 may encode a signaling ligand for the GLP-1 and LIN-12 receptors of *C. elegans*. *Development*, 120(10):2913–24.
- Hintsch, G, Zurlinden, A, Meskenaite, V, Steuble, M, Fink-Widmer, K, Kinter, J & Sonderegger, P (2002). The calsynenins—a family of postsynaptic membrane proteins with distinct neuronal expression patterns. *Mol Cell Neurosci*, 21(3):393–409.
- Hirabayashi, S, Nishimura, W, Iida, J, Kansaku, A, Kishida, S, Kikuchi, A, Tanaka, N & Hata, Y (2004). Synaptic scaffolding molecule interacts with axin. *J Neurochem*, 90(2):332–9.
- Hirao, K, Hata, Y, Ide, N, Takeuchi, M, Irie, M, Yao, I, Deguchi, M, Toyoda, A, Sudhof, T C & Takai, Y (1998). A novel multiple PDZ domain-containing molecule interacting with N-methyl-D-aspartate receptors and neuronal cell adhesion proteins. *J Biol Chem*, 273(33):21105–10.
- Hirao, K, Hata, Y, Yao, I, Deguchi, M, Kawabe, H, Mizoguchi, A & Takai, Y (2000). Three isoforms of synaptic scaffolding molecule and their characterization. Multimerization between the isoforms and their interaction with N-methyl-D-aspartate receptors and SAP90/PSD-95-associated protein. *J Biol Chem*, 275(4):2966–72.
- Hock, B, Böhme, B, Karn, T, Yamamoto, T, Kaibuchi, K, Holtrich, U, Holland, S, Pawson, T, Rubsamen-Waigmann, H & Strebhardt, K (1998). PDZ-domain-mediated interaction of the Eph-related receptor tyrosine kinase EphB3 and the ras-binding protein AF6 depends on the kinase activity of the receptor. *Proc Natl Acad Sci U S A*, 95(17):9779–84.
- Hofmann, M, Schuster-Gossler, K, Watabe-Rudolph, M, Aulehla, A, Herrmann, B G & Gossler, A (2004). WNT signaling, in synergy with T/TBX6, controls Notch signaling by regulating Dll1 expression in the presomitic mesoderm of mouse embryos. *Genes Dev*, 18(22):2712–7.
- Hrabé de Angelis, M, McIntyre, J 2nd & Gossler, A (1997). Maintenance of somite borders in mice requires the Delta homologue Dll1. *Nature*, 386(6626):717–21.
- Ide, N, Hata, Y, Deguchi, M, Hirao, K, Yao, I & Takai, Y (1999). Interaction of S-SCAM with neural plakophilin-related Armadillo-repeat protein/delta-catenin. *Biochem Biophys Res Commun*, 256(3):456–61.
- Ikeuchi, T & Sisodia, S S (2003). The Notch ligands, Delta1 and Jagged2, are substrates for presenilin-dependent "gamma-secretase" cleavage. *J Biol Chem*, 278(10):7751–4.

References

- Itoh, M, Kim, C-H, Palardy, G, Oda, T, Jiang, Y-J, Maust, D, Yeo, S-Y, Lorick, K, Wright, G J, Ariza-McNaughton, L, Weissman, A M, Lewis, J, Chandrasekharappa, S C & Chitnis, A B (2003). Mind bomb is a ubiquitin ligase that is essential for efficient activation of Notch signaling by Delta. *Dev Cell*, 4(1):67–82.
- Jarriault, S, Brou, C, Logeat, F, Schroeter, E H, Kopan, R & Israel, A (1995). Signalling downstream of activated mammalian Notch. *Nature*, 377(6547):355–8.
- Jelen, F, Oleksy, A, Smietana, K & Otlewski, J (2003). PDZ domains - common players in the cell signaling. *Acta Biochim Pol*, 50(4):985–1017.
- Johnston, S H, Rauskolb, C, Wilson, R, Prabhakaran, B, Irvine, K D & Vogt, T F (1997). A family of mammalian Fringe genes implicated in boundary determination and the Notch pathway. *Development*, 124(11):2245–54.
- Joutel, A, Andreux, F, Gaulis, S, Domenga, V, Cecillon, M, Battail, N, Piga, N, Chapon, F, Godfrain, C & Tournier-Lasserre, E (2000). The ectodomain of the Notch3 receptor accumulates within the cerebrovasculature of CADASIL patients. *J Clin Invest*, 105(5):597–605.
- Joutel, A, Corpechot, C, Ducros, A, Vahedi, K, Chabriat, H, Mouton, P, Alamowitch, S, Domenga, V, Cecillon, M, Marechal, E, Maciasek, J, Vayssiere, C, Cruaud, C, Cabanis, E A, Ruchoux, M M, Weissenbach, J, Bach, J F, Bousser, M G & Tournier-Lasserre, E (1996). Notch3 mutations in CADASIL, a hereditary adult-onset condition causing stroke and dementia. *Nature*, 383(6602):707–10.
- Joutel, A, Vahedi, K, Corpechot, C, Troesch, A, Chabriat, H, Vayssiere, C, Cruaud, C, Maciasek, J, Weissenbach, J, Bousser, M G, Bach, J F & Tournier-Lasserre, E (1997). Strong clustering and stereotyped nature of Notch3 mutations in CADASIL patients. *Lancet*, 350(9090):1511–5.
- Kamakura, S, Oishi, K, Yoshimatsu, T, Nakafuku, M, Masuyama, N & Gotoh, Y (2004). Hes binding to STAT3 mediates crosstalk between Notch and JAK-STAT signalling. *Nat Cell Biol*, 6(6):547–54.
- Kibar, Z, Vogan, K J, Groulx, N, Justice, M J, Underhill, D A & Gros, P (2001). Ltap, a mammalian homolog of Drosophila Strabismus/Van Gogh, is altered in the mouse neural tube mutant Loop-tail. *Nat Genet*, 28(3):251–5.
- Klein, T & Arias, A M (1998). Interactions among Delta, Serrate and Fringe modulate Notch activity during Drosophila wing development. *Development*, 125(15):2951–62.

References

- Kopan, R, Schroeter, E H, Weintraub, H & Nye, J S (1996). Signal transduction by activated mNotch: importance of proteolytic processing and its regulation by the extracellular domain. *Proc Natl Acad Sci U S A*, 93(4):1683–8.
- Krantz, I D, Piccoli, D A & Spinner, N B (1997). Alagille syndrome. *J Med Genet*, 34(2):152–7.
- Krebs, L T, Iwai, N, Nonaka, S, Welsh, I C, Lan, Y, Jiang, R, Saijoh, Y, O'Brien, T P, Hamada, H & Gridley, T (2003). Notch signaling regulates left-right asymmetry determination by inducing Nodal expression. *Genes Dev*, 17(10):1207–12.
- Kullander, K & Klein, R (2002). Mechanisms and functions of Eph and ephrin signalling. *Nat Rev Mol Cell Biol*, 3(7):475–86.
- Kusumi, K, Sun, E S, Kerrebrock, A W, Bronson, R T, Chi, D C, Bulotsky, M S, Spencer, J B, Birren, B W, Frankel, W N & Lander, E S (1998). The mouse pudgy mutation disrupts Delta homologue Dll3 and initiation of early somite boundaries. *Nat Genet*, 19(3):274–8.
- Lai, E C, Deblandre, G A, Kintner, C & Rubin, G M (2001). Drosophila neuralized is a ubiquitin ligase that promotes the internalization and degradation of delta. *Dev Cell*, 1(6):783–94.
- LaVoie, M J & Selkoe, D J (2003). The Notch ligands, Jagged and Delta, are sequentially processed by alpha-secretase and presenilin/gamma-secretase and release signaling fragments. *J Biol Chem*, 278(36):34427–37.
- Leenders, F, Tesdorpf, J G, Markus, M, Engel, T, Seedorf, U & Adamski, J (1996). Porcine 80-kDa protein reveals intrinsic 17 beta-hydroxysteroid dehydrogenase, fatty acyl-CoA-hydratase/dehydrogenase, and sterol transfer activities. *J Biol Chem*, 271(10):5438–42.
- Levy, D E & Darnell, J E Jr (2002). Stats: transcriptional control and biological impact. *Nat Rev Mol Cell Biol*, 3(9):651–62.
- Li, L, Krantz, I D, Deng, Y, Genin, A, Banta, A B, Collins, C C, Qi, M, Trask, B J, Kuo, W L, Cochran, J, Costa, T, Pierpont, M E, Rand, E B, Piccoli, D A, Hood, L & Spinner, N B (1997). Alagille syndrome is caused by mutations in human Jagged1, which encodes a ligand for Notch1. *Nat Genet*, 16(3):243–51.
- Lieber, T, Kidd, S & Young, M W (2002). kuzbanian-mediated cleavage of Drosophila Notch. *Genes Dev*, 16(2):209–21.
- Logeat, F, Bessia, C, Brou, C, LeBail, O, Jarriault, S, Seidah, N G & Israel, A (1998). The Notch1 receptor is cleaved constitutively by a furin-like convertase. *Proc Natl Acad Sci U S A*, 95(14):8108–12.

References

- Lowell, S & Watt, F M (2001). Delta regulates keratinocyte spreading and motility independently of differentiation. *Mech Dev*, 107(1-2):133–40.
- Lowry, O H, Rosebrough, N J, Farr, A L & Randall, R J (1951). Protein measurement with the Folin phenol reagent. *J Biol Chem*, 193(1):265–75.
- Luo, B, Aster, J C, Hasserjian, R P, Kuo, F & Sklar, J (1997). Isolation and functional analysis of a cDNA for human Jagged2, a gene encoding a ligand for the Notch1 receptor. *Mol Cell Biol*, 17(10):6057–67.
- Maga, G & Hubscher, U (2003). Proliferating cell nuclear antigen (PCNA): a dancer with many partners. *J Cell Sci*, 116(Pt 15):3051–60.
- Manley, J L & Tacke, R (1996). SR proteins and splicing control. *Genes Dev*, 10(13):1569–79.
- Markwell, M A, Haas, S M, Tolbert, N E & Bieber, L L (1981). Protein determination in membrane and lipoprotein samples: manual and automated procedures. *Methods Enzymol*, 72(0076-6879):296–303.
- Mathew, D, Gramates, L S, Packard, M, Thomas, U, Bilder, D, Perrimon, N, Gorczyca, M & Budnik, V (2002). Recruitment of scribble to the synaptic scaffolding complex requires GUK-holder, a novel DLG binding protein. *Curr Biol*, 12(7):531–9.
- McCright, B, Lozier, J & Gridley, T (2002). A mouse model of Alagille syndrome: Notch2 as a genetic modifier of Jag1 haploinsufficiency. *Development*, 129(4):1075–82.
- Meyer, G, Varoqueaux, F, Neeb, A, Oschlies, M & Brose, N (2004). The complexity of PDZ domain-mediated interactions at glutamatergic synapses: a case study on neuroligin. *Neuropharmacology*, 47(5):724–33.
- Montcouquiol, M, Rachel, R A, Lanford, P J, Copeland, N G, Jenkins, N A & Kelley, M W (2003). Identification of Vangl2 and Scrb1 as planar polarity genes in mammals. *Nature*, 423(6936):173–7.
- Mori, T, Li, Y, Hata, H & Kochi, H (2004). NIRF is a ubiquitin ligase that is capable of ubiquitinating PCNP, a PEST-containing nuclear protein. *FEBS Lett*, 557(1-3):209–14.
- Mori, T, Li, Y, Hata, H, Ono, K & Kochi, H (2002). NIRF, a novel RING finger protein, is involved in cell-cycle regulation. *Biochem Biophys Res Commun*, 296(3):530–6.
- Morrison, A, Hodgetts, C, Gossler, A, Hrabé de Angelis, M & Lewis, J (1999). Expression of Delta1 and Serrate1 (Jagged1) in the mouse inner ear. *Mech Dev*, 84(1-2):169–72.

References

- Mumm, J S, Schroeter, E H, Saxena, M T, Griesemer, A, Tian, X, Pan, D J, Ray, W J & Kopan, R (2000). A ligand-induced extracellular cleavage regulates gamma-secretase-like proteolytic activation of Notch1. *Mol Cell*, 5(2):197–206.
- Murdoch, J N, Doudney, K, Paternotte, C, Copp, A J & Stanier, P (2001). Severe neural tube defects in the loop-tail mouse result from mutation of *Lpp1*, a novel gene involved in floor plate specification. *Hum Mol Genet*, 10(22):2593–601.
- Murdoch, J N, Henderson, D J, Doudney, K, Gaston-Massuet, C, Phillips, H M, Paternotte, C, Arkell, R, Stanier, P & Copp, A J (2003). Disruption of scribble (*Scrb1*) causes severe neural tube defects in the circletail mouse. *Hum Mol Genet*, 12(2):87–98.
- Nguyen, D N, Liu, Y, Litsky, M L & Reinke, R (1997). The sidekick gene, a member of the immunoglobulin superfamily, is required for pattern formation in the *Drosophila* eye. *Development*, 124(17):3303–12.
- Nguyen, M M, Nguyen, M L, Caruana, G, Bernstein, A, Lambert, P F & Griep, A E (2003). Requirement of PDZ-containing proteins for cell cycle regulation and differentiation in the mouse lens epithelium. *Mol Cell Biol*, 23(24):8970–81.
- Nishimura, W, Yao, I, Iida, J, Tanaka, N & Hata, Y (2002). Interaction of synaptic scaffolding molecule and Beta -catenin. *J Neurosci*, 22(3):757–65.
- Nourry, C, Grant, S G N & Borg, J-P (2003). PDZ domain proteins: plug and play! *Sci STKE*, 2003(179):RE7.
- Oda, T, Elkahloun, A G, Pike, B L, Okajima, K, Krantz, I D, Genin, A, Piccoli, D A, Meltzer, P S, Spinner, N B, Collins, F S & Chandrasekharappa, S C (1997). Mutations in the human *Jagged1* gene are responsible for Alagille syndrome. *Nat Genet*, 16(3):235–42.
- Ohashi, M, Sakurai, M, Higuchi, M, Mori, N, Fukushi, M, Oie, M, Coffey, R J, Yoshiura, K, Tanaka, Y, Uchiyama, M, Hatanaka, M & Fujii, M (2004). Human T-cell leukemia virus type 1 Tax oncoprotein induces and interacts with a multi-PDZ domain protein, MAGI-3. *Virology*, 320(1):52–62.
- Ohtsuka, T, Hata, Y, Ide, N, Yasuda, T, Inoue, E, Inoue, T, Mizoguchi, A & Takai, Y (1999). nRap GEP: a novel neural GDP/GTP exchange protein for rap1 small G protein that interacts with synaptic scaffolding molecule (S-SCAM). *Biochem Biophys Res Commun*, 265(1):38–44.

References

- Oka, C, Nakano, T, Wakeham, A, de la Pompa, J L, Mori, C, Sakai, T, Okazaki, S, Kawaichi, M, Shiota, K, Mak, T W & Honjo, T (1995). Disruption of the mouse RBP-J kappa gene results in early embryonic death. *Development*, 121(10):3291–301.
- Pan, D & Rubin, G M (1997). Kuzbanian controls proteolytic processing of Notch and mediates lateral inhibition during Drosophila and vertebrate neurogenesis. *Cell*, 90(2):271–80.
- Panin, V M, Papayannopoulos, V, Wilson, R & Irvine, K D (1997). Fringe modulates Notch-ligand interactions. *Nature*, 387(6636):908–12.
- Paranjape, S M, Krumm, A & Kadonaga, J T (1995). HMG17 is a chromatin-specific transcriptional coactivator that increases the efficiency of transcription initiation. *Genes Dev*, 9(16):1978–91.
- Parks, A L, Klueg, K M, Stout, J R & Muskavitch, M A (2000). Ligand endocytosis drives receptor dissociation and activation in the Notch pathway. *Development*, 127(7):1373–85.
- Pavlopoulos, E, Pitsouli, C, Klueg, K M, Muskavitch, M A, Moschonas, N K & Delidakis, C (2001). neuralized Encodes a peripheral membrane protein involved in delta signaling and endocytosis. *Dev Cell*, 1(6):807–16.
- Pestova, T V, Kolupaeva, V G, Lomakin, I B, Pilipenko, E V, Shatsky, I N, Agol, V I & Hellen, C U (2001). Molecular mechanisms of translation initiation in eukaryotes. *Proc Natl Acad Sci U S A*, 98(13):7029–36.
- Przemeck, G K H, Heinzmann, U, Beckers, J & Hrabé de Angelis, M (2003). Node and midline defects are associated with left-right development in Delta1 mutant embryos. *Development*, 130(1):3–13.
- Ramain, P, Khechumian, K, Seugnet, L, Arbogast, N, Ackermann, C & Heitzler, P (2001). Novel Notch alleles reveal a Deltex-dependent pathway repressing neural fate. *Curr Biol*, 11(22):1729–38.
- Raya, A, Kawakami, Y, Rodriguez-Esteban, C, Buscher, D, Koth, C M, Itoh, T, Morita, M, Raya, R M, Dubova, I, Bessa, J G, de la Pompa, J L & Belmonte, J C I (2003). Notch activity induces Nodal expression and mediates the establishment of left-right asymmetry in vertebrate embryos. *Genes Dev*, 17(10):1213–8.
- Rebay, I, Fleming, R J, Fehon, R G, Cherbas, L, Cherbas, P & Artavanis-Tsakonas, S (1991). Specific EGF repeats of Notch mediate interactions with Delta and Serrate: implications for Notch as a multifunctional receptor. *Cell*, 67(4):687–99.

References

- Sambrook, J., Fritsch, E.F. & Maniatis, T. (1989). *Molecular cloning*. Cold Spring Harbor Laboratory Press, 2. Ausg.
- Schägger, H & von Jagow, G (1987). Tricine-sodium dodecyl sulfate-polyacrylamide gel electrophoresis for the separation of proteins in the range from 1 to 100 kDa. *Anal Biochem*, 166(2):368–79.
- Shoji, H, Tsuchida, K, Kishi, H, Yamakawa, N, Matsuzaki, T, Liu, Z, Nakamura, T & Sugino, H (2000). Identification and characterization of a PDZ protein that interacts with activin type II receptors. *J Biol Chem*, 275(8):5485–92.
- Six, E, Ndiaye, D, Laabi, Y, Brou, C, Gupta-Rossi, N, Israel, A & Logeat, F (2003). The Notch ligand Delta1 is sequentially cleaved by an ADAM protease and gamma-secretase. *Proc Natl Acad Sci U S A*, 100(13):7638–43.
- Six, E M, Ndiaye, D, Sauer, G, Laabi, Y, Athman, R, Cumano, A, Brou, C, Israel, A & Logeat, F (2004). The notch ligand Delta1 recruits Dlg1 at cell-cell contacts and regulates cell migration. *J Biol Chem*, 279(53):55818–26.
- Spana, E P, Kopczynski, C, Goodman, C S & Doe, C Q (1995). Asymmetric localization of numb autonomously determines sibling neuron identity in the Drosophila CNS. *Development*, 121(11):3489–94.
- Spinner, N B, Colliton, R P, Crosnier, C, Krantz, I D, Hadchouel, M & Meunier-Rotival, M (2001). Jagged1 mutations in alagille syndrome. *Hum Mutat*, 17(1):18–33.
- Spörle, R & Schughart, K (1998). Paradox segmentation along inter- and intrasomatic borderlines is followed by dysmorphology of the axial skeleton in the open brain (opb) mouse mutant. *Dev Genet*, 22(4):359–73.
- Struhl, G, Fitzgerald, K & Greenwald, I (1993). Intrinsic activity of the Lin-12 and Notch intracellular domains in vivo. *Cell*, 74(2):331–45.
- Sun, X & Artavanis-Tsakonas, S (1996). The intracellular deletions of Delta and Serrate define dominant negative forms of the Drosophila Notch ligands. *Development*, 122(8):2465–74.
- Tam, P P (1981). The control of somitogenesis in mouse embryos. *J Embryol Exp Morphol*, 65 Suppl(0022-0752):103–28.
- Thomas, M, Laura, R, Hepner, K, Guccione, E, Sawyers, C, Lasky, L & Banks, L (2002). Oncogenic human papillomavirus E6 proteins target the MAGI-2 and MAGI-3 proteins for degradation. *Oncogene*, 21(33):5088–96.

References

- Tolkacheva, T, Boddapati, M, Sanfiz, A, Tsuchida, K, Kimmelman, A C & Chan, A M (2001). Regulation of PTEN binding to MAGI-2 by two putative phosphorylation sites at threonine 382 and 383. *Cancer Res*, 61(13):4985–9.
- Tomlinson, A & Struhl, G (1999). Decoding vectorial information from a gradient: sequential roles of the receptors Frizzled and Notch in establishing planar polarity in the *Drosophila* eye. *Development*, 126(24):5725–38.
- Trieschmann, L, Alfonso, P J, Crippa, M P, Wolffe, A P & Bustin, M (1995a). Incorporation of chromosomal proteins HMG-14/HMG-17 into nascent nucleosomes induces an extended chromatin conformation and enhances the utilization of active transcription complexes. *EMBO J*, 14(7):1478–89.
- Trieschmann, L, Postnikov, Y V, Rickers, A & Bustin, M (1995b). Modular structure of chromosomal proteins HMG-14 and HMG-17: definition of a transcriptional enhancement domain distinct from the nucleosomal binding domain. *Mol Cell Biol*, 15(12):6663–9.
- Tsuchida, K, Matsuzaki, T, Yamakawa, N, Liu, Z & Sugino, H (2001). Intracellular and extracellular control of activin function by novel regulatory molecules. *Mol Cell Endocrinol*, 180(1-2):25–31.
- Tsuda, L, Nagaraj, R, Zipursky, S L & Banerjee, U (2002). An EGFR/Ebi/Sno pathway promotes delta expression by inactivating Su(H)/SMRTER repression during inductive notch signaling. *Cell*, 110(5):625–37.
- Varnum-Finney, B, Purton, L E, Yu, M, Brashem-Stein, C, Flowers, D, Staats, S, Moore, K A, Le Roux, I, Mann, R, Gray, G, Artavanis-Tsakonas, S & Bernstein, I D (1998). The Notch ligand, Jagged-1, influences the development of primitive hematopoietic precursor cells. *Blood*, 91(11):4084–91.
- Vazquez, F, Grossman, S R, Takahashi, Y, Rokas, M V, Nakamura, N & Sellers, W R (2001). Phosphorylation of the PTEN tail acts as an inhibitory switch by preventing its recruitment into a protein complex. *J Biol Chem*, 276(52):48627–30.
- Vogt, L, Schrimpf, S P, Meskenaite, V, Frischknecht, R, Kinter, J, Leone, D P, Ziegler, U & Sonderegger, P (2001). Calsyntenin-1, a proteolytically processed postsynaptic membrane protein with a cytoplasmic calcium-binding domain. *Mol Cell Neurosci*, 17(1):151–66.
- Wallingford, J B & Harland, R M (2002). Neural tube closure requires Dishevelled-dependent convergent extension of the midline. *Development*, 129(24):5815–25.

References

- Wallingford, J B, Rowning, B A, Vogeli, K M, Rothbacher, U, Fraser, S E & Harland, R M (2000). Dishevelled controls cell polarity during *Xenopus* gastrulation. *Nature*, 405(6782):81–5.
- Weissman, A M (2001). Themes and variations on ubiquitylation. *Nat Rev Mol Cell Biol*, 2(3):169–78.
- Wharton, K A, Johansen, K M, Xu, T & Artavanis-Tsakonas, S (1985). Nucleotide sequence from the neurogenic locus notch implies a gene product that shares homology with proteins containing EGF-like repeats. *Cell*, 43(3 Pt 2):567–81.
- Wood, J D, Yuan, J, Margolis, R L, Colomer, V, Duan, K, Kushi, J, Kaminsky, Z, Kleiderlein, J J, Sharp, A H & Ross, C A (1998). Atrophin-1, the DR-PLA gene product, interacts with two families of WW domain-containing proteins. *Mol Cell Neurosci*, 11(3):149–60.
- Wright, G J, Leslie, J D, Ariza-McNaughton, L & Lewis, J (2004). Delta proteins and MAGI proteins: an interaction of Notch ligands with intracellular scaffolding molecules and its significance for zebrafish development. *Development*, 131(22):5659–69.
- Wu, J Y, Wen, L, Zhang, W J & Rao, Y (1996). The secreted product of *Xenopus* gene lunatic Fringe, a vertebrate signaling molecule. *Science*, 273(5273):355–8.
- Wu, X, Hepner, K, Castelino-Prabhu, S, Do, D, Kaye, M B, Yuan, X J, Wood, J, Ross, C, Sawyers, C L & Whang, Y E (2000a). Evidence for regulation of the PTEN tumor suppressor by a membrane-localized multi-PDZ domain containing scaffold protein MAGI-2. *Proc Natl Acad Sci U S A*, 97(8):4233–8.
- Wu, Y, Dowbenko, D, Spencer, S, Laura, R, Lee, J, Gu, Q & Lasky, L A (2000b). Interaction of the tumor suppressor PTEN/MMAC with a PDZ domain of MAGI3, a novel membrane-associated guanylate kinase. *J Biol Chem*, 275(28):21477–85.
- Xu, J, Paquet, M, Lau, A G, Wood, J D, Ross, C A & Hall, R A (2001). beta 1-adrenergic receptor association with the synaptic scaffolding protein membrane-associated guanylate kinase inverted-2 (MAGI-2). Differential regulation of receptor internalization by MAGI-2 and PSD-95. *J Biol Chem*, 276(44):41310–7.
- Yamagata, M, Weiner, J A & Sanes, J R (2002). Sidekicks: synaptic adhesion molecules that promote lamina-specific connectivity in the retina. *Cell*, 110(5):649–60.

References

- Yao, I, Hata, Y, Ide, N, Hirao, K, Deguchi, M, Nishioka, H, Mizoguchi, A & Takai, Y (1999). MAGUIN, a novel neuronal membrane-associated guanylate kinase-interacting protein. *J Biol Chem*, 274(17):11889–96.
- Yao, R, Natsume, Y & Noda, T (2004). MAGI-3 is involved in the regulation of the JNK signaling pathway as a scaffold protein for frizzled and Ltap. *Oncogene*, 36(6023-30).
- Zanetti, M, Braghetta, P, Sabatelli, P, Mura, I, Doliana, R, Colombatti, A, Volpin, D, Bonaldo, P & Bressan, G M (2004). EMILIN-1 deficiency induces elastogenesis and vascular cell defects. *Mol Cell Biol*, 24(2):638–50.
- zur Lage, P & Jarman, A P (1999). Antagonism of EGFR and notch signalling in the reiterative recruitment of *Drosophila* adult chordotonal sense organ precursors. *Development*, 126(14):3149–57.

Appendix

Publication list

Pfister, S., Przemeck, G.K.H., Gerber, J-K., Beckers, J., Adamski, J., Hrabé de Angelis, H. (2003). Interaction of the MAGUK Family Member Acvrinp1 and the Cytoplasmic Domain of the Notch Ligand Delta1. *Journal of Molecular Biology* 333(2): 229-235

Alessandrini, F., Pfister, S., Kremmer, E., Stachowith, S., Gerber, J-K., Ring, J., Behrendt, H. (2004) Alteration of the Level of β -Glucocerebrosidase in the Skin of Patients with Psoriasis Vulgaris. *Journal of Investigative Dermatology* 123(6): 1030-1036

Table 4.2: Oligonucleotides

primer name	number	length (bp)	5'-3' sequence	T _m (°C)
<i>Dll1</i> rev XhoI	32546	30	ATA TCT CGA GCA TCG CTT CCA TCT TAC ACC	64.2
<i>Dll1</i> cyto for EcoRI	32547	36	ATA GAA TTC GGC GCC GGC CTG AAG CTA CAG	79.5
<i>Acvrinp1</i> for EcoRI	41316	25	GAA TTC GGT CCC TGG AGT GGA CTA C	60
<i>Acvrinp1</i> ΔPDZ4-5 rev XhoI	41317	26	CTC GAG CTA GTT GCT GTT GGA GTA GG	58.8
<i>Acvrinp1</i> PDZ5 for EcoRI	41318	25	GAA TTC ATG TCT CCA GAC ACC AGG C	59.7
<i>Acvrinp1</i> ΔPDZ5 rev XhoI	41319	22	CTC GAG CTA CAA GGG TGG GGG C	62.7
<i>Acvrinp1</i> rev XhoI	41320	24	CTC GAG AGG ATG TCT TCG AGG GAG	59.4
<i>Acvrinp1</i> ΔPDZ1-5 rev XhoI	41321	28	CTC GAG CTA CTT TGC TCC AAG TTC TGT G	61.7
<i>Acvrinp1</i> PDZ1 for EcoRI	41322	27	GAA TTC ATG TTC CGA GAA AAG CCA CTC	61.2
<i>Acvrinp1</i> PDZ4 for EcoRI	41323	25	GAA TTC ATG AGC AGC AAT GCC TCA C	60.8
<i>Acvrinp1</i> for Sall	42238	25	GTC GAC GGA TGG AAT TGG AGA AAA G	60.8
<i>Acvrinp1</i> rev NotI	42245	22	GCG GCC GCA GGA TGT CTT CGA G	66.5
<i>Dll1</i> cyto for Sall	42278	24	GTC GAC TTG TCC GGC TGA AGC TAC	60.1
<i>Dll1</i> rev NotI	42279	24	GCG GCC GCT TAC ACC TCA GTC GCT	67.8
<i>Dll1</i> cytoΔPDZ-BD for	47376	40	GAA AAG GAT GAG TGT GTT ATA TAA GAT GGA AGC GAT GCT C	68.7
<i>Dll1</i> cytoΔPDZ-BD rev	47377	40	GAG CAT CGC TTC CAT CTT ATA TAA CAC ACT CAT CCT TTT C	68.7
<i>Jag1</i> rev XhoI	51347	31	CTC GAG CTA TAC GAT GTA TTC CAT CCG GTT C	65.1
<i>Jag1</i> cyto for EcoRI	51548	26	GAA TTC CGG AAG CCG CGG AAG CCC AG	73
<i>Magi3</i> rev	52809	31	TTA ATG TTG CTC AGG TTT CAC GTA GGA GCA C	64.9
<i>Magi3</i> PDZ1 for	52931	30	GAC AGG CTG AAA TTC ATT CTG CAA AAA CAG	63.8
<i>Magi3</i> PDZ1 for MluI	54598	30	ACG CGT TGG GAC AGG CTG AAA TTC ATT CTG	70.1
<i>Magi3</i> PDZ1 for EcoRI	MWG5	31	GAA TTC ATG GGA CAG GCT GAA ATT CAT TCT G	65.5
<i>Magi3</i> rev NotI	MWG6	29	GCG GCC GCT TAA TGT TGC TCA GGT TTC AC	69.5
<i>Jag1</i> cytoΔPDZ-BD for	57525	39	CCC AGA GCT TGA ACC GGA TGT AGC TCG AGG AAG CTT GGC	78.7
<i>Jag1</i> cytoΔPDZ-BD rev	57526	39	GCC AAG CTT CCT CGA GCT ACA TCC GGT TCA AGC TCT GGG	78.7

Table 4.3: Plasmid constructs

construct	vector	gene (accession number)	bp of cds	amino acids	primer	template	restriction sites
pGBKT7 <i>DIII</i> /cyto	pGBKT7	<i>DIII</i> (NM_007865)	1705-2182	569-722	32547; 32546	pCRIID <i>III</i> /full ¹	EcoRI; XhoI (EcoRI; Sall of pGBKT7)
pGEX <i>DIII</i> /cyto	pGEXΔBamHI	<i>DIII</i> (NM_007865)	1705-2182	569-722	32547; 32546	pCRIID <i>III</i> /full ¹	EcoRI; XhoI
pGEX <i>DIII</i> ΔPDZ- BD	pGEXΔBamHI	<i>DIII</i> (NM_007865)	1705-2170	569-718	47376; 47377	pGEX <i>DIII</i> /cyto	EcoRI; XhoI
pGEX <i>Jag1</i> /cyto	pGEXΔBamHI	<i>Jag1</i> (NM_013822)	3281-3657	1095-1218	51548; 51347	IMAG p998A0914407Q3	EcoRI; XhoI
pGEX <i>Jag1</i> ΔPDZ-BD	pGEXΔBamHI	<i>Jag1</i> (NM_013822)	3281-3645	1095-1214	57525; 57526	pGEX <i>Jag1</i> /cyto	EcoRI; XhoI
pcDNA3 <i>Acvrinp1</i> GUKWW	pcDNA3	<i>Acvrinp1</i> (NM_015823)	1-708	1-236	41316; 41321	CMV-FLAG-ARIP1 ²	EcoRI; XhoI
pcDNA3 <i>Acvrinp1</i> PDZ1-5	pcDNA3.1	<i>Acvrinp1</i> (NM_015823)	727-3339	243-1113	41322; 41320	CMV-FLAG-ARIP1 ²	EcoRI; XhoI
pcDNA3 <i>Acvrinp1</i> ΔPDZ4-5	pcDNA3.1	<i>Acvrinp1</i> (NM_015823)	1-2199	1-733	41316; 41317	CMV-FLAG-ARIP1 ²	EcoRI; XhoI
pcDNA3 <i>Acvrinp1</i> PDZ4-5	pcDNA3	<i>Acvrinp1</i> (NM_015823)	2212-3339	738-1113	41323; 41320	CMV-FLAG-ARIP1 ²	EcoRI; XhoI
pcDNA3 <i>Acvrinp1</i> ΔPDZ5	pcDNA3.1	<i>Acvrinp1</i> (NM_015823)	1-2847	1-949	41316; 41319	CMV-FLAG-ARIP1 ²	EcoRI; XhoI
pcDNA3 <i>Acvrinp1</i> PDZ5	pcDNA3	<i>Acvrinp1</i> (NM_015823)	2863-3339	955-1113	41318; 41320	CMV-FLAG-ARIP1 ²	EcoRI; XhoI
pcDNA3 <i>Magi-3</i> PDZ1-5	pcDNA3	<i>Magi-3</i> (AF213258)	1150-3381	384-743	MWG5; MWG6	pCRIIM <i>agi-3</i> PDZ1-5	EcoRI; NotI
pACT <i>DIII</i> /cyto	pACT	<i>DIII</i> (NM_007865)	1705-2182	569-722	42278; 42279	pGBKT7 <i>DIII</i> /full	Sall; NotI
pBIND <i>Acvrinp1</i>	pBIND	<i>Acvrinp1</i> (NM_015823)	full-length	full-length	42238; 42245	CMV-FLAG-ARIP1	Sall; NotI
pBIND <i>Magi-3</i> PDZ1-5	pBIND	<i>Magi-3</i> (AF213258)	1150-3381	384-743	54598; MWG6	pcDNA3 <i>Magi-3</i> PDZ1-5	MluI; NotI

Table 4.4: RNA probes

construct	vector	gene (accession number)	bp of cds	primer	template	orientation
pCRIIA <i>Acvrinp1</i> PDZ1-5	pCRII	<i>Acvrinp1</i> (NM_015823)	727-3339	41322; 41320	CMV-FLAG-ARIP1 ²	T7
pCRIIM <i>Magi-3</i> PDZ1-5	pCRII	<i>Magi-3</i> (AF213258)	1151-3381	52931; 52809	mouse d10 cDNA ³	T7

¹ kindly provided by Dr. Josef-Karl Gerber

² kindly provided by Kunihiro Tsuchida (University of Tokushima, Japan)

³ kindly provided by Dr. Rebekka Mindnich

List of Figures

1.1	Notch signal transduction pathway	10
1.2	Cell fate determination	11
2.1	GST pull-down assay	24
2.2	Gal4 yeast two-hybrid system	32
2.3	Mammalian two-hybrid system	33
3.1	Sequence analysis of Dll1 homologues	41
3.2	Sequence analysis of mouse Delta and Jagged proteins	41
3.3	Sequence analysis of Acvrinp1 and Magi-3	43
3.4	Induction and purification of GST fusion proteins	47
3.5	Interaction of Dll1cyto and Acvrinp1 <i>in vitro</i>	48
3.6	Generation of Magi-3 cDNA	49
3.7	Interaction of Dll1cyto and Jag1cyto with Acvrinp1 and Magi-3 <i>in vitro</i>	49
3.8	Structural model of Acvrinp1 PDZ4 complexed with Dll1 PDZ-ligand	51
3.9	Interaction of Dll1 with Acvrinp1 and Magi-3 <i>in vivo</i>	52
3.10	Comparison of <i>Acvrinp1</i> and <i>Dll1</i> gene expression	55
3.11	Analysis of <i>Magi-3</i> gene expression	55
4.1	Model of JNK activation by Magi-3	64

List of Tables

3.1	Dll1 interacting proteins	44
4.1	NLS, PDZ-BD and Fringe inhibition of DSL ligands	58
4.2	Oligonucleotides	82
4.3	Plasmid constructs	83
4.4	RNA probes	84

Danksagung

Ganz besonders möchte ich mich bei meinem Doktorvater Martin Hrabé de Angelis bedanken, der mir durch sein Vertrauen sehr viel Freiraum für eigene Ideen gegeben hat. Auch dafür, dass er es mir ermöglicht hat, meine Ergebnisse bei vielen Gelegenheiten zu präsentieren, bin ich sehr dankbar.

Bei Jurek Adamski bedanke ich mich für zahlreiche interessante Diskussionen und Anregungen, für die gute Betreuung und für das Probelesen dieser Arbeit. Gerhard Przemeck hat mich bei unzähligen Gelegenheiten unterstützt. Er hatte bei allen Fragen und Problemen stets ein offenes Ohr und war mir eine unersetzliche Hilfe bei der Durchführung und beim Schreiben dieser Arbeit. Vielen Dank dafür!

Christina Höfer danke ich für neue interessante Ideen und wünsche Ihr noch viel Spass und Erfolg bei Ihrer Doktorarbeit.

Bei Josef-Karl Gerber bedanke ich mich für seine hervorragende Betreuung, die noch weit über das Ende der Diplomarbeit hinausging.

Bedanken möchte ich mich auch bei Francesca Alessandrini. Die Arbeit mit ihr hat mir besonders viel Freude gemacht.

Johannes Beckers danke ich für seine Hilfe beim Schreiben des Manuskripts. Den Mitgliedern meiner Arbeitsgruppe Gabriele Möller, Dominga Deluca, Cornelia Prehn, Rebekka Mindnich, Thomas Ohnesorg, Christina Guggenberger, Brigitte Keller, Florian Grädler, Inge Laaser, Gabriele Ziegelmeier, Marion Schieweg, André Enseleit, Marc Maier und Martina Brandl möchte ich für die angenehme Atmosphäre im Labor danken.

Vielen Dank auch den Praktikanten Veronica Leiss, Stefanie Piegisch, Denise Ilgen und Maximilian Adolf, die an unterschiedlichen Teilprojekten mitgewirkt haben.

Zu guter Letzt möchte ich auch meiner Familie und meinen Freunden danken, die mich die ganze Zeit über unterstützt haben.

Lebenslauf

Persönliche Daten:

Geburtsdatum: 23.09.1978
Geburtsort: München
Staatsangehörigkeit: deutsch

Schulbildung:

1988-1995 Theresiengymnasium München
1995-1997 Ludwigsgymnasium München
Abschluß: Abitur

Hochschulausbildung:

10/97-01/02 Studium der Biologie an der Technischen Universität München
05/01-01/02 Diplomarbeit am Institut für Experimentelle Genetik, GSF-Neuherberg
Titel: Suche nach Protein-Interaktoren des cytoplasmatischen Anteils von mD111 mit Hilfe des Hefe Gal4 Zwei-Hybrid-Systems
Abschluß: Diplom

Dissertation:

Seit 03/2002 Doktorandin am Institut für Experimentelle Genetik, GSF-Neuherberg